

# Finite-state transducers for substitution tilings

Simon Tatham

2025-12-18

## Abstract

We present a suite of algorithmic techniques for handling substitution tilings by treating a tile's hierarchy of supertiles in a purely combinatorial fashion using finite state automata. The resulting techniques are very convenient for practical generation of patches of aperiodic tilings such as hats, Spectres and Penrose tiles, both random and deliberately selected. They also permit some analyses of the represented tiling. A particular product of this process is two substitution systems for the hat tiling which are 'unambiguous' in that a single tile address uniquely determines the rest of the plane.

## 1 Introduction

Well-known aperiodic tilings such as the Penrose P2 and P3 tilings [Pen79], the Ammann-Beenker tiling ([GS86], Figures 10.4.14 and 10.4.15), the hat tiling [SMKGS24a] and the Spectre tiling [SMKGS24b], are generated by *substitution systems*, in which one tiling of the plane is converted ('*deflated*') into another, by consistently substituting a set of smaller tiles for each original tile. In some substitution systems, every level of this system looks the same; in others, a set of *metatiles* is repeatedly deflated, and then a different final substitution step turns the metatiles into the tiles of the desired end-product tiling.

In some substitution systems, the tilings before and after deflation correspond geometrically, with the *subtiles* deflated from each *supertile* occupying exactly the same region of the plane (under an appropriate scaling), or failing that, occupying a region that overlaps the edges of the original supertile in a consistent fashion. In others, such as the *HTPF* system of metatiles for the hat tiling, the geometry is much more distorted by the deflation process, and even the metatiles themselves change their shape slightly in every deflation. It is therefore desirable to find ways to deal with these tilings which do not need to consider the geometry of any tiles except those in the final end-product tiling.

The substitution system itself provides an alternative way to identify each tile in a tiling of the plane, via an infinitely long *address* [GS99] describing the relationship of a particular tile  $t_0$  to its supertile  $t_1$  (both what type of tile  $t_1$  is, and which subtile of  $t_1$  is  $t_0$ ), and the relationship of that in turn to the second-order supertile  $t_2$ , and so on. These addresses can be regarded as strings of symbols from a finite alphabet, and [GS99] suggests that finite state automata can be used to manipulate those strings. In particular an automaton is suggested which accepts the addresses of *two* tiles, one symbol at a time from each (as if they were combined by the `zip` operation in programming languages such as Python), and determines whether the two addresses describe tiles that are adjacent in the tiling.

This article develops that idea into a full system of algorithms for working with tilings in this way. The automaton described in [GS99] is modified slightly so that its input includes a choice of *edge* of each of the two input tiles, and reports not only whether the tiles could be adjacent at all, but whether they are adjacent along that specific pair of edges. A second automaton is constructed from this, which receives only a single edge address as input, and generates the address of its neighbour as output. This second automaton cannot always be constructed, but if it cannot, the substitution system can be modified to remove the obstacle, with the modified system always being a 'refinement' of the old one – identical except that some tile types have been duplicated into multiple 'subtypes' carrying additional information about their role in the tiling. Algorithms for all of these constructions are presented.

Some results of the refinement process are also described, including two substitution systems for the hat tiling not previously published to the best of my knowledge.

## 2 Specifying a substitution system

In order to handle a substitution tiling algorithmically, it must first be specified, in a form that provides all the necessary data.

The algorithms described in this article work entirely on a *combinatorial* description of the tiling. The only information required is about what tiles and edges exist, which of them are adjacent to which, and which map

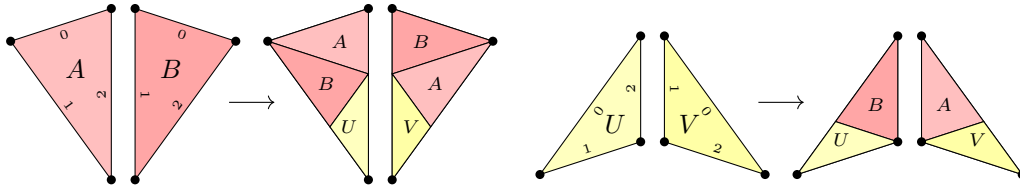


Figure 1: Substitution system for Penrose P2 tiling using Robinson triangles

to which under deflation. Lengths, angles and position in the plane are not required. Therefore, *calculation* in real or complex numbers is also not required: all these algorithms are discrete in character, manipulating strings or sequences of elements from small finite sets.

We shall present small examples first, and work up to the full description of a combinatorial substitution system at the end of the section.

Section 2.7 describes a geometric representation of the tiling from which the combinatorial details can conveniently be generated. This geometric representation is not used directly by any of the algorithms, although the proofs that the algorithms work will depend on the combinatorial data corresponding to some geometric tiling.

## 2.1 Constraints

The term ‘substitution system’, or ‘substitution tiling’, has both general and specific usages.

In a general sense, a ‘substitution system’ might be any set of rules that transforms one family of tiles (or perhaps other objects) systematically into another. An example in this general sense might be a dissection of a single polygon into multiple polygons similar to itself, but of different sizes. Iterating this substitution leads to the number of differently sized polygons growing without bound. One might also choose to iterate the substitution a different number of times for each sub-polygon, e.g. continuing to substitute polygons as long as they exceed some threshold size.

Here, we are concerned with the more specific usage of ‘substitution system’ that applies to aperiodic tilings. For the purposes of this article, we expect a substitution system to meet some more stringent constraints:

**Every tile is substituted the same number of times.** We only consider systems in which an entire tiling of the plane is transformed into an entire new tiling, by applying the substitution rules to every tile exactly once. That transformation can be iterated, so that each tile goes through substitution  $n$  times, but we still expect that every tile has been substituted the same number of times.

**Finitely many tile types up to congruence.** We consider systems with a finite set of ‘prototiles’ (reference subsets of the plane) fixed in advance, so that no matter how many times the substitution rules are applied, every tile remains congruent (not merely similar) to one of those prototiles. The example above violates this assumption because of the unbounded set of different sizes of tile.

**Deflation makes more tiles.** We expect that after applying the substitution system to a whole tiling to create a deflated tiling, the total number of tiles is increased. This need not be true for a single tile in a single deflation, but it must be true that as  $n \rightarrow \infty$ , the total number of tiles in the  $n$ -times deflation of any starting tile increases without bound.

For example, there exists a substitution system that interchanges between the Penrose P2 and P3 tilings in each deflation, with the property that each P2 kite turns into just one P3 thick rhomb. But in the next deflation that P3 rhomb turns into two P2 tiles (a kite and a dart), and that number grows further as you iterate more times.

## 2.2 Sub-tiles, sub-edges, and adjacency map

As an initial example, we shall use a substitution system for the Penrose P2 tiling, in which the usual ‘kite’ and ‘dart’ tiles are each subdivided into two isosceles *Robinson triangles* [Rob75]. During deflation, each triangle is subdivided into either 2 or 3 smaller triangles, according to the rules shown in figure 1.

To describe this substitution system combinatorially, one says that there are four *types* of tile, here referred to as  $A, B, U, V$ . For each tile we index its edges, in an arbitrary manner: here, we adopt the convention (also shown in figure 1) that edges are indexed 0,1,2 in anticlockwise order around the triangle, with the base of each isosceles triangle having index 0.

During deflation, each *supertile* generates a number of *subtiles*; again we must assign each subtile an arbitrary index, and specify which tile type each subtile is. Indices can be anything you like as long as they are

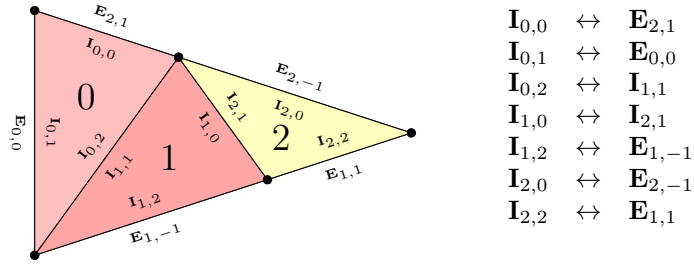


Figure 2: Adjacency map for the type- $A$  Robinson triangle

distinguishable. Here we shall keep things simple for a computer implementation, by using integers  $0, 1, 2, \dots$  for the subtiles of each tile.<sup>1</sup>

Next, we must specify how the tiles arising from deflation are arranged relative to each other, by providing an *adjacency map* for each supertile, listing pairs of subtile edges that meet in its deflation. For example, in the deflation of the  $A$  triangle, the adjacency map says that edge 0 of the subtile of type  $B$  and edge 1 of the subtile of type  $U$  are adjacent to each other.

Finally, we must describe how adjacency of supertiles is related to adjacency of subtiles. If that  $A$  supertile is deflated *twice*, so that its  $B$  and  $U$  subtiles each turn into two or three sub-subtiles, then the adjacency map for the  $B$  subtile shows how its three sub-subtiles are arranged relative to each other, and similarly for the  $U$ , but to lay out the full set of sub-subtiles of the original  $A$ , we must also know which sub-subtiles of the  $B$  are adjacent to which of the  $U$ .

To answer this, we also specify what happens to the edges of tiles during deflation. Each edge of a supertile is divided into a number of *sub-edges*, and we specify how many sub-edges arise from each edge. For example, when deflating the  $B$  tile, edges 1 and 2 are each divided into two sub-edges, and edge 0 is not divided at all, generating only a single (trivial) sub-edge.

When the edges of two supertiles meet, their sub-edges must match up, in reversed order. For this reason it is convenient to index sub-edges in a way that is symmetric about 0, so that sub-edge  $i$  of one supertile meets sub-edge  $-i$  of the other. So when an edge is divided into  $n$  sub-edges, we assign them indices  $-n + 1, -n + 3, \dots, n - 3, n - 1$ .<sup>2</sup> In this example, every edge either has a single sub-edge with index 0, or two sub-edges with indices  $-1, +1$ .

Finally, we extend the adjacency map for each supertile so that it also lists edge pairs consisting of one edge of a sub-tile, and one sub-edge of a supertile edge. Formally, we use a symbol of the form  $\mathbf{I}_{i,j}$  to denote edge  $j$  of sub-tile  $i$  of the supertile, and  $\mathbf{E}_{u,v}$  to denote sub-edge  $v$  of edge  $u$  of the supertile (connoting ‘interior’ and ‘exterior’ edges respectively). Then the adjacency map specifies an involution on the set of all of these symbols, with no fixed point.

Figure 2 shows an example: the full adjacency map for the deflation of a triangle of type  $A$ , and the geometric diagram it is derived from. The other adjacency maps are calculated similarly. The full set can be found in Figure 22.

### 2.3 Spurs

As a second example, we show an alternative substitution system for the Penrose P2 tiling, this one based on whole kites and darts rather than Robinson triangles. This system can be derived from the previous one by first merging the deflation diagrams of the  $A$  and  $B$  triangles to obtain the deflation of a whole kite, and similarly merging the  $U$  and  $V$  diagrams to deflate a whole dart. After this, every  $A$  and  $B$  sub-tile in either deflation diagram appears next to its counterpart, so we merge those into whole kites, obtaining a deflation of a kite and a dart into kites,  $U$  triangles, and  $V$  triangles. Finally, we replace each  $U$  triangle with a whole dart sticking out past the edge of the supertile’s outline, and to compensate, we remove the  $V$  triangles completely. (As if  $U$  had bulged along the line connecting it to  $V$ , and  $V$  had shrunk correspondingly, until  $U$  had occupied all of the dart and  $V$  had reached zero size.)

The resulting substitution system is shown in figure 3. In this system, the deflation of a tile no longer occupies precisely the same geometric space as the original tile. Some supertile edges, under deflation, become

<sup>1</sup>This Robinson triangle system, and the corresponding one for the Penrose P3 tiling, both have the convenient property that no two subtiles of the same tile have the same type. As a result, you don’t really need a subtile index at all: you could reuse the subtile’s type as its index. But this property is rare and we shall not depend on it.

<sup>2</sup>Indexing the sub-edges in the more obvious fashion, from 0 at one end, is also possible, but less convenient. In this representation, sub-edge  $i$  of one supertile meets sub-edge  $n - 1 - i$  of the other, so every time an algorithm needs to compute one of those indices from the other, it must look up the value of  $n$  based on the tile type and edge index in question. The symmetric indexing approach allows this common query to be performed by simply negating  $i$ , with no auxiliary table lookup.

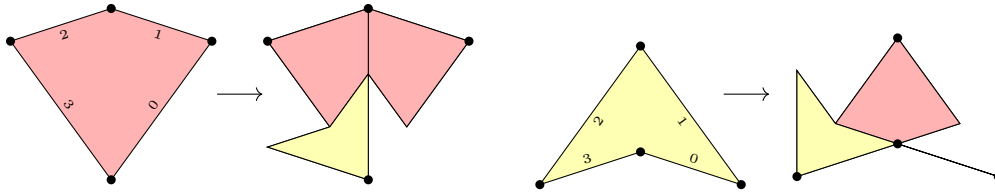


Figure 3: Substitution system for Penrose P2 whole tiles

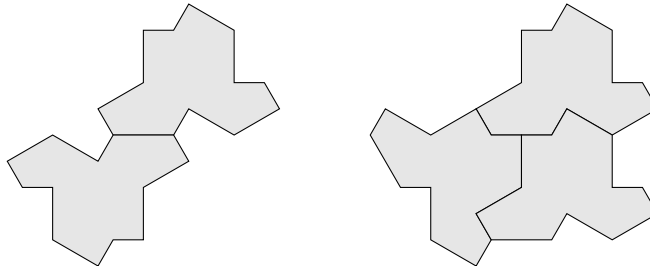


Figure 4: The long edge of a hat monotile can meet one hat or two

crooked paths of three sub-edges with angles between them. However, the system is still consistent: any two edges which can appear next to each other in a full Penrose tiling of the plane have matching shapes in their deflations. For example, when two kites meet along a long edge, sharing their apex, their deflations fit too, because the protrusion from one of the long edges fits exactly into the hole in the other.

The new feature in this system is a *zero-thickness spur*, sticking out from the right of the dart's deflation, running along a former edge of the vanished  $V$  triangle. This spur is invisible in the final deflated tiling: it protrudes from one supertile's deflation between the deflation of two others, and contributes no subtiles to the output. But for the purposes of the algorithms presented here, a spur such as this cannot be disregarded completely, because the deflation of edge 1 of a dart must still have the same number of sub-edges as that of any edge it can meet (such as edge 2 of a dart, or edge 3 of a kite), so that every sub-edge has its counterpart in the other supertile.

We represent this in the combinatorial description of the tiling by allowing the adjacency map to contain entries which pair up two *exterior* edges (symbols of type  $\mathbf{E}_{u,v}$ ), along with the entries already seen which pair up two interior edges, or one interior to one exterior edge. For example, in this diagram, the 'upper' side of the spur is the first of three sub-edges of the dart's edge 1. Since those three sub-edges are indexed symmetrically as  $-2, 0, +2$ , the spur sub-edge will be  $\mathbf{E}_{1,-2}$  in our notation. The 'lower' side of the spur is the single sub-edge of the dart's edge 0. So the adjacency map for the dart will contain an entry pairing up  $\mathbf{E}_{1,-2} \leftrightarrow \mathbf{E}_{0,0}$ . The full adjacency maps for this system, including this pairing of two external edges, can be seen in Figure 28.

## 2.4 Edges are not always polygon edges

A background assumption made by this representation of a tiling is that, whenever two tiles  $t, u$  are adjacent in the tiling, they meet 'edge to edge': along the shared boundary, vertices of  $t$  correspond exactly to vertices of  $u$ , and each edge of tile  $t$  on the boundary meets the whole of a single edge of tile  $u$ . If this were not true, the adjacency map described in previous sections could not be written down in the form of a one-to-one mapping, because some edge  $\mathbf{I}_{t,k}$  would not meet another single edge, but might instead meet two or more other edges, or *parts* of two other edges.

If 'edge' is taken to mean an edge of a polygon in the usual sense – a maximal straight segment of the shape's boundary – then this property is not always satisfied. The hat monotile [SMKGS24a], regarded as a polygon, has 13 edges, consisting of six of length 1, six of length  $\sqrt{3}$ , and one of length 2. When it tiles the plane, the length-2 edge of the hat sometimes meets the length-2 edge of a neighbouring hat, but more often meets length-1 edges of two different hats, so that the midpoint of the length-2 edge is a point where three tiles meet. Figure 4 shows both of these possibilities.

Fortunately, the solution is simple. For the purposes of describing a tiling in this combinatorial form, we regard the length-2 edge of the hat as two separate length-1 edges with a vertex in between them, so that the hat has 14 vertices and 14 edges, and it so happens that two consecutive edges are collinear.

In general, for the purposes of a combinatorial description of this kind, one chooses how to divide the boundary of each tile into 'edges' by placing a vertex at any point on the boundary where it is possible for two other tiles to meet, and then propagating those vertices transitively to other tiles by placing a vertex anywhere that a neighbouring tile's vertex can appear. Once this procedure has iterated to closure, the edges can be

taken to be maximal segments of each tile’s boundary not containing a vertex. (Additional vertices can be placed if desired for any other reason.)

## 2.5 Layers

Some substitution tilings use an auxiliary system of ‘metatiles’, which do not appear in the final tiling of the plane. One way to generate the hat tiling [SMKGS24a] uses a system of metatiles labelled  $H, T, P, F$ , with a set of substitution rules to deflate metatiles into other metatiles, and another set to deflate metatiles into hats. So one can generate a large patch of hat tiles by starting with a single metatyle, say  $H$ ; deflating it to a larger and larger patch of smaller sub-metatiles, for as many iterations as desired; and finally applying the other set of substitution rules just once, to turn each of the smallest sub-sub- $\dots$ -sub-metatiles into a small number of actual hats.

To express a tiling of this type, we introduce the concept of a *layer*, defining a subset of the tiles involved in the entire substitution system. Each complete tiling of the plane, between deflations, contains tiles from only one layer. For example, in the  $HTPF$  hat system, there are two layers: a ‘hats’ layer containing the hat and its reflection, and a ‘metatiles’ layer containing the  $H, T, P, F$  metatiles.

To define the relationship between layers, we say that the final tiling of the plane we are trying to generate is the *base layer* of the system. Then, for each layer  $L$ , we specify a *parent layer*  $P$ , containing whatever set of supertiles deflate to the tiles in  $L$ . For example, in the  $HTPF$  system, the parent of the ‘hats’ layer is the ‘metatiles’ layer, and the parent of the ‘metatiles’ layer is *also* the ‘metatiles’ layer.

These parenthood relationships inductively define a sequence of higher- and higher-order layers, indexed by  $\mathbb{N}_0$ : we define the 0th layer to be the base layer, and the  $(n + 1)$ th layer to be the parent of the  $n$ th. In general this sequence will be eventually periodic: with a finite number of layers, a layer must be repeated, and then the same sequence of parents appears for ever.

However, the period can be greater than 1: the layer structure of a substitution system need not terminate in a layer which is its own parent. An example, already mentioned in section 2.1, is that the Penrose P2 tiling (kites and darts) can be deflated to the P3 tiling (thin and thick rhombs), and *vice versa*, creating a two-layer substitution system in which each layer’s parent is the other layer, and each deflation swaps between a P2 and P3 tiling of the plane. (Some details of this are given in [de 81a].)

## 2.6 Complete description of a combinatorial system

To summarise, here is the full set of information required to describe a tiling substitution system in the combinatorial manner described here.

- **Tiles.** List the tile types that exist. For each one, state how many edges it has.
- **Layers.** List the layers that exist. For each one, identify its parent layer, and list the tile types that appear in it.
- **Deflations.** For each pair  $(L, P)$  of a layer  $L$  and its parent layer  $P$ , give information about how each tile type  $t$  in  $P$  deflates to tiles in  $L$ . Specifically:
  - **Number of sub-edges.** For each edge of  $t$ , state how many sub-edges it turns into during deflation from  $P \rightarrow L$ .
  - **Set of sub-tiles.** List the sub-tiles of  $t$  when deflated from  $P \rightarrow L$ . Assign each one a distinct index, and give its tile type.
  - **Adjacency map.** As described in section 2.2, give the adjacency map for the deflation of  $t$  from  $P \rightarrow L$ , mapping symbols of the forms  $\mathbf{I}_{t,e}$  and  $\mathbf{E}_{e,s}$  to each other in pairs.

## 2.7 Geometric ‘source code’

All the algorithms described in this article can work using only the combinatorial representation of a tiling described above. However, that representation is not convenient for data entry. For more complicated substitution systems, when tiles have many edges and deflation of a tile creates many sub-tiles, the adjacency maps can be large and unwieldy (see Figures 46 and 48 for examples!). Also, since so much information about tile shape and position is missing from the combinatorial data, there is very little chance to cross-check it automatically to catch human error.

In practice the author has generally found it more convenient to describe the tiling by its geometric details, and have a computer program calculate the combinatorial data from that. However, this is not *required*: if the data listed in section 2.6 can be obtained by some other means, that is just as acceptable.

To describe a tiling geometrically for conversion into this combinatorial form, we introduce the extra concept of classifying the tile edges into *edge types*. Any two tile edges that meet in a tiling must have the same type; any two edges that behave differently under deflation must have different types.

Edge types are often *directed*, by arbitrarily nominating one of their end points to be a ‘source’ and the other a ‘target’. This is required if any deflation of the edge is asymmetric, and introduces the extra constraint that when two edges of a directed type meet in the tiling, the direction must match as well as the type, with the target vertices of the two tiles’ edges coinciding. Alternatively, an edge type can be undirected, in which case all its deflations must be symmetric under  $180^\circ$  rotation, including types and directions of the sub-edges.

For each edge type, the geometric tiling description specifies a vector in  $\mathbb{R}^2$ , or (equivalently and more conveniently) a complex number. The description of each tile states the type and direction of every edge, and a rotation of that edge relative to its reference orientation. Finally, for each deflation from layer  $P \rightarrow L$ , the description specifies not just *how many* sub-edges each edge type deflates to, but what all their types and directions are, and by what angle each sub-edge is rotated relative to the original edge.

This is enough information to determine the precise geometric outline of the deflation of a tile  $t$  from layer  $P \rightarrow L$ : for each edge of  $t$ , look up its sequence of sub-edges, and concatenate those sequences, each transformed by the same rotation that was specified for that edge of the original tile.<sup>3</sup> In particular, this makes it possible to automatically identify pairs of edges in the deflated tile outline which retrace each other to form the zero-thickness spurs described in section 2.3.

After discounting those spurs, the remaining outline of the tile deflation encloses a region of the plane which must be filled with sub-tiles from the layer  $L$ . Each tile can be placed by specifying just one entry from the adjacency map. For example, one might place the first sub-tile, with index  $t$ , by saying that its edge  $\mathbf{I}_{t,i}$  matches some  $\mathbf{E}_{u,v}$  identifying a boundary edge. That is enough information to locate the tile in the plane, and any other pairs of matching edges can then be detected automatically. Each further sub-tile is placed similarly, either adjacent to another boundary edge, or adjacent to an edge of an already placed sub-tile.

A full example of this process is shown in a later section. Figure 50 shows the six tiles involved in the *HTPF* system for the hat tiling (the four metatiles, and the two handednesses of hat), with the metatiles using five distinct edge types and the hats two. Figures 51 and 52 show the edge deflation rules for the processes of deflating the metatiles into more metatiles, or to hats, respectively. Finally, Figures 53 and 54 show the result of deflating each tile’s outline according to each set of those rules, and the correct tiling of the interior of the patch with metatiles or hats respectively. (The edge types and directions are not shown, but if they were, the edge types in the patch outlines would correctly match those of the subtiles filling them.) Several of these diagrams show zero-thickness spurs, such as the one in the top left of the  $H \rightarrow H$  deflation which matches  $\mathbf{E}_{2,4} \leftrightarrow \mathbf{E}_{3,-2}$ .

This geometric representation is more convenient for data entry than specifying the full combinatorial adjacency data directly. The user need only specify one entry of the adjacency map per sub-tile, and all the others are calculated automatically, by finding pairs of edges sharing both endpoints<sup>4</sup>, and matching up each edge from  $u \rightarrow v$  with one from  $v \rightarrow u$ .

Moreover, the system of edge types permits a large amount of automatic cross-checking: *every* entry in the adjacency map, whether manually specified or automatically calculated, can be checked to ensure it really does match two edges of the same type and direction. For this reason, it is usually convenient to treat the geometric representation as ‘source code’ – a concise high-level description entered manually by a human – and generate the combinatorial representation by a process strongly analogous to software compilation, in that it first performs a thorough check for type mismatches and other inconsistencies, and then generates all the low-level details that were too tedious to write by hand.

Of course, one other advantage of specifying the geometric shapes of the tiles is that *after* the algorithms in this article have been used to determine the structure of a patch of tiling, the geometric information can be reused to draw the tiling as output!

## 2.8 Addresses of tiles and edges

In a plane tiling generated by a substitution system, we can assign to any tile an *address* [GS99] which gives its position within the combinatorial tile hierarchy.

If the original tiling  $\mathcal{T}_0$  is deflated from some tiling of supertiles  $\mathcal{T}_1$ , then one can imagine identifying a tile  $t_0 \in \mathcal{T}_0$  by (inductively) identifying its supertile  $t_1 \in \mathcal{T}_1$ , and stating which subtile of  $t_1$  is  $t_0$ . Our combinatorial data has assigned each of  $t_1$ ’s subtiles a distinct index. So this suggests it might only be necessary to specify that index, so that the full address of  $t_0$  consists of a sequence of indices: the index of  $t_0$  as a subtile of  $t_1$ , the index of  $t_1$  as a subtile of its supertile  $t_2$ , and so on.

<sup>3</sup>In some substitution systems, such as the one for the Spectre tiling given in section 7.3, a particular deflation  $P \rightarrow L$  can be *reflecting*, meaning that after constructing each deflated tile outline in this manner it is reflected before filling it with subtiles.

<sup>4</sup>It is possible to find that a deflation diagram includes a pair of points  $u, v$  such that there are *multiple* edges  $u \rightarrow v$ , making the adjacency map non-unique. Examples of this are shown in Figures 43 and 48. In this situation one expects the same number of edges from  $u \rightarrow v$  as there are from  $v \rightarrow u$ , and then pairs them up arbitrarily. The different choices will only affect questions that do not change the output tiles, such as which side of one zero-thickness spur another one is considered to lie.

However, this is not necessarily enough information to even identify the *type* of the original tile  $t_0$ . For example, in the system of Penrose tiles shown in figure 3, suppose the subtiles are indexed so that subtile 1 of a kite is one of the sub-kites, and subtile 1 of a dart is the sub-dart. Then the index sequence  $1, 1, 1, \dots$  could represent a kite all of whose supertiles are kites, *or* a dart all of whose supertiles are darts. An ambiguous sequence of indices of this kind could potentially begin at any point in the sequence, even if the lower-order indices in the sequence were unambiguous.

Therefore, we must also specify the type of the starting tile and each of its supertiles. So the full address of a tile is a sequence of the form

$$t_0 \xleftarrow{i_1} t_1 \xleftarrow{i_2} t_2 \xleftarrow{i_3} t_3 \dots$$

in which the  $(t_n)$  are tile types, and the  $(i_n)$  are subtile indices. The notation  $t_{n-1} \xleftarrow{i_n} t_n$  means that the  $(n-1)$ th- and  $n$ th-order supertiles have types  $t_{n-1}$  and  $t_n$  respectively, and that the former is the  $(i_n)$ th subtile of the latter.

For a full tiling of the plane, the address is an infinite sequence, describing larger and larger supertiles without bound. In other situations one can also consider a *finitely* long address, which stops after specifying some particular supertile type  $t_n$ , and says nothing about what larger tiling (if any) that supertile might be part of.

We shall present algorithms to handle these addresses using finite state automata. We must therefore represent each address in the form of a sequence of symbols from a finite alphabet. The alphabet we choose consists mainly of symbols of the form  $(\xleftarrow{i} t)$ , where  $t$  is a tile type and  $i$  is one of its subtile indices in some deflation<sup>5</sup>. These symbols can represent every part of an address except for the initial tile type, for which we require a set of extra symbols specifying *only* a tile type. So every tile address starts with a bare tile type, followed by an infinite sequence of  $(\xleftarrow{i} t)$  symbols:

$$(t_0), (\xleftarrow{i_1} t_1), (\xleftarrow{i_2} t_2), (\xleftarrow{i_3} t_3), \dots$$

The main aim of our algorithms is to determine the address of a tile's neighbour from that of the tile itself. Therefore, we must have a way to specify *which* neighbour is desired. To place the two tiles relative to each other in the plane, we must also know how the neighbour is oriented relative to the initial tile. In other words, we want to specify a particular *edge* of the original tile  $t_0$ , and receive an answer telling us not only what type of tile is adjacent to  $t_0$  along that edge, but also which of its edges coincides with the edge we specified.

Therefore, we need another kind of address that specifies a particular edge of a tile. We modify the initial symbol so that instead of being a plain tile type, it is a pair  $(t, e)$ , indicating edge  $e$  of tile  $t$  according to whatever arbitrary indexing scheme we have assigned to our tile edges. So the address of a tile *edge* consists of one of these modified initial symbols, but thereafter, uses the same set of supertile symbols  $(\xleftarrow{i} t)$  as the address of a tile:

$$(t_0, e), (\xleftarrow{i_1} t_1), (\xleftarrow{i_2} t_2), (\xleftarrow{i_3} t_3), \dots$$

### 3 Relation to regular languages

We have described representations of the address of a tile, and the address of a tile edge, in terms of sequences of symbols from a finitely large alphabet. The aim was to calculate further addresses within the same tiling by string-processing techniques, rather than geometric ones.

The simplest type of string processing known to computer science is a finite state automaton. These are reliably fast, and easy to analyse and reason about. So if we can possibly use finite state automata to process tile addresses, it's worth a try.

Let  $\mathcal{E}$  denote the set of finite strings of symbols of the correct form to be the edge address of a tile within an  $n$ th-order supertile for some  $n$ . That is, strings of the form

$$(t_0, e), (\xleftarrow{i_1} t_1), (\xleftarrow{i_2} t_2), \dots, (\xleftarrow{i_n} t_n)$$

satisfying the necessary consistency criteria:  $e$  must be the index of an edge of tile type  $t_0$ , and each  $t_n$  must be the correct tile type to be subtile  $i_{n+1}$  of a tile of type  $t_{n+1}$ .

It is easy to see that  $\mathcal{E}$  is a regular language, because a DFA can be constructed for it trivially, consisting of a special START state and a state for every *(layer, tile type)* pair, with a transition between two states of the

<sup>5</sup> Which deflation? In a tiling with multiple layers, the meaning of a symbol  $(\xleftarrow{i} t)$  can vary depending on where in the address it appears. For example, in the *HTPF* hat system, if it appears as the first supertile symbol, it will describe one of the hats in the deflation from a metatile to the base hat layer, but if it appears any later, it will describe one of the *metatiles* in the deflation from metatiles to other metatiles. This does not cause a problem in the algorithms, because they can always keep track of what layer they are currently in, and disambiguate the meaning of each symbol.

latter type whenever the supertile type and subtile index in a symbol are consistent with the source state of the transition.

Similarly, let  $\mathcal{T}$  denote the language of strings giving the address of a tile rather than an edge, identical to  $\mathcal{E}$  except that the first symbol is a bare tile type  $t_0$  instead of a pair  $(t_0, e)$ . This too is regular, by the same reasoning.

Let  $\mathcal{T} \times \mathcal{T}$  denote the set of ordered pairs of two tile addresses of the same length, represented as a sequence of ordered pairs containing one symbol from each address, as if they had been combined by Python `zip`. That is, if  $(\sigma_0, \sigma_1, \dots, \sigma_n), (\sigma'_0, \sigma'_1, \dots, \sigma'_n) \in \mathcal{T}$ , then  $((\sigma_0, \sigma'_0), (\sigma_1, \sigma'_1), \dots, (\sigma_n, \sigma'_n)) \in \mathcal{T} \times \mathcal{T}$ . We define  $\mathcal{E} \times \mathcal{E}$  similarly.

Let the *neighbour language*  $\mathcal{N} \subset \mathcal{E} \times \mathcal{E}$  denote the set of pairs of edge addresses  $(A, A')$  which are neighbours within the  $n$ -times deflation of some common supertile. That is, the tiles identified by the two addresses are adjacent in the  $n$ th-order deflation of the supertile, and moreover, they meet along the edges specified by  $A$  and  $A'$ .

**Theorem 1.**  *$\mathcal{N}$  is a regular language.*

*Proof.* We begin by showing this for a restricted class of substitution systems: those in which the deflation of each tile type can be scaled to occupy the same region of the plane as the original tile, with no zero-thickness spurs or geometric distortion. An example is the Robinson-triangle system for the P2 tiling, shown in Figure 1.

If a substitution system has this property under a single deflation, then it has it under any finite number of deflations. So if two tiles  $t, u$  are adjacent within the deflation of an order- $n$  supertile, then for every  $0 < i < n$ , either their order- $i$  supertiles coincide, or are themselves adjacent along a whole edge, with the edge separating  $t, u$  being part of that longer supertile edge.

Therefore, as we ascend from the tiles  $(t, u)$  to their supertiles  $(t_1, u_1), \dots, (t_n, u_n)$ , each pair of supertiles is adjacent, until the first pair that coincide. After that, all further supertile pairs coincide.

This allows us to directly construct a state machine which matches  $\mathcal{N}$ . For the initial segment of a string before two supertiles coincide, each state  $S(L, t, u, e, f)$  describes a layer  $L$  of the system; a pair of tile types  $t, u$  within that layer; and a pair of edge indices  $e, f$  of those tiles, indicating their adjacency: edge  $e$  of tile  $t$  meets edge  $f$  of tile  $u$ .

Transitions can be determined using the adjacency maps, such as the one shown in Figure 2. In a state  $S(L, t, u, e, f)$ , if there exist tile types  $t', u'$  in  $L$ 's parent layer  $P$ , and indices  $i, j, k, e', f'$  such that

- subtile  $i$  of tile type  $t'$  (when deflated from  $P \rightarrow L$ ) is type  $t$
- subtile  $j$  of tile type  $u'$ , similarly, is type  $u$
- the adjacency map for deflating tile  $t'$  maps  $\mathbf{I}_{i,e} \leftrightarrow \mathbf{E}_{e',k}$
- the adjacency map for deflating tile  $u'$  maps  $\mathbf{I}_{j,f} \leftrightarrow \mathbf{E}_{f',-k}$

then this is saying that  $t, u$  occupy compatible positions along the boundaries of two edges of  $t', u'$ , such that if edge  $e'$  of  $t'$  meets edge  $f'$  of  $u'$ , then their subtiles would meet in the way described by the original state  $S(L, t, u, e, f)$ . Hence, a transition exists from  $S(L, t, u, e, f) \rightarrow S(P, t', u', e', f')$ , on a symbol pair  $\left( \left( \overset{i}{\leftarrow} t' \right), \left( \overset{j}{\leftarrow} u' \right) \right)$ .

At the point where the supertiles of  $t, u$  coincide, we enter a second family of states, describing a single tile in a particular layer, say  $A(L, t)$ . These are the accepting states of our automaton. The first transition into an accepting state occurs when subtiles  $i, j$  of a supertile type  $s$  match the types  $t, u$  from an existing state, and those subtiles meet internally to the supertile's deflation, along the correct edges. That is, if  $s$ 's adjacency map includes the entry  $\mathbf{I}_{i,e} \leftrightarrow \mathbf{I}_{j,f}$ , then a transition exists from  $S(L, t, u, e, f) \rightarrow A(P, s)$  on the symbol pair  $\left( \left( \overset{i}{\leftarrow} s \right), \left( \overset{j}{\leftarrow} s \right) \right)$ . Thereafter, transitions between accepting states require both symbols in the pair to be identical, and to continue to spell out a valid tile address, exactly as in the natural DFA matching  $\mathcal{T}$ .

Now we must extend this construction to more general substitution systems: those in which tile edges deflate to non-straight outlines, and especially those with zero-thickness spurs. In these systems, it need not be true that two tiles  $t, u$  sharing an edge have supertiles  $t', u'$  also sharing an edge.

In systems meeting the constraints described in section 2.1, iterating the geometric deflation process and re-scaling each deflated tile shape to the same overall area as the original tile causes the tile outlines to converge to a fractal. An example, based on the P2 whole-tile substitution system in Figure 3, is shown in Figure 5. Transforming the substitution system into this form, with every tile having a fractal outline and every tile edge being a fragment of that outline, restores the property that the deflation of a tile occupies the same plane region as the tile itself. Hence, when two tiles are adjacent along a segment of their outline, their two supertiles must also be: see Figure 6 for an example case. So we can still construct a set of automaton states based on two tiles sharing a segment of boundary.

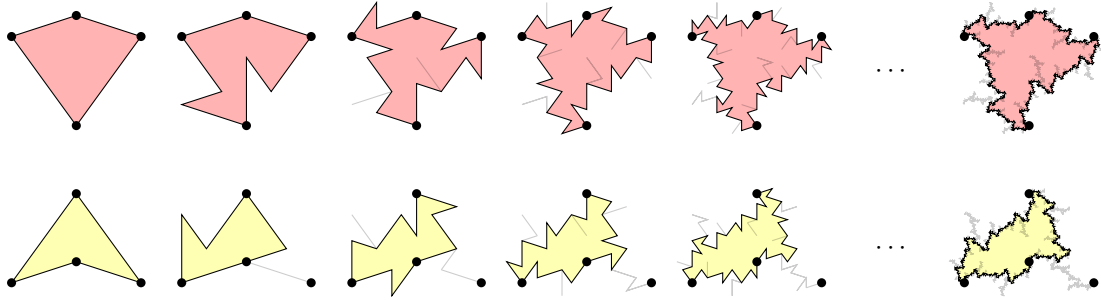


Figure 5: Converging to fractal tile outlines for the P2 whole-tiles system

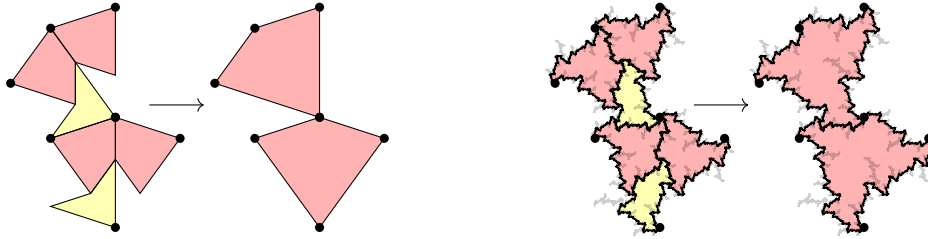


Figure 6: Adjacent tiles may not have adjacent supertiles, but the fractal versions do

We must also show that there are *finitely* many such states, which is no longer obvious when all we know is that two tiles share *some segment of boundary* instead of one of a discrete set of edges.

To see this, we observe that the fractal tile shapes are bounded. In a tiling of the plane using tiles from some particular layer, there are only finitely many ways to tile a disc of radius  $r$  with a given tile  $t$  at a fixed location in the centre, and the fractal forms of those patches exhibit all the ways that the fractal outline of tile  $t$  can be adjacent to that of any other tile. No other forms of adjacency need be considered, because even if two fractal tile outlines  $t, u$  physically fit together in some other way, that adjacency cannot occur between a pair of supertiles within the context of a legal tile address, since any such pair of supertiles form part of a tiling of the whole plane.  $\square$

Calculating the fractal tile shapes and their adjacencies is potentially awkward. We shall show a further useful property of  $\mathcal{N}$ , which we shall use in the next section to derive an easier, purely combinatorial algorithm for finding a recogniser for  $\mathcal{N}$ .

The extra property relates to *reversibility*. A DFA that recognises a regular language  $L$  can always be turned into a recogniser for the language  $L^R$  consisting of the reversal of every string of  $L$ , by simply reversing all the arrows in the state transition diagram and interchanging the starting and accepting states. Usually the reversed recogniser is no longer deterministic, and must be determinised again if a DFA for  $L^R$  is desired. [Ang82] defines the concept of a *zero-reversible acceptor* to be a DFA for a language  $L$  which remains deterministic under this reversal<sup>6</sup>, because there is a unique accepting state, and no two distinct states have transitions to the same state on the same symbol. A *zero-reversible language* is one that admits a zero-reversible acceptor.

Our neighbour language  $\mathcal{N}$  cannot in general be zero-reversible, because it has an accepting state for every supertile type, i.e. usually more than one. However, it can be written as the disjoint union of zero-reversible languages in a natural way.

We define the sublanguage  $\mathcal{N}(L, t) \subset \mathcal{N}$  to be the set of edge address pairs which represent adjacent tiles whose highest-order supertiles *not* shared are in layer  $L$  of the substitution system, and their lowest-order shared supertile is a tile of type  $t$  in layer  $P$ , the parent of  $L$ . Sublanguages of the form  $\mathcal{N}(L, t)$  are pairwise disjoint, and partition  $\mathcal{N}$ .

**Theorem 2.**  $\mathcal{N}(L, t)$  is zero-reversible.

*Proof.* From the proof of Theorem 1, we can directly construct a DFA for  $\mathcal{N}$  in which each non-accepting state describes two tiles  $s, s'$  in layer  $L$  adjacent along subsets  $b, b'$  of their boundary. (In a system with spurs, these boundary subsets may not correspond to single edges of the original tiles, but nonetheless, there will be a finite set of possible boundary subsets that  $s, s'$  can legally share.) Accepting states describe a single tile  $s$  in layer  $L$ . We denote these types of state as  $S(L, s, b, s', b')$  and  $A(L, s)$  respectively.

<sup>6</sup>Why ‘zero-reversible’ and not just ‘reversible’? [Ang82] defines the weaker condition of  $k$ -reversibility to mean that the reversed automaton need not be deterministic already, but if multiple transitions on the same symbol are available then  $k$  extra symbols of lookahead suffice to rule out all but one of them. ‘Reversible’ by itself is used to mean ‘ $k$ -reversible for some  $k \geq 0$ ’.

We consider  $b, b'$  to be the maximal subsets of each tile's boundary shared with the other's. In some substitution systems, the geometry of two tiles means that if they are adjacent along some pair of edges  $e, e'$  then they are also adjacent along another edge pair  $f, f'$ . For these purposes we regard  $b, b'$  as being the union of both of those edges, and any further edges the two tiles might share. Thus, we do not consider  $S(L, s, e, s', e')$  and  $S(L, s, f, s', f')$  to be distinct DFA states.

A DFA for  $\mathcal{N}(L, t)$  can be constructed from the DFA for  $\mathcal{N}$  itself by removing all the accepting states except for  $A(P, t)$ , and giving that state no outgoing transitions, so that the two input tile addresses must specify just enough symbols to reach the first shared supertile.

This DFA has a unique accepting state, by construction: we made it by deleting all the other accepting states. So we only need to show that no state has two distinct predecessors with transitions to it on the same symbol.

A transition to the accepting state is of the form  $S(L, s, b, s', b') \rightarrow A(P, t)$ , on the symbol  $\left(\left(\overset{i}{\leftarrow} t\right), \left(\overset{i'}{\leftarrow} t\right)\right)$ . Such a transition is only valid if subtiles  $i$  and  $i'$  of  $t$  have types  $s, s'$  respectively. Then subtiles  $i, i'$  of  $t$  have a fixed geometric relationship, and there is only one maximal pair of boundary segments  $b, b'$  along which they can meet. So  $A(P, t)$  has at most one predecessor for any symbol.

Similarly, consider a transition between two non-accepting states  $S(M, s, b, s', b') \rightarrow S(Q, t, c, t', c')$  (where  $Q$  is the parent layer of  $M$ ) on the symbol  $\left(\left(\overset{i}{\leftarrow} t\right), \left(\overset{i'}{\leftarrow} t'\right)\right)$ . Again,  $s$  is constrained to be the tile type of subtile  $i$  of  $u$ , and  $s'$  similarly; and placing the fractal tile shapes of  $t, t'$  next to each other along boundary segments  $c, c'$  fixes their relative position in the plane, and leaves only one possibility for which segments  $b, b'$  of those subtiles can meet.  $\square$

## 4 Algorithms for handling addresses

In the previous section we showed that the combinatorics of a tiling can be handled by finite state automata. In this section we present concrete algorithms for constructing two different forms of automaton. The ultimate aim is to create a deterministic finite-state transducer which takes a tile edge address as input, and produces its neighbour edge address as output.

### 4.1 Computing neighbours recursively

We first present a recursive algorithm to calculate the neighbour of a tile. For some applications, this recursive algorithm is adequate by itself to generate patches of tiling. It is also used to generate the input to the algorithm in section 4.2.1.

As input, this algorithm requires a combinatorial tiling description, and the address of a specific tile edge, in the form shown in section 2.8:

$$(t_0, e), \left(\overset{i_1}{\leftarrow} t_1\right), \left(\overset{i_2}{\leftarrow} t_2\right), \left(\overset{i_3}{\leftarrow} t_3\right), \dots$$

It computes and returns an address in the same form, describing the neighbour of the input tile along that edge, and which edge of it meets  $e$ .

The algorithm begins by inspecting the deflation diagram of tile  $t_1$ , one of whose tiles is  $t_0$ . The tiling description provides an adjacency map describing this deflation diagram. In that map, the symbol  $\mathbf{I}_{i_1, e}$  describes edge  $e$  of the subtile with index  $i_1$  – that is, exactly the edge we have been asked about. So the first step is to look up that symbol in the map, to see what it is paired with.

In the simple case, the result of that lookup is another interior symbol, i.e. one of the form  $\mathbf{I}_{i'_1, e'}$ . This means that the sub-tile adjacent to the starting one is another sub-tile of the same supertile  $t_1$ . So the algorithm need only replace the two low-order symbols of the input address, by looking up the tile type  $t'_0$  of the new sub-tile, and returning the modified address

$$(t'_0, e'), \left(\overset{i'_1}{\leftarrow} t_1\right), \left(\overset{i_2}{\leftarrow} t_2\right), \left(\overset{i_3}{\leftarrow} t_3\right), \dots$$

In the more complicated case,  $\mathbf{I}_{i_1, e}$  turns out to be paired with an exterior edge  $\mathbf{E}_{u, v}$ , so that edge  $e$  of the input tile  $t_0$  is part of the boundary of its supertile  $t_1$ . In that case, we must find the neighbouring *supertile* of  $t_1$  – we'll call that  $t'_1$  – and decide which subtile of that is the answer to the original query.

To find the neighbour of  $t_1$ , we invoke this entire algorithm a second time, recursively. The input address is formed by removing the two low-order symbols from our original input, and replacing them with a symbol describing the supertile  $t_1$ , and in particular the edge of it that contains our original query edge. The adjacency

---

**Algorithm 1** Recursively compute the neighbour of an edge address

---

```

let  $(t_0, e), (\overset{i_1}{\leftarrow} t_1), \text{address-tail} = \text{input-address};$ 
lookup-result  $\leftarrow$  look up  $\mathbf{I}_{i_1, e}$  in adjacency map for  $t_1$ ;
while lookup-result is of the form  $\mathbf{E}_{u, v}$  do
  let  $\text{supertile-address} = (t_1, u), \text{address-tail};$ 
  recurse to find  $(t'_1, u'), \text{new-address-tail} = \text{neighbour of } \text{supertile-address};$ 
  lookup-result  $\leftarrow$  look up  $\mathbf{E}_{u', -v}$  in adjacency map for  $t'_1$ ;
  replace  $(t_1, \text{address-tail}) \leftarrow (t'_1, \text{new-address-tail});$ 
end while
now expect that lookup-result is of the form  $\mathbf{I}_{i'_1, e'}$ ;
let  $t'_0 = \text{type of subtile } i'_1 \text{ of } t_1;$ 
return  $(t'_0, e'), (i'_1, t_1), \text{address-tail};$ 

```

---

map lookup result  $\mathbf{E}_{u, v}$  says that the original query edge is part of edge  $u$  of  $t_1$ , in particular sub-edge  $v$  of it. So we must find out what supertile borders on edge  $u$  of  $t_1$ , and therefore we recursively query the address

$$(t_1, u), (\overset{i_2}{\leftarrow} t_2), (\overset{i_3}{\leftarrow} t_3), (\overset{i_4}{\leftarrow} t_4), \dots$$

We also slightly modify the tiling description provided to the recursive call, by changing its base layer to be the one containing  $t_1$ , i.e. the parent of the original base layer.

The recursive invocation of the algorithm returns the full address of an edge of another tile in the parent layer:

$$(t'_1, u'), (\overset{i'_2}{\leftarrow} t'_2), (\overset{i'_3}{\leftarrow} t'_3), (\overset{i'_4}{\leftarrow} t'_4), \dots$$

So we know that edge  $u'$  of this supertile borders on edge  $u$  of the original supertile. The smaller tile edge we really wanted to know about was not the whole of edge  $u$ , but sub-edge  $v$  of it. This meets sub-edge  $-v$  of the new supertile's edge (as discussed in section 2.2). So to determine what sub-tile of  $t'_1$  we need, we look up the symbol  $\mathbf{E}_{u', -v}$  in the adjacency map for  $t'_1$ .

If this lookup in the adjacency map returns an interior symbol  $\mathbf{I}_{i'_1, e'}$ , then we can terminate the algorithm by adding those details to the address returned from the recursive call. Find out the tile type  $t'_0$  of subtile  $i'_1$  of  $t'_1$ , and return

$$(t'_0, e'), (\overset{i'_1}{\leftarrow} t'_1), (\overset{i'_2}{\leftarrow} t'_2), (\overset{i'_3}{\leftarrow} t'_3), \dots$$

There is one remaining possibility. After a recursive call, the lookup of  $\mathbf{E}_{u', -v}$  in the new supertile's adjacency map might return *another* exterior symbol. This occurs when the algorithm encounters one of the zero-thickness spurs described in section 2.3. We have tried to step in to the deflation of tile  $t'_1$ , and found that we've landed on a zero-thickness spur, not a real tile – so we must step straight off the other side of the spur to find out what real tile lies beyond it.

In this situation, the algorithm does the same thing it would have done if the *original* lookup had returned an exterior symbol. It makes another recursive call to compute the neighbour  $t''_1$  of  $t'_1$ , and loops round again, until it reaches a supertile  $t_1^{(k)}$  in which the adjacency map lookup finally returns an interior symbol.

A summary of this algorithm, in pseudocode, is shown as Algorithm 1.

## 4.2 Computing neighbours using a transducer

The recursive algorithm described above is adequate for some purposes, but in complicated substitution systems it has to recurse repeatedly up and down its input string rewriting symbols, which makes it slower, and also difficult to reason about. Moreover, Section 5 will describe a class of tiling instances it cannot handle at all.

A finite-state transducer is a better way to calculate neighbour addresses, if one can be constructed. In this section we present algorithms to do so.

### 4.2.1 Recogniser for neighbour edge pairs

In section 3 we showed that the neighbour language  $\mathcal{N}$ , consisting of all zipped-together pairs of tile edge addresses of the same finite length describing two tiles sharing an edge, is a regular language. Our first step is to construct a DFA to recognise  $\mathcal{N}$ .

One way to construct this DFA would be to follow the structure of the proof of Theorem 1: make a state for every possible adjacent pair of tiles or their fractalizations, together with START and the required accepting states, and fill in the transitions by considering the geometry of the tiles.

---

**Algorithm 2** Build a DFA for neighbouring edge address pairs

---

```
make an empty automaton with just a START state;
add all accepting states  $A(L, t)$  and their transitions;
done  $\leftarrow \emptyset$ ; ▷ set of edge address prefixes already processed
for  $k$  in  $1, 2, \dots$  do ▷ length of strings in input corpus
  for  $A_1$  in edge addresses of length  $k$  with no prefix in done do
    let  $A_2 =$  neighbour of  $A_1$  according to Algorithm 1;
    if Algorithm 1 did not fail by overrunning the end of  $A_1$  then
      call ADDSTRING(automaton, zip( $A_1, A_2$ )); ▷ see Algorithm 3
      done  $\leftarrow$  done  $\cup \{A_1\}$ ;
    end if
  end for
call MERGESTATES(automaton); ▷ see Algorithm 4
return if ISCOMPLETE(automaton); ▷ see Algorithm 5
end for
```

---

---

**Algorithm 3** Subroutine to add new states to an NFA to make it recognise one extra string, labelling the states with layers of the substitution system

---

```
procedure ADDSTRING(automaton, string) ▷ each  $p_i$  is a symbol pair
  let  $(p_1, p_2, \dots, p_k) =$  string;
  add states  $s_1, \dots, s_{k-1}$  to automaton;
  set layer( $s_1$ ) = parent( $B$ ), layer( $s_{i+1}$ ) = parent(layer( $s_i$ ));
  let  $L =$  layer( $s_{k-1}$ ),  $t =$  tile type specified in both symbols of  $p_k$ ;
  add transitions START  $\xrightarrow{p_1}$   $s_1 \xrightarrow{p_2}$   $\dots \xrightarrow{p_{k-1}}$   $s_{k-1} \xrightarrow{p_k}$   $A(L, t)$ ;
end procedure
```

---

However, using the geometry of the tiling complicates implementation (the coordinates may well involve algebraic numbers, requiring either elaborate exact computation or risky floating-point approximation), as well as requiring more information as input. In this section we instead present a purely combinatorial algorithm to construct the same DFA from only the data described in section 2.6, based on Theorem 2 which tells us that  $\mathcal{N}$  is the union of a set of zero-reversible languages.

In [Ang82] an algorithm is given to infer a DFA for a zero-reversible language from a finite corpus of strings of the language. Paraphrased, one first constructs an NFA consisting of a single START state, an ACCEPT state, and a separate path from START to ACCEPT for each string in the corpus. Then merge<sup>7</sup> any two states  $A, B$  which have transitions  $U \xrightarrow{s} A, U \xrightarrow{s} B$  from the same predecessor  $U$  on the same symbol  $s$ , and conversely, merge any two states with transitions to the same *successor* on the same symbol, i.e.  $A \xrightarrow{s} V, B \xrightarrow{s} V$  for some  $s, V$ . Iterate both of those merging operations to closure. The first policy guarantees to make the NFA deterministic; the second makes its reversal deterministic too, so that the resulting DFA is still a DFA if the arrows are reversed and START swapped with ACCEPT.

In the process, the DFA is transformed from one that matched *only* the strings in the finite input corpus into one that matches their ‘zero-reversible closure’, the smallest zero-reversible language containing the input corpus. For example, if the input corpus was  $\{abc, abdbc\}$ , then its zero-reversible closure would be the language  $ab(db)^*c$ , because the state reached via  $ab$  and the one reached via  $abdb$  have been merged, permitting any number of repetitions of  $db$  to cycle back to that state before finishing the string with a  $c$ .

The recursive algorithm in the previous section can be used to make a corpus of strings from  $\mathcal{N}$ , by feeding it every possible input string  $A$  up to some chosen length  $k$ , and if it successfully returns an output string  $B$  at all, adding zip( $A, B$ ) to the corpus. This algorithm can fail, by recursing so deeply that it finds itself needing to read a symbol from beyond the end of  $A$ . For this application, we must detect that error, and handle it by abandoning the attempt to determine the neighbour address of  $A$  and moving on to the next possibility.

Given a corpus of this kind, it is straightforward to classify each string into one of the sublanguages  $\mathcal{N}(L, t)$  described in section 3, partitioning the corpus into sub-corpuses. Each of these sub-corpuses is a sample from a zero-reversible language, so the state-merging algorithm described above can be used to make a DFA for it. Then those DFAs can be recombined into one with multiple accepting states.

Rather than literally separating the input corpus into subsets, it is simpler to build the whole combined DFA in one go, by making a single NFA with one START state and a full set of  $A(L, t)$  accepting states. Then, as before, create a separate path of states from START to an appropriate accepting state for each string of the

---

<sup>7</sup>The description in [Ang82] suggests constructing the initial DFA in the form of a trie, so that states with the same predecessor start off already merged. This is equivalent.

---

**Algorithm 4** Subroutine to merge states in an NFA, turning it into a DFA matching a union of zero-reversible languages

---

```

procedure MERGESTATES(automaton)
  repeat
    if  $\exists$  transitions  $A \xrightarrow{p} C, B \xrightarrow{p} C$  and  $\text{layer}(A) = \text{layer}(B)$  then
      merge states  $A, B$  and all their transitions;
    end if
    if  $\exists$  transitions  $A \xrightarrow{p} B, A \xrightarrow{p} C$  and  $\text{layer}(B) = \text{layer}(C)$  then
      merge states  $B, C$  and all their transitions;
    end if
  until neither type of merge is possible
end procedure

```

---

**Algorithm 5** Subroutine to check an automaton has a neighbour for every legal input

---

```

function ISCOMPLETE( $A : \text{automaton}$ )
  let  $B$  be a DFA matching any valid edge address;
   $discovered \leftarrow \{(\text{START}_A, \text{START}_B)\}$ ;
   $visited \leftarrow \emptyset$ ;
  while  $discovered \setminus visited$  contains a state pair  $(s_A, s_B)$  do
    add  $(s_A, s_B)$  to  $visited$ ;
    for all  $(b, t_B)$  such that  $B$  has a transition  $s_B \xrightarrow{b} t_B$  do
      if  $\nexists(a, t_A) : A$  has a transition  $s_A \xrightarrow{(a,b)} t_A$  then
        return false; ▷ automaton is incomplete!
      else
        add  $(t_A, t_B)$  to  $discovered$  for all such pairs  $(a, t_A)$ ;
      end if
    end for
  end while
  return true;
end function

```

---

input corpus. Inductively annotate every state with a layer of the substitution system: START is associated with the base layer, and any successor of a state  $s$  is associated with the parent of  $s$ 's layer. Now repeatedly merge states which have the same predecessor on the same symbol, or which have the same successor on the same symbol, *except* that two states may only be merged if they are annotated with the same layer. This precaution avoids the mistake of merging states from different layers  $L, L'$  with transitions to the same accepting state  $A(P, t)$ , where  $P$  is the common parent of both  $L$  and  $L'$ . (Recall from Theorem 2 that the sublanguages  $\mathcal{N}(L, t)$  are distinguished by the last layer *before* entering an accepting state, so such a merge would mix up the states from two of those sublanguages' DFAs, and create nonsense.)

This procedure terminates in a DFA recognising some sublanguage of the full language  $\mathcal{N}$ . (Specifically, the union of the zero-reversible closure of each sub-corpus; each of those closures is a sublanguage of one  $\mathcal{N}(L, t)$ .) However, it may not be all of  $\mathcal{N}$ .

By Theorem 1, the whole neighbour language  $\mathcal{N}$  is regular. Therefore, there is some finite length  $k$  such that every state of a minimal DFA for  $\mathcal{N}$  is reached by some edge address pair of length  $\leq k$ . However, this  $k$  is not known in advance, and may be greater than the length of strings we generated for our input corpus. So the final part of our algorithm is to detect if the output DFA is complete, and if not, retry with a corpus of longer address pairs. Since  $\mathcal{N}$  is regular, sooner or later, an attempt will succeed.

To detect completeness, we reinterpret our DFA for a language of edge-address pairs as an NFA for a language of *single* edge addresses, by replacing each symbol pair  $(a, b)$  on a transition with just  $a$ . (Choosing  $b$  instead should give the same results, because the construction process is symmetric.) Then we search that NFA to find any legal edge address which it does not accept. This is done by constructing the DFA for the language  $\mathcal{E}$  of *all* legal edge addresses, and performing a graph search over the cross product of the two automata to find pairs of states reachable from START via the same sequence of symbols. If this search encounters any state pair and symbol from which the DFA for  $\mathcal{E}$  has a transition and the newly built NFA does not, then we have not constructed a recogniser for all of  $\mathcal{N}$ , and must try again.

A pseudocode sketch of the full algorithm for constructing a DFA for  $\mathcal{N}$  is shown in Algorithm 2, with subroutines given in more detail by Algorithms 3, 4 and 5.

---

**Algorithm 6** Try to make a deterministic transducer from a recogniser for  $\mathcal{N}$

---

```

discovered  $\leftarrow \{ \{(\text{START}, \epsilon) \} \}$ ;
visited  $\leftarrow \emptyset$ ;
transitions  $\leftarrow \emptyset$ ;
while discovered \ visited contains an element src-dfa-state do
  add src-dfa-state to visited;
  for all symbols a do
    dest-dfa-state  $\leftarrow \emptyset$ ;
    for (src-rec-state, output) in src-dfa-state do
      for each src-rec-state  $\xrightarrow{(a,b)}$  dest-rec-state in the recogniser for  $\mathcal{N}$  do
        add (dest-rec-state, output  $\circ$  b) to dest-dfa-state;
      end for
    end for
    let prefix = longest common prefix of all output strings in dest-dfa-state;
    remove prefix from start of every output string in dest-dfa-state;
    add dest-dfa-state to discovered;
    mark dest-dfa-state as accepting if the NFA states in it are accepting;
    add src-dfa-state  $\xrightarrow{a}$  dest-dfa-state to transitions with output prefix;
  end for
end while
return (discovered, transitions);

```

---

A full example of a recogniser generated by this algorithm is shown in Figure 7. In this case, since the substitution system is simple enough that adjacent tiles always have adjacent supertiles, it is possible to label each state of the recogniser with a specific pair of tile edges. In more complicated recognisers this is not always possible.

#### 4.2.2 Deterministic transducer

The DFA built in the previous section solves the problem of deciding whether two tile edge addresses are neighbours of each other. However, this is not the problem we typically want to solve! Usually we have *one* tile edge address, and want to calculate the address of its neighbour.

By changing our point of view, we can reinterpret our existing DFA as a finite-state *transducer*, with each transition on a symbol pair  $(a, b)$  reinterpreted as a transition on the input symbol  $a$ , producing  $b$  as output.

This change of viewpoint renders the automaton nondeterministic. Interpreted as a recogniser for neighbouring pairs, it could have two state transitions  $S \xrightarrow{a,b} T, S \xrightarrow{a,c} U$ , with the left-hand symbol  $a$  in common, and going to different states depending on whether the right-hand symbol is  $b$  or  $c$ . When  $b$  or  $c$  is provided as input, the choice of which transition to take is forced, and the automaton can be deterministic. But interpreted as a transducer accepting  $a$  as input and emitting one of  $b$  or  $c$  as output, this is less helpful – the automaton now has multiple choices of transition to take from that state on the input  $a$ .

The next algorithm attempts to convert this nondeterministic transducer into a deterministic one. This transformation loses the invariant that every transition outputs exactly one symbol: instead, each transition on an input symbol outputs a *string* of output symbols, which may be empty, or contain more than one symbol. So the output of the automaton will lag behind its input, in situations such as the one just described, where the input symbol  $a$  does not give enough information to know whether the corresponding output symbol should be  $b$  or  $c$ . However, if the transducer has finitely many states, the lag is bounded, so with a sufficiently long input string every output symbol will be generated eventually.

The procedure for doing this is very similar to the procedure for converting an ordinary (recogniser-style) NFA into a DFA, in which each DFA state is identified with a subset of the states of the NFA. To apply this procedure to transducers rather than recognisers, permitting uncertain output to be delayed until all but one of the possibilities has been eliminated, each DFA state must be identified not with a plain set of NFA states, but with a set of pairs (*NFA state*, *string*), where the *string* is ‘pending output’: output generated by the path through the NFA to that state, which has not yet been emitted as output from the DFA.

To calculate a transition from one DFA state to the next on a symbol  $a$ , we enumerate all the transitions on  $a$  from each of the corresponding NFA states, and in each case, construct an output (*state*, *string*) pair with the NFA’s output symbol appended to the output string. Then, before converting this set of pairs into a DFA state, we examine it to find out whether all the state pairs agree on a prefix of their output strings. If so, then we remove that shared prefix from all of the output strings, and record it as the *deterministic* output of the

DFA transition we are calculating.

For each state of the DFA, we expect its set of associated NFA states to either all be accepting, or all non-accepting. In the former case the DFA state is also marked as accepting.

(Proof: if the DFA construction made a state containing an accepting and a non-accepting state, it would mean that there was an  $m$ -symbol input string  $A$  with two possible output strings  $B, C$  such that the pair  $(A, B)$  reached an accepting state of the NFA while  $(A, C)$  reached a non-accepting state. There must be some extension of  $(A, C)$  which does reach an accepting state, say by appending extra symbols  $a, c$  to the two strings to make an  $n$ -symbol pair  $(Aa, Cc)$ . Then  $(Aa, Ba)$  must also be acceptable to the NFA, because after  $(A, B)$  reaches an accepting state, further symbol pairs with both elements equal are legal inputs and remain in an accepting state. So  $Aa$  is an  $n$ -symbol input with  $Ba, Cc$  as distinct possible outputs, and since both end in an accepting state, the  $n$ th-order supertile type is the same in both cases. But this means that  $Ba$  and  $Cc$  identify different lowest-level tiles within that  $n$ th-order supertile – a contradiction, since two different subtiles of that supertile cannot both be adjacent to the same input tile along the same edge.)

Algorithm 6 shows this procedure in pseudocode. An example transducer built by the algorithm is shown in Figure 8.

Including these pending output strings as part of the description of a DFA state makes the set of potential states infinite, because strings can be arbitrarily long. So, unlike the technique for determining an NFA recogniser for a language, this algorithm can fail to terminate. Indeed, for some important substitution systems, it does. We discuss this in the next section.

### 4.3 Ambiguous substitution systems

The transducer built by Algorithm 6 can emit no symbols, or more than one symbol, on any given transition. But it is the determination of a transducer that emitted exactly one output symbol per input symbol, so it retains the invariant that the number of output symbols it has emitted, plus the length of any pending output string in its current state, must equal the number of input symbols it has so far received.

Hence, if Algorithm 6 terminates, then there is an integer  $k$  such that the length of any pending output string in any DFA state is  $< k$ . That is, the transducer is able to determine the  $n$ th output symbol of any edge address after examining at most  $n + k$  input symbols.

Conversely, if there is a  $k$  such that  $n + k$  input symbols are always enough to rule out all but one possibility for the  $n$ th output symbol, then Algorithm 6 must terminate, because the set of possible  $(NFA\ state, string)$  pairs becomes finite if the strings all have length  $\leq k$ .

We shall define a substitution system as **unambiguous** if Algorithm 6 terminates successfully, and otherwise, **ambiguous**.

#### 4.3.1 Detecting ambiguous systems

Conveniently, the failure of Algorithm 6 to terminate can be detected reliably, enabling it to be converted into a terminating algorithm which either determines its input transducer, or reports that it cannot.

Given a nondeterministic transducer which is not determinisable, there is no upper bound on the length of ‘pending output’ strings that can appear in DFA states constructed by Algorithm 6. In particular, this means that for any  $k$ , there exists some input string  $I$  of length  $m + k$  for which only the first  $m$  output symbols can be uniquely determined. In the nondeterministic transducer, this means that there exist two legal paths  $P_1, P_2$  from START for that input string which differ in their  $(m + 1)$ st output symbol, say one path visits states START,  $s_1, s_2, \dots, s_{m+k}$  and the other START,  $s_1, s_2, \dots, s_m, s'_{m+1}, s'_{m+2}, \dots, s'_{m+k}$ . By choosing  $k$  sufficiently large we can find two integers  $m < u < v < k$  after that symbol for which the state pairs  $(s_u, s'_u) = (s_v, s'_v)$ . The segment of input and output between those positions can be pumped: if the transducer is given the first  $v$  symbols of  $I$ , followed by infinitely many repetitions of the segment between  $u$  and  $v$ , there is a valid output sequence corresponding to each of these, by similarly repeating each path’s output between  $u, v$ . So the  $(m + 1)$ st output symbol never becomes unambiguous, because both of these paths with different values for that symbol can be legally continued indefinitely.

To detect this condition in practice, given a set of states constructed by an unfinished execution of Algorithm 6, it is enough to form a directed graph  $G$  as follows, and check it for cycles. Each vertex of  $G$  corresponds to a set of ordered pairs of the form  $(NFA\ state, symbol)$ , and is made from a state of the half-constructed DFA (which is a set of pairs  $(NFA\ state, string)$ ) by discarding all but the first symbol in each pending output string. (States in which the pending output strings are empty need not be considered.) Edges of  $G$  correspond to only those state transitions in the DFA which generate no deterministic output.

Then a cycle in  $G$  corresponds to a path between two DFA states which generated no definite output and only appended more symbols to each possible pending output, with the property that repeating the same sequence of input symbols will have the same effect indefinitely. Conversely, if the transducer is not

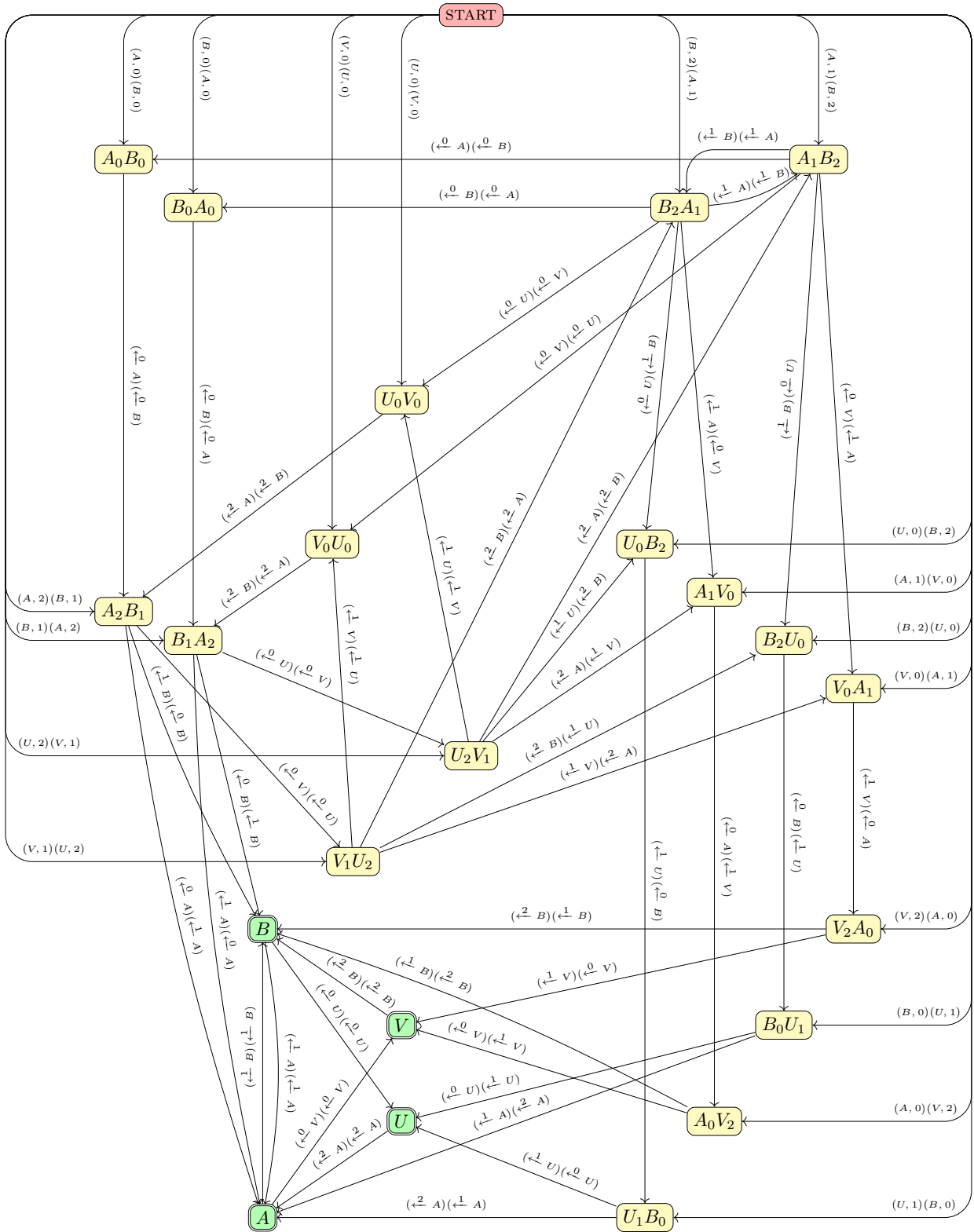


Figure 7: Example recogniser for neighbour edge pairs, in the P2 Robinson triangle system from Figure 22. Non-accepting states are labelled with two tile types and the edges of those tiles that meet. Accepting states (double outline) are labelled with a single tile type.

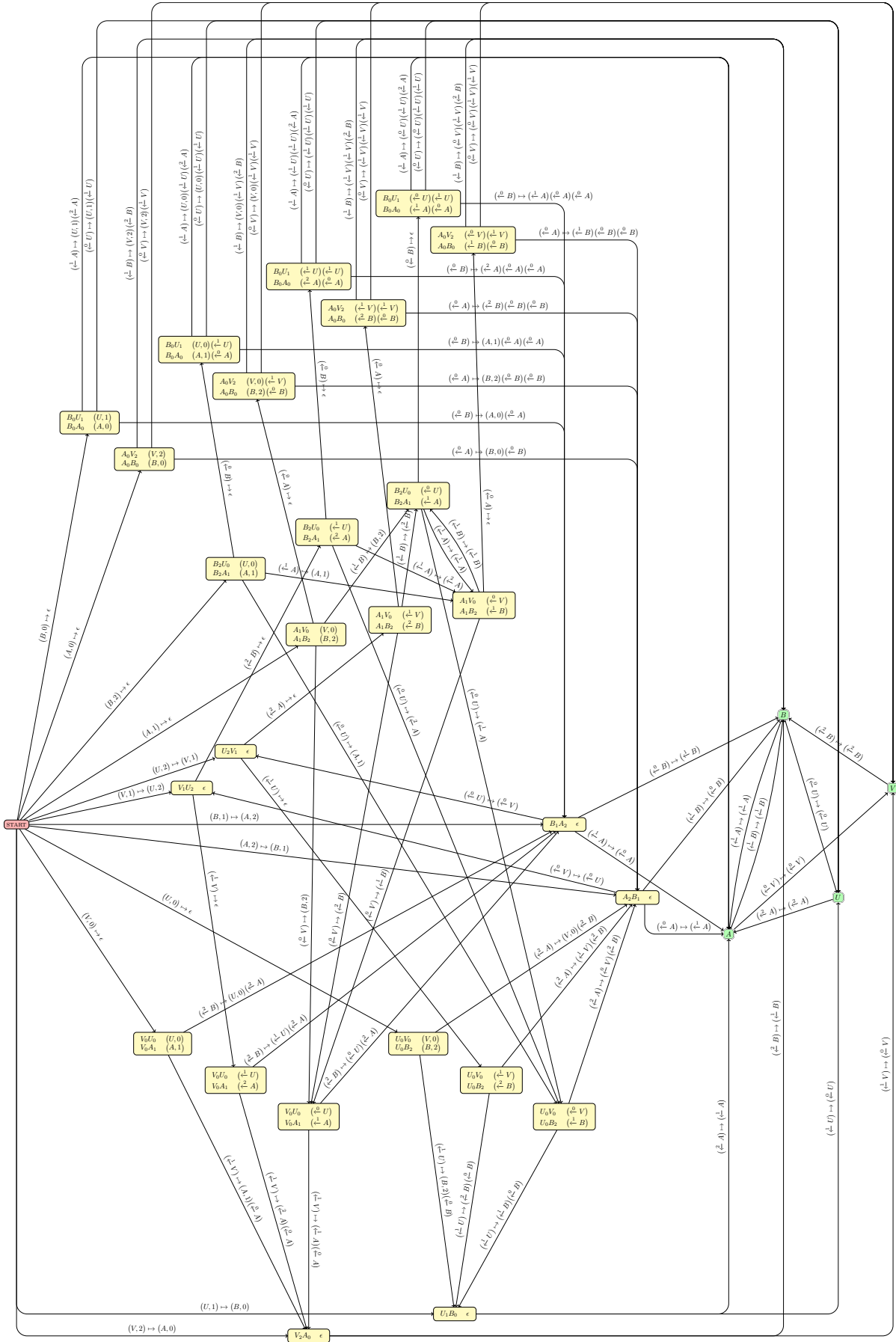


Figure 8: Example transducer for the P2 Robinson triangle system (Figure 22). States other than START and accepting states are annotated with a set of (recogniser state, pending output) pairs, one on each line. The recogniser states are the same as the ones shown in Figure 7.

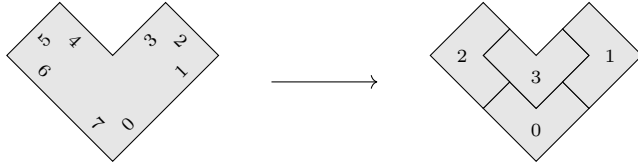


Figure 9: Substitution system for the simple ‘chair’ tiling

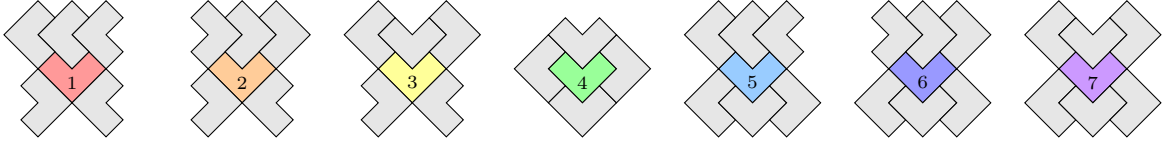


Figure 10: All the neighbourhoods of a single chair

determinisable, then a situation of this kind must eventually arise from the construction given above, because after each repetition of the section of  $I$  between positions  $u, v$ , the transducer must have returned to a state where *two* particular  $(m + 1)$ th output symbols are still possible, and even if other possible  $(m + 1)$ th symbols are ruled out by going round the cycle, eventually the set of possible symbols must stop decreasing while still being greater than 1.

Hence, we enhance Algorithm 6 so that, interleaved with the main algorithm, it periodically pauses the discovery of new transducer states, constructs the graph  $G$  described above, and checks it for a cycle. If a cycle is ever found, the algorithm reports failure; sooner or later, either that must happen, or the determinisation must succeed.

#### 4.3.2 Neighbourhood-based refinement

The existence of ambiguous substitution systems is theoretically interesting, but practically awkward, because a deterministic transducer is a very convenient thing to have for a tiling, and it would be nice if that convenience were always available.

The essential problem, in an ambiguous system, is that there is some sequence of input symbols for which it is difficult to determine even the first output symbol, i.e. the lowest-order tile adjacent to the tile  $t$  described by the first input symbol. (The start of the difficult sequence need not coincide with the beginning of the entire input edge address, although it often does in practice.) One way to work around a problem like this is to provide extra information in advance. In this case, that means *refining* the tiling, by cloning the tile type  $t$  into multiple subtypes, and arranging that each of the possible neighbour tiles can only legally appear next to one of those subtypes. This requires more information to be provided in the input tile address, but for some practical purposes this is no difficulty (if you are generating a *random* patch of tiling, then you can invent more detailed tile subtypes at random as easily as less detailed ones), and we shall also see in section 5 that for some purposes it is unavoidable.

Of course, it is one thing to say ‘clone tile  $t$ ’, but another to do it in practice. How many clones of  $t$  do you need? When  $t$  appears in the deflation diagram of another tile type (or even of one of the clones of  $t$  itself), which kind of  $t$  should it be replaced with? How many other tile types need to be cloned so that different versions of them can deflate to different kinds of  $t$ ? Where does the cloning end?

In this section we present an algorithm which automates this process, by taking an input substitution system and outputting a refinement of it: a finite number of distinct versions of each original tile type, and a description of how to derive the new system’s deflation diagrams from the old system. This description only needs to provide new information not present in the original system’s deflation diagrams, relating to which clone of each subtile appears where, and whether it depends on which clone of the supertile is being deflated. All the other details, like edge subdivisions and neighbour maps, are unchanged.

Since the purpose of creating clones of a tile is to restrict what neighbours can appear next to them, the essential idea is to make a clone of each tile type corresponding to each of its possible neighbourhoods.

A natural definition of the ‘neighbourhood’ of a tile in a tiling is to list, for each of the tile’s edges, what type of tile is adjacent to that edge, and which edge of the neighbour tile. We show an example of classifying tiles by this type of neighbourhood, based on the hierarchical substitution system of L-triominoes (or ‘chairs’) from [GS99] with a single tile type. Figure 9 shows the substitution rule for the chair tiling. It also numbers all the edges of the chair tile, and assigns identifiers for the four subtiles in a deflation ( $B, L, R, C$  for ‘bottom’, ‘left’, ‘right’ and ‘centre’). Figure 10 shows the seven possible neighbourhoods of a single chair that can arise in a tiling generated by this system.

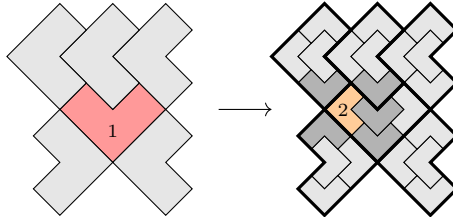


Figure 11: Deriving the subtype of a tile in a deflation diagram

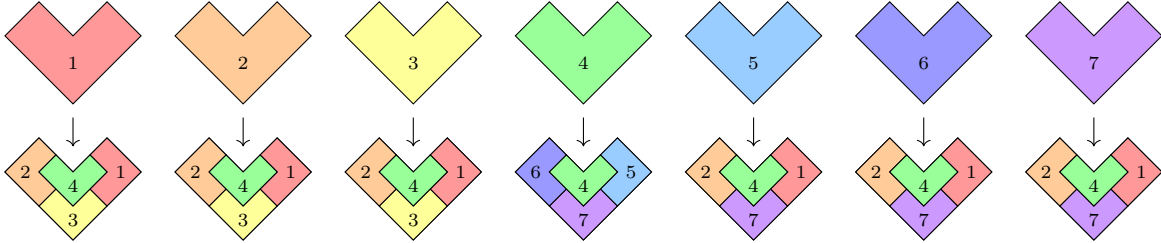


Figure 12: Full deflation diagrams for the 7-chair refinement

If we are to make a refined substitution system using these seven possibilities as the subtypes of the chair tile, then we must construct the deflation diagram for each subtype. These deflation diagrams will be refinements of the diagram for the chair itself (Figure 9); the only new decision to make, for each subtype of chair being deflated, is which subtype of chair appears in each position in its deflation diagram.

To determine this, we start from the neighbourhood diagram for the subtype of the larger chair; deflate that entire diagram into smaller chairs; and from there, determine the neighbourhood (and hence the subtype) of each chair deflated from the original tile. Figure 11 shows an example of this, demonstrating that when deflating a chair of subtype 1 (according to the numbering in Figure 10), the leftmost subtile has subtype 2. Repeating this procedure for all the subtiles of all seven chair types, we obtain a full set of deflation diagrams for the refined chair tiling. Figure 12 shows these diagrams in full.

The chair substitution system is ambiguous. With just one chair type, Algorithm 2 successfully constructs a recogniser for neighbouring edge address pairs, but Algorithm 6 fails to convert it into a deterministic transducer. However, the refined system with seven chair types is unambiguous: it *does* admit a deterministic transducer.

To see why this helps, here is a concrete reason why the original chair tiling is ambiguous. Consider a tile which is subtile 0 of its supertile, which is subtile 0 of its supertile in turn, and so on  $n$  times. That is, its address is of the form

$$\text{chair} \underbrace{\overset{0}{\leftarrow} \text{chair} \overset{0}{\leftarrow} \text{chair} \overset{0}{\leftarrow} \dots \overset{0}{\leftarrow} \text{chair} \overset{0}{\leftarrow}}_{n \text{ steps}} \text{chair}$$

so that the lowest-order tile occupies the very bottom corner of the  $n$ th-order supertile, in the orientation shown in figure 9. What borders that tile on one of its lower edges – say, edge 0 from the same figure? It depends on what borders the  $n$ th-order supertile, and the various possibilities do not all lead to the same orientation of the *smallest* chair: this  $n$ th-order chair might be either back-to-back with the next one or nested inside it, and the two touching lowest-order chairs will have the same relationship as the high-order ones in each case. So a transducer for this substitution system cannot generate even the first output symbol without looking at the  $(n + 1)$ th input symbol. But  $n$  was arbitrary. So the transducer cannot have finitely many states.

The refined chair tiling resolves this problem by requiring the input tile address to be specified in more detail. The deflation diagrams in Figure 12 show that subtile 0 of any chair has either type 3 or type 7: for chair types 1,2,3, subtile 0 has type 3, and for types 4,5,6,7, it has type 7. In particular, each of types 3 and 7 has a subtile 0 of the same type as itself. So the input address must now be specified in one of the following forms:

$$\begin{aligned} \text{chair}_3 \overset{0}{\leftarrow} \text{chair}_3 \overset{0}{\leftarrow} \text{chair}_3 \overset{0}{\leftarrow} \dots \overset{0}{\leftarrow} \text{chair}_3 \overset{0}{\leftarrow} \text{chair}_t & \quad t \in \{1, 2, 3\} \\ \text{chair}_7 \overset{0}{\leftarrow} \text{chair}_7 \overset{0}{\leftarrow} \text{chair}_7 \overset{0}{\leftarrow} \dots \overset{0}{\leftarrow} \text{chair}_7 \overset{0}{\leftarrow} \text{chair}_t & \quad t \in \{4, 5, 6, 7\} \end{aligned}$$

This allows the transducer to know, when it sees the *first* symbol of the address, whether the  $n$ th symbol is going to be in the set  $\{1, 2, 3\}$  or the set  $\{4, 5, 6, 7\}$ . More immediately, because the lowest-order tile has either type 3 or 7, the neighbourhood diagrams in Figure 10 show what orientation of chair tile borders it along the lower edges. So the transducer has information it did not have in the original substitution system.

---

**Algorithm 7** Answer the list of refinement queries for a tile

---

```
procedure ANSWERQUERIES(information  $T_0$  identifying the starting tile)
   $A_0 \leftarrow \text{tile-type}(T_0);$  ▷  $Q_0$  always asks for the starting tile type
  for queries  $Q_n$  for  $n = 1, 2, \dots$  do
    let  $(m, u, e) = Q_n;$  ▷ ‘if  $Q_m$  was a tile of type  $u$ , try its edge  $e$ ’
    if  $A_m$  has tile type  $u$  then
       $(T_n, e') \leftarrow$  neighbour of tile  $T_m$  across edge  $e;$ 
       $A_n \leftarrow (\text{tile-type}(T_n), e');$ 
    else ▷ including the case  $A_m = \perp$ 
       $A_n \leftarrow \perp;$ 
    end if
  end for
  return the list of  $(A_n);$ 
end procedure
```

---

(This does not derive from any magical foresight involved on the part of the transducer! Rather, changing the address notation in this way has required the *user providing the input tile address* to compensate for the transducer’s inability to look arbitrarily far into the future, by giving the necessary information early in the address rather than leaving it until later.)

This example with the chair tiling illustrates the basic procedure for refining a substitution system. However, it isn’t as simple as that in every case, because if the substitution system has zero-thickness spurs, then knowing the type of every formal neighbour of a tile  $t$  may not be enough information to know the type of every neighbour of  $t$ ’s subtiles in a particular deflation: even if the neighbours of  $t$  fully surround  $t$  leaving no exposed edge, the same might not be true after deflating all the tiles.

To account for this, the refinement algorithm must be prepared to use a more general definition of ‘neighbourhood’. The strategy is to make a list of *queries* about tiles in the tiling:

- the initial query  $Q_0$  is simply ‘What type is the central tile?’
- immediate followups are of the form ‘If the answer to query  $Q_0$  was a tile of type  $t$ , what type is that tile’s neighbour along edge  $e$ , and what edge of that neighbour meets edge  $e$ ?’
- further followups name the full answer to the previous query, including a tile type and an edge: ‘If the answer to query  $Q_n$  was edge  $e$  of a tile of type  $u$ , what type is that tile’s neighbour along edge  $f$ , and what edge of that neighbour meets edge  $f$ ?’

A query need only be answered if its precondition is satisfied. If a query  $Q_n$ ’s predecessor query  $Q_m$  had an answer other than the one assumed by  $Q_n$ , then the answer to  $Q_n$  is  $\perp$ , or ‘not applicable’. The same is true if the predecessor query’s answer was itself  $\perp$ .

The simple definition of ‘neighbourhood’ for the chair system is easily converted into this form:

- $Q_0$ . What type is the central tile? (in this case it will always be ‘chair’)
- $Q_1$ . If the answer to  $Q_0$  was ‘chair’, what borders that chair on edge 0?
- $Q_2$ . If the answer to  $Q_0$  was ‘chair’, what borders that chair on edge 1?
- ⋮
- $Q_8$ . If the answer to  $Q_0$  was ‘chair’, what borders that chair on edge 7?

To refine a general substitution system, we initialise the list of queries in this fashion: for each tile type, we make a set of queries following up  $Q_0$  and asking about every edge of that tile. Then we find tile subtypes by searching the substitution system for finitely long tile addresses which provide enough information to answer all queries in the list. Then we attempt to determine the deflation diagram for each of those subtypes, by answering the same list of queries about each of its subtiles, using no information except the answers to the same queries for the supertile. If this attempt fails due to not being able to determine what is on the other side of a spur, the failure comes with a description of an additional query that would have allowed the algorithm to make more progress. We collect as many of these extra queries as possible, and then restart the algorithm from scratch with the extended query list.

The algorithm terminates when both the set of queries and the set of tile subtypes are closed: the set of queries is such that knowing the answers for a supertile allows the answers for all its subtiles to be determined, and every tile subtype appearing as a subtile in a deflation diagrams is also a subtype for which a deflation diagram is known in turn.

The key part of this algorithm is finding the answers to the list of subtype-determining queries. Algorithm 7 gives the general procedure for doing this, supposing that it has access to some type of information identifying

---

**Algorithm 8** Compute the neighbour of a subtile in the deflation of a supertile subtype

---

```
procedure SUPERTILENEIGHBOUR(answers, query, e)
  let answer = answer to query in answers;
  if answer named edge e of a tile type t then
    let u, f be such that query asked about edge f of tile u;
    let query = predecessor of query;
    return (query, u, f);
  else
    let new-query = (query, e);
    if new-query is not in the query list then
      return failure, and recommend adding new-query to the list;
    else
      let (u, f) = new-answer = answer to new-query in answers;
      return (new-query, u, f);
    end if
  end if
end procedure

procedure SUBTILENEIGHBOUR(i1, answers, query, t1)
  lookup-result ← look up Ii1,e in adjacency map for t1;
  while lookup-result is of the form Eu,v do
    new-query, t'1, u' ← SUPERTILENEIGHBOUR(answers, query, t1, u);
    lookup-result ← look up Eu',-v in adjacency map for t'1;
    replace (t1, query) ← (t'1, new-query);
  end while
  now expect that lookup-result is of the form Ii'1,e';
  return (i'1, query, t1);
end procedure
```

---

a particular tile, allowing the tile's type to be determined, and a method for identifying the neighbour of the tile.

To determine a starting list of tile subtypes, Algorithm 7 is used in a form where the 'information identifying a tile' is a finitely long tile address giving the tile's position within a deflation of some particular supertile, and a tile's neighbour is determined by passing that address to Algorithm 1 to calculate the similar address of the neighbour. If this procedure completes without Algorithm 1 recursing too deep and running off the end of the input address, then the tile's subtype is successfully determined.

However, when determining the subtype of a tile in a deflation diagram, a full address for the subtype is not available, because it is necessary to ensure that the subtypes of subtiles can be derived *only* from the answers to the queries for the supertile. So for this purpose we reuse Algorithm 7 using a different representation of a tile identity, and a modified algorithm for determining its neighbour.

At the layer of the supertile *t*, for which we know the answers to all the subtype queries, our representation of a tile identity for these purposes simply nominates a particular query  $Q_i$ , and the tile referred to is whichever tile  $Q_i$  is asking about. Given a tile identity specified in that form, finding the neighbour of the tile along some edge *e* is normally done by extending the query  $Q_i$  into a longer one, incorporating the answer given in the tile identity: 'If the answer to  $Q_i$  was [this edge of that tile], what's on the other side of its edge *e*?'. The only exception is if *e* is the same edge that  $Q_i$  asked about, in which case we instead *shorten* the previous query by a step, returning to whatever query it was itself a followup to.

However, when determining tile subtypes in a deflation diagram, we need to find neighbours at the *subtile* layer, not the supertile layer. So the full algorithm for finding neighbours in this context uses the same structure as the recursive Algorithm 1, using the adjacency map for each supertile, but where Algorithm 1 recursed by calling itself, this method instead calls the supertile neighbour procedure described in the previous paragraph. Algorithm 8 shows this in full.

Algorithm 9 shows the top-level structure of the overall refinement procedure, using all the previous algorithms in this section as subroutines.

One aspect omitted from the pseudocode for brevity is handling substitution systems involving multiple layers. Tile types at all layers potentially need refining into multiple subtypes. So when Algorithm 9 iterates over all tile addresses of length *n*, it must include addresses of tiles *at all layers*, not just length-*n* addresses of tiles in the base layer. If a tile type appears in multiple layers, it should be considered to be a separate tile of the same shape for each layer it appears in, so that the list of queries for each layer can vary independently.

---

**Algorithm 9** Compute a refinement of a whole tiling

---

```
queries  $\leftarrow$   $\{Q_0\} \cup \{(0, t, e)\}$ ;  
for  $n = 1, 2, 3, \dots$  do ▷ length of tile address to explore  
  subtypes  $\leftarrow \emptyset$ ;  
  for all finite tile addresses of length  $n$  do  
    let answers = ANSWERQUERIES(address); ▷ via Algorithm 1  
    if all queries answered successfully then  
      subtypes  $\leftarrow$  subtypes  $\cup \{(t, answers)\}$ ;  
    end if  
  end for  
  incomplete  $\leftarrow$  (subtypes  $\neq \emptyset$ ); ▷ need at least one subtype  
  for  $(t, super\text{-}answers)$  in subtypes do ▷ make deflation diagrams  
    for each deflation of  $t$  do  
      for each subtile index  $i$  of that subtype do  
        let sub-answers = ANSWERQUERIES(super-answers,  $Q_0$ ); ▷ via Algorithm 8  
        if Algorithm 8 failed and suggested an extra query then  
          add the new query to queries;  
          incomplete  $\leftarrow$  true;  
        end if  
        if sub-answers  $\notin$  subtypes then  
          incomplete  $\leftarrow$  true;  
        end if  
        enter sub-answers as type of subtile  $i$  in deflation of subtype;  
      end for  
    end for  
  end for  
  if not incomplete then  
    return subtypes and deflation diagrams;  
  end if  
end for
```

---

It is logical that this refinement procedure should be able to transform an ambiguous substitution system into an unambiguous one, because it incorporates information into each tile type about that tile's immediate neighbourhood – i.e. about exactly what a transducer needs to know to produce its output.

However, a single run of the refinement algorithm is not always sufficient. The Ammann-Beenker tiling ([GS86], Figures 10.4.14 and 10.4.15) is an example of a substitution system requiring two passes of this refinement algorithm before a transducer can be successfully generated. Figure 13 shows the substitution system in a form suitable for use with these algorithms. The Ammann-Beenker tiling includes a constraint about the order of tiles that can appear around each vertex, shown in the figure as shaded markings which are required to form into a thick arrow shape around the vertex. The markings on the rhombus are asymmetric, and in order to meet the constraint, both mirror-image forms of it must occur in a specific pattern around any vertex where 8 rhombus tiles meet, shown in Figure 14.

An unambiguous version of the system must therefore distinguish all 8 of the rhombi around such a vertex. Knowing each tile's immediate neighbours is not enough to distinguish all 8 rhombi, because (for example) there are two instances of a green rhombus with both neighbours red. But a second run of the refinement algorithm includes information about the *once-refined* type of each of the rhombus's neighbours, i.e. information about the original type of the rhombus's *second-order* neighbours, which includes 5 of the rhombuses around an 8-rhombus vertex – and that *is* enough information to distinguish all 8, because between 5 rhombuses are 4 of the vertex's 8 incident edges, and one of those must be the green/green or red/red edge. Full details of the necessary refinement are given in section 7.2.

The more times this algorithm is run on a system, the more each tile type incorporates information from a larger and larger area of the tiling around the tile. After some finite number of refinements, each tile will describe a neighbourhood of itself sufficiently large that, given any full tile address containing those refined tile types, the regions of the plane forced by the neighbourhoods of larger and larger supertiles expand in all directions and cover the whole plane. So it should always be possible to make a substitution system unambiguous after applying the refinement algorithm enough times.

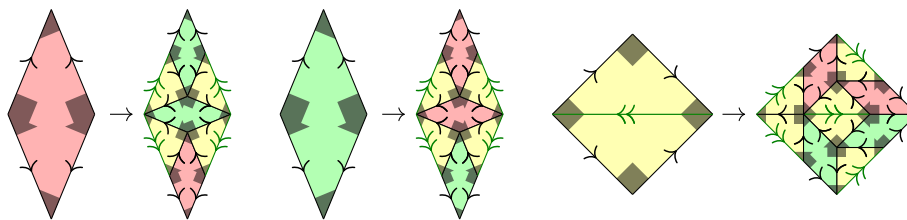


Figure 13: Deflation diagrams for the Ammann-Beenker tiling

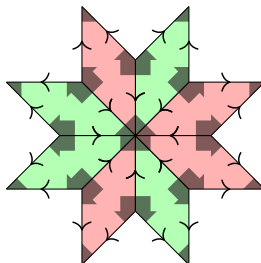


Figure 14: The only way 8 Ammann-Beenker rhombi can meet at a vertex

### 4.3.3 Remerging tile types

In the previous section, as an example, we derived a refinement of the chair substitution system containing 7 different tile types. That refinement is unambiguous, where the original system is ambiguous.

In the deflation diagrams shown in Figure 12, chair types 1, 2 and 3 all have identical deflation diagrams. So do chair types 5, 6 and 7. We can reduce the number of tile types by merging each of those sets into a single combined type, obtaining (say) types  $x = \{1, 2, 3\}$ ,  $y = \{4\}$ ,  $z = \{5, 6, 7\}$ , to produce the resulting simpler system shown in Figure 15.

This system remains unambiguous: merging the synonymous tile types does not cause Algorithm 6 to fail. That is to be expected, because a ‘coarse’ tile address given in terms of the three types  $x, y, z$  can be readily converted back to a ‘fine’ one using the seven original types  $1, \dots, 7$  with only a finite amount of lookahead: to recover the fine subtype of a chair at level  $n$ , it is necessary only to look at its coarse supertile type at level  $n + 1$ . All the fine types merged into that coarse type had exactly the same deflation diagram, so the coarse supertile type plus the subtype index is enough to recover the fine type of the subtype.

Even if this reduction were performed more than once (if the first round of merging tile types caused some deflation diagrams to become identical which were previously not), this argument would still hold: each reduction can be undone by a finite state machine using a single symbol of lookahead, therefore finitely many reductions can be undone using finite lookahead. So there is no reason why reducing a system in this way should prevent a finite-state transducer from being able to handle it.

## 4.4 Putting it all together

The algorithms presented in this section combine into a general-purpose method for computing a deterministic finite-state transducer for tiling substitution systems.

Given a substitution system, one first uses Algorithm 2 (section 4.2.1) to make a DFA that matches the neighbour language  $\mathcal{N}$  of pairs of neighbouring tile edge addresses. Then Algorithm 6 (section 4.2.2) converts that into a transducer capable of taking one tile edge address as input, and producing the neighbouring one as output. If Algorithm 6 cannot succeed, this can be detected via the technique in Section 4.3.1. In that situation, the substitution system is ambiguous, but all hope is not lost: run Algorithm 9 (section 4.3.2) to refine it into a substitution system more likely to be unambiguous, and try the whole procedure again.

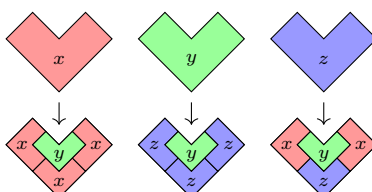


Figure 15: Deflation diagrams for the 3-chair refinement

All of these algorithms are practical in their running time, and suitable for real-world use in software. In the author’s own implementations, compiled code (in Rust) can process a typical substitution system in well under a second, and even unoptimised interpreted code (in Sage) in under a minute. And a transducer only needs to be constructed once for a given tiling, and then can be reused for as much work as is needed.

Some applications of these finite-state automata are given in section 6.

## 5 Infinite supertile boundaries

So far, we have discussed the question of finding the address of a tile’s neighbour on the assumption that the two tiles share an  $n$ th-order supertile, for some  $n$ . The recursive Algorithm 1 must ascend the levels of supertiles until it reaches such an  $n$  before it can begin generating any output at all; the transducer constructed by Algorithm 6 signals that a shared supertile has been reached by entering an accepting state, and if further input symbols are provided after that, emitting them unchanged as output (checking them for validity as a side effect).

But  $n$  can be arbitrarily large. For any  $n$ , it is easy to find examples of adjacent tiles which have no supertile in common before the  $n$ th layer, simply by making a single  $n$ th-order tile  $T$ , deflating it  $n$  times, and choosing two 0th-order tiles that came from different immediate subtiles of  $T$ . It follows that arbitrarily long paths exist through the transducer state machine which never enter an accepting state.

The transducer has finitely many states. So if *arbitrarily* long paths exist in it which never reach an accepting state, then there must also exist *infinitely* long paths with the same property. That is, there exists an infinite sequence of input symbols for which the transducer never enters an accepting state – but it still produces an infinite sequence of output, since no transducer state has more than a finite amount of pending output, and the invariant is always maintained that total length of output (including pending output in the current state) equals the total length of input consumed so far.

An input sequence like this describes a tile  $t$ , and its output a neighbouring tile  $t'$ , such that the two tiles have no supertile in common at all. The union of the patches of tiling deflated from  $t$ ’s supertiles does not cover the whole plane, and the same is true for  $t'$ . [GS99] describes these as ‘infinitely large supertiles’; one might also describe them as supertiles of infinite *order*. They are both, so we shall simply say ‘infinite supertile’.

The recursive Algorithm 1 cannot handle tile addresses of this type. It cannot begin generating any output until it has found an  $n$ th-order supertile in common between its input and output tiles, and in this case, no such supertile exists. So it will keep recursing until it runs out of stack, and never generate any useful output. If one imagines each  $n$ th-order supertile’s patch of tiling to be surrounded by a wall of height  $n$ , then Algorithm 1 must climb over such a wall step by step in order to get over it to the next tile – but an *infinite* supertile boundary, being the union of a wall of every integer height, prevents it from passing at all.

However, our deterministic transducer has no trouble crossing those infinitely high walls, because it generates its output address from the low order upwards, before even *knowing* that the wall is infinitely high. Indeed, it never receives enough information to be certain of that. For all the transducer knows, at any point, the next few symbols might lead to an accepting state, and there might be a shared finite-order supertile between its input and output after all.

Proper infinite supertiles (that is, not covering the entire plane) often occur in the most interesting instances of a given aperiodic tiling, such as instances with full reflective or rotational symmetry, or ‘singular’ tilings with near-symmetry. So an algorithm for calculating neighbour addresses which can cross their boundaries is desirable, because it allows those particularly interesting tiling instances to be generated and investigated conveniently.

An example of an infinite supertile boundary occurs in the P2 Robinson triangle substitution system shown in Figure 1. From that figure we can see that the upper part of edge 1 of the  $A$  triangle, under deflation, becomes edge 2 of a  $B$  triangle (which we have indexed as subtile number 1 in figure 2). Conversely, the upper part of edge 2 of a  $B$  becomes edge 1 of an  $A$  (again subtile number 1). So we can construct the following address, describing an  $A$  tile whose sequence of supertile types alternates between  $B$  and  $A$  forever, and in particular describing edge 1 of the lowest-order  $A$ :

$$\mathcal{A} = (A, 1), (\overset{1}{\leftarrow} B), (\overset{1}{\leftarrow} A), (\overset{1}{\leftarrow} B), (\overset{1}{\leftarrow} A), (\overset{1}{\leftarrow} B), (\overset{1}{\leftarrow} A), \dots$$

This is a concrete example of an address that will cause Algorithm 1 to attempt to recurse to infinite depth, and fail to terminate. Every time it is called to traverse edge 1 of a type- $A$  tile, it will recurse to attempt to traverse edge 2 of its type- $B$  supertile, and *vice versa*.

The infinite supertile containing this address is a half-plane, whose boundary is a straight line. From first principles we can construct an address for a supertile that can occupy the other half-plane and fit next to this one, by symmetry. The Robinson-triangle system is invariant under the combined transformation of replacing each tile with its mirror image, and interchanging the tile types  $A \leftrightarrow B, U \leftrightarrow V$ . (This also interchanges edge

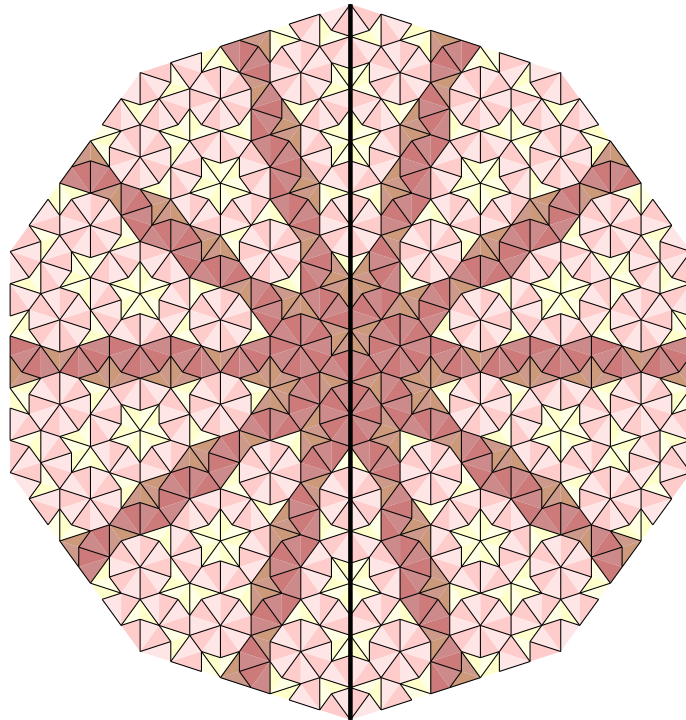


Figure 16: The Penrose P2 infinite cartwheel pattern

indices 1 and 2, since the edges of each triangle are indexed anticlockwise.) The image of address  $\mathcal{A}$  under this symmetry gives rise to a mirror-image half-plane, with the same pattern of long and short tile edges along its boundary, fitting exactly to the first one:

$$\mathcal{B} = (B, 2), (\overleftarrow{1} A), (\overleftarrow{1} B), (\overleftarrow{1} A), (\overleftarrow{1} B), (\overleftarrow{1} A), (\overleftarrow{1} B), \dots$$

This is perhaps the simplest example of an infinite-order supertile boundary. It is also a good example of the principle that tile addresses of this kind tend to coincide with tilings of particular interest, because these tile addresses represent the two tiles at the centre of the famous ‘infinite cartwheel pattern’, an instance of P2 which not only has reflection symmetry but *almost* has 10-way rotation symmetry too<sup>8</sup>, in that *most* of the plane is invariant under a rotation of  $36^\circ$ , with only the centre of the image and a few thin spokes varying. Figure 16 shows this pattern, with the non-rotationally-symmetric parts shaded, and the line of true reflection symmetry running vertically down the centre.

The example transducer in Figure 8 demonstrates that these two addresses  $\mathcal{A}, \mathcal{B}$  are indeed mapped to one another, without any difficulty arising from the infinite supertile boundary: the symbols of address  $\mathcal{B}$  shown above are generated as output from the transducer, if one follows transitions from START on the symbols of  $\mathcal{A}$ , and *vice versa*.

## 5.1 Eventually periodic tile addresses

The address  $\mathcal{A}$  shown above has the useful property of being *eventually periodic*. Apart from the initial special symbol containing an edge type instead of a supertile index, the rest of the address repeats the two symbols  $(\overleftarrow{1} B), (\overleftarrow{1} A)$  for ever.

Eventually periodic tile addresses are particularly well suited to a finite-state transducer, because given a description of an eventually periodic address in the form (initial segment, repeating segment), a finitely long computation can deliver the neighbouring tile’s address in the same form, simply by waiting until a second visit is made to the same combination of a state of the transducer and a position in the repeating part of the input. Then all the output generated since the first visit to that combination is guaranteed to repeat forever, since in every subsequent repetition, the transducer will receive the same sequence of input symbols starting

<sup>8</sup>This phenomenon of near-symmetry derives from the ‘singular pentagrids’ described in [de 81b]: the tiling is ultimately generated from a pentagrid which *actually* has the symmetry group of a decagon, but at the points where more than two pentagrid edges meet, gaps are created which can be filled with Penrose tiles in multiple ways, and no way to fill the gaps can preserve all the symmetry. We shall use the word ‘singular’ for other nearly-symmetric instances of substitution tilings, by analogy.

from the same state.<sup>9</sup>

It follows that the class of eventually periodic tile addresses is closed under the neighbour relation: every tiling of the plane based on a substitution system is either composed entirely of eventually periodic addresses, or has none of them at all.

Since the class of eventually periodic addresses appears to include many (if not all) of the tilings of special interest, like symmetric and singular tilings, it's useful to have a way to talk about them concisely. A useful notation is to describe a whole *infinite supertile* at a time, by mentioning only the eventually repeating segment of the tile address, normalised to be (a) of minimum length (never talk about repetitions of *abab* when you can just say *ab*), and (b) starting at a position in the address which is a multiple of its own length.

For example, the address  $\mathcal{A}$  in the previous section is part of the infinite supertile  $\left[ \left( \overset{1}{\leftarrow} A \right), \left( \overset{1}{\leftarrow} B \right) \right]^*$ , whereas its neighbour  $\mathcal{B}$  is part of the infinite supertile  $\left[ \left( \overset{1}{\leftarrow} B \right), \left( \overset{1}{\leftarrow} A \right) \right]^*$ . The repeating sequence in each of these infinite supertiles is a cyclic rotation of the other, implying that the two supertiles can be obtained from one another by deflation. In this case they also appear in the same tiling of the whole plane with a boundary between them, but in other cases, they are entirely separate tilings.

## 5.2 Uniqueness

When a deterministic transducer crosses an infinite supertile boundary and returns a unique address for the tile on the far side, it does not necessarily mean that it has found the only *layout of tiles* that physically fits to the far side of the boundary (even counting matching rules implicit in the substitution system, such as types and directions of edges).

A transducer constructed by this method only permits tile adjacencies that would arise in finitely large patches generated by the input substitution system. Any other way to fit tiles together is not considered. So a transducer will only be able to say that there is a unique layout of tiles, with their types, such that every finitely large patch crossing the boundary is consistent with the substitution system.

If an infinite supertile does extend to the rest of the plane in multiple ways that physically fit, then it will have multiple representations in the tile addressing system, and which one you give as input to the transducer controls which of the possible extensions you receive as output. Sections 7.3 and 7.4 exhibit example cases in which this occurs.

## 6 Applications

Now that we have a suite of algorithms for dealing with substitution tilings using finite state automata, what are they useful for?

### 6.1 Tiling generation

Most obviously, a finite-state transducer for a substitution system provides a highly practical method of generating patches of the tiling described by the system, for whatever purpose you might need one – mathematical research, puzzle games, or simply pretty pictures.

Perhaps the most obvious method of generating a patch of a Penrose tiling, or hats, or Spectres, is to start from a single order- $n$  tile or metatile, for some  $n$  large enough for your purposes; apply the substitution system  $n$  times to deflate that single  $n$ th-order tile into a large patch of 0th-order tiles; then pick out from that patch a smaller region of whatever size and shape you really wanted, and throw the rest of the output tiles away.

In place of that approach, we present a family of approaches based on knowing an address for each tile plotted. In general, one chooses a starting tile, equipped with both a position in the plane and an address within the substitution system. Then one calculates the address of a neighbouring tile via the combinatorial algorithms presented in Section 4, obtaining in particular its lowest-order tile type, and finding out which pair of edges of the two tiles coincide, which is enough to place that tile in the plane too – so now that second tile also has known plane coordinates and a known address, enabling the same procedure to be repeated. One can search outwards from the starting tile in any pattern desired, discovering new tiles on demand, and stop as soon as all the tiles overlapping the desired region have been found.

The simplest method of doing this is to run the neighbour algorithm *in full* to compute a complete address for each new tile. One could give the starting tile's address to a deterministic transducer, and run it until

---

<sup>9</sup>As a by-product of this algorithm, it is also possible to detect the boundary between two infinite supertiles. An edge between two tiles is part of an infinite supertile boundary precisely when a transducer generates infinite output without ever entering an accepting state. In the case of eventually periodic tile addresses, the transducer's sequence of state transitions is also eventually periodic, so this can be determined in finite time.

the transducer reaches an accepting state. (Equivalently, and requiring less complicated programming, one could not bother constructing any transducers at all, and do this same job directly by using the recursive Algorithm 1.)

This approach only works if there is no possibility – or, failing that, at least zero probability – of encountering an infinite supertile boundary, since in that situation disaster occurs: the transducer will *never* reach an accepting state, or Algorithm 1 will recurse forever and overflow its stack. If the input coordinates are generated at random, then this disaster has probability 0 (although in principle arbitrarily high-order boundaries are still possible, so however large your stack is, it *could* overflow). If the aim is to plot an entire patch of tiling deflated from some single  $n$ th-order supertile, then the disaster is *by definition* impossible, since either algorithm will report failure by running out of input rather than running for ever.

To plot non-random instances of a tiling which involve infinite supertile boundaries with *eventually periodic* addresses, this approach can still be used, but instead of running the transducer until it reaches an accepting state, one runs it until it has calculated the full eventually periodic address of the destination tile, by the procedure described in section 5.1. This also allows infinite supertile boundaries to be detected, and displayed on the diagram if desired.

What about plotting a *fully general* patch of tiling, given only a stream of symbols from an input tile address about which you know nothing? In this case, neither of these approaches works: there is no guarantee that a transition algorithm will reach an accepting state or terminate its recursion, and even if it does begin repeating a periodic cycle of output, the algorithm cannot know that, without knowing the same thing about the input. In this situation, the simple approach of computing each tile’s address before moving on to the next tile cannot work reliably.

An alternative algorithm in this situation is to propagate symbols of the address one by one across the set of tiles generated so far. Keep track of a tree of links between the tiles, with each tile linked to a unique ‘parent’, being the neighbour tile from which it was first discovered. For each tile other than the starting tile, store the currently known prefix of its address, and remember the current state of a transducer that is generating its address from that of its parent. Then, for each new symbol received from the input stream, append it to the address of the starting tile, and propagate that symbol outwards to all the tile’s children by feeding it to each child’s transducer. If a transducer emits one or more output symbols as a result, propagate those in turn to that tile’s children, and so on. A transducer is initialised for each exposed edge of a known tile, and a new tile is added to the collection as soon as that transducer generates the first output symbol for that tile, allowing its type and position to be known.

At every stage of this algorithm, a finite number of symbols propagate along each edge of this tree, so no intermediate step can fail to terminate. And every desired tile must eventually be discovered, because the lag between the deterministic transducer’s input and output is bounded by a constant  $k$ , so that if  $n$  symbols of a parent tile’s address are known, then so are at least  $n - k$  symbols of its child. By induction, if a tile is separated from the starting tile by  $m$  edges of the tree, then at least  $n - mk$  of its symbols can be calculated from  $n$  symbols of the starting tile. So for any finite output region, a finite number of input symbols suffices to discover at least the lowest-order type and position of every tile in the region.

This family of techniques in general has many advantages over the approach of deflating a single starting tile:

**Only generate the tiles you really need.** Generating a much larger patch than necessary, only to throw most of the tiles away, is a waste of computation. The transducer technique does not calculate the address of any tile until it is already known that the tile overlaps the target region of the plane.

In some cases the deflation technique can reduce its computational costs by detecting early when a high-order intermediate tile will not overlap the output region at all, and discarding it from the list of tiles to deflate to the next level. This approach works well in systems such as Robinson triangles, where a supertile and its subtiles occupy exactly the same region of the plane, and that region is geometrically simple. But it works badly in the hat and Spectre tilings, where the  $n$ -times deflation of an order- $n$  supertile becomes a more and more complicated shape and the geometry of the tiling is distorted during each deflation, so it is hard work to determine *whether* a high-order supertile will contribute to the output region.

**Ignores higher-order tile geometry completely.** The geometric distortion at every layer of the hat or Spectre tiling does not complicate the transducer approach at all. This entire suite of algorithms is completely unconcerned with the geometry of tiles, only with their combinatorics. It matters not at all to them whether the geometric effects of deflation are simple or complex. Even the reflecting nature of Spectre substitution systems, in which the whole plane reverses handedness in every deflation, is ignored as irrelevant.

**Avoids dealing with very large or precise coordinates.** One way or another, the deflation technique needs to handle plane coordinates at high precision, because even if it does not *generate* every single tile in the large patch corresponding to its starting tile, it must at least consider locations everywhere in that patch to decide which of them to process further. Storing and processing large numbers is inconvenient and error-prone: if the algorithm runs in floating point, then rounding errors become more significant as the coordinates become more precise, and if plane coordinates are instead represented exactly as an integer linear combination of some set of algebraic numbers, then the integer coefficients risk overflowing.

The transducer technique never needs to consider any plane coordinate that is not a vertex of a tile in the final output. All the information about large supertiles is encapsulated in the combinatorial tile addresses, without dealing with their locations in the plane. Those tile addresses are essentially discrete, so it is easy for algorithms to handle them without any risk of imprecision. Overflow is still possible, but it manifests as running off the end of a finitely long address string and needing to extend it.

**No need to commit to  $n$  in advance.** In the deflation technique, you begin by choosing how large a patch to generate, by deciding on how high-order a supertile to begin from. In the transducer technique, you *can* work the same way, but more flexible approaches are also possible.

In particular, if you want to generate a *random* patch of a substitution tiling, then there is no need to precommit to the length of the tile addresses at all. Instead, you can literally ‘make it up as you go along’, by starting with a very short initial address, and extending it lazily as necessary: if the symbols of the starting tile address turn out to be insufficient to fill the whole output region, choose additional symbols at random to extend it, and proceed with tiling generation as if those additional symbols had been known all along.

**Random tilings from the exact limiting distribution.** Continuing on the theme of generating a random patch of tiling: in a typical substitution tiling the relative density of tile types in the plane will converge to a limiting distribution the larger a patch you consider (namely, the eigenvector with the largest eigenvalue of the matrix that describes how many of each subtile type are produced by deflating each supertile type).

Using the deflation technique for making a patch of tiling from a single  $n$ th-order supertile, you can approach this limiting distribution as closely as you like by choosing  $n$  sufficiently large, but the computational cost increases as you do so, so you must trade off how closely you want to approximate the limiting distribution with the amount of work you are prepared to do.

The transducer technique requires no tradeoff. When you invent each supertile symbol to extend the input address, you can choose that supertile symbol *directly* from the exact limiting distribution.

**Can handle infinite supertile boundaries.** As discussed already, transducer-based techniques can describe and successfully generate a region of tiling intersecting an infinite supertile boundary, because they do not depend on having any finite-order supertile in common between a pair of neighbouring tiles.

## 6.2 Address-finding

In the previous section we discussed the problem of turning a tile address into a patch of tiling. Another application of tiling automata is to go in the opposite direction. Suppose you are given a patch of tiles covering a region of the plane, and you wish to find an address that describes the same patch in terms of a particular substitution system.

(Perhaps the patch of tiles was generated by a different substitution system for the same tiling; or perhaps from a different method, such as a cut-and-project scheme. Or perhaps you do not even know that, and have merely received a patch in the form of a drawing, from some unknown source.)

The input to this procedure is precisely the output of the previous one: a collection of tiles, each one given its type, and the knowledge of which pairs of tiles are adjacent, along which edge of each one. We aim to recover an address describing one of the tiles in the patch – any one will do – such that regenerating a tiling from that address as described in the previous section will produce the same layout of tiles as the input.

To begin with, there is no hope of finding a *unique* tile address. The argument in the previous section is sufficient: if the maximum input/output lag of the transducer for a substitution system is  $d$ , and two tiles have a path of length  $j$  between them, then  $jd$  symbols of the address of one tile are sufficient to determine the type of the other. So a finite patch of tiling can only constrain finitely many symbols of the address of any of its tiles.

Therefore, an address-finding algorithm must deal in a representation of many possible tile addresses at once. A convenient representation is an NFA.

As a first step, we use Algorithm 2 from section 4.2.1 to generate a recogniser  $R$  for pairs of neighbouring edge addresses. As mentioned in section 4.2.2, this can also be regarded as a nondeterministic transducer taking one edge address as input and producing another as output. (For these purposes, a nondeterministic transducer is good enough, and it is convenient that this form of automaton has no lag between the input and the output.)

To analyse a patch of tiles, the essential plan is to focus on one tile at a time, and have an NFA  $A$  that matches all possible addresses for that tile that we have not yet ruled out. We begin by choosing a starting tile within the input patch, and initialising our NFA  $A$  to one that recognises any legal address at all for a tile of that type. (This is easy to construct from first principles as a DFA, and of course that is also a valid NFA.)

Next, we step across edge  $e$  of the starting tile  $t$ , arriving in its neighbour tile of type  $u$  via edge  $f$ . We must now construct a new NFA  $A'$  for the possible addresses of that destination tile.

To do this, we construct the Cartesian product  $A \times R$  of the previous NFA with the neighbour-recogniser automaton. A state of  $A \times R$  is an ordered pair consisting of a state  $a \in A$  and a state  $r \in R$ ; the product automaton has a transition  $(a, r) \xrightarrow{\alpha} (a', r')$  on a symbol  $\alpha$  if there exists  $\beta$  such that the transition  $a \xrightarrow{\beta} a'$  exists in  $A$ , and  $r \xrightarrow{(\beta, \alpha)} r'$  exists in  $R$ . That is, the NFA for  $t$ 's address accepts  $\beta$  as the next symbol from state  $a$ , and the neighbour recogniser accepts  $\alpha$  as the next symbol of  $u$ 's address if  $\beta$  is the next symbol of  $t$ 's. Finally, we delete every transition from the start state of the product machine which does not take  $(t, e)$  as the first input symbol and deliver  $(u, f)$  as the output symbol.

The resulting NFA describes a set of infinitely long tile addresses which are consistent with being the address of a tile of type  $u$ , whose neighbour via the edges  $e, f$  is a tile of type  $t$  described by the input NFA  $A$ . We reduce this NFA by deleting unreachable states, and translate to a canonical form (converting complex ordered-pair representations of its states back to something computationally simple like integers), to produce  $A'$ .

By repeating this procedure, we can walk around the entire input patch of tiling, via a path that visits every tile. (A Hamilton cycle is not necessary; visiting a tile more than once is harmless.) As we move around, our NFA evolves in two ways: it changes to reflect the tile we are currently standing on, and it also becomes more and more refined as the algorithm incorporates more knowledge about nearby tiles in the tiling.

Once we have visited all tiles, the NFA should be such that any valid path through it describes an address consistent with the tiles visited. For a reasonably large patch of tiling, it is likely that the NFA will give the first few symbols of the output tile address unambiguously.

If desired, at this point the output NFA can be determinised, via the usual technique of making a DFA whose states correspond to sets of NFA states. A DFA is easier to read, because it will begin with a unique transition for each address symbol that is uniquely determined. (In the NFA, one might have to trace many branches with the same symbols on them to check if one of them had a different idea.)

The remaining challenge is to choose just one address. For some purposes (depending on what the output is going to be used for), it is enough to choose randomly, or arbitrarily. However, if the input patch of tiling was a particularly interesting instance, such as a singular or symmetric one, then probably one of the possible addresses is the one most desired, and it is probably a simple, eventually periodic address with a short period. The author has found that a good approach is to end the walk around the tiling on a tile as close as possible to the pattern's centre of symmetry, and then search the NFA to find the *simplest* eventually periodic address that it accepts, measured by the combined length of its initial segment and repeating segment. This in turn can be done by iterating over candidate pairs of lengths in increasing order, and for each one, searching the automaton to find whether any address of that shape is accepted at all.

### 6.3 Analyses of tilings

One more possibility, given a finite-state automaton describing a tiling, is to transform the automaton in various ways to derive automata that describe classes of addresses, or address pairs, of particular interest.

For example, suppose one is interested in infinite supertile boundaries in general. As mentioned in section 5.1, an edge between two tiles is part of an infinite supertile boundary if and only if the neighbour address recogniser, given both tiles' addresses as input, never enters an accepting state. Therefore, by deleting all accepting states from the neighbour recogniser, a DFA is obtained which matches precisely those pairs of addresses that lie on such a boundary.

If two address pairs lie on the same infinite supertile boundary, then they have some finite-order supertile in common, so their paths through this DFA will at some point reach the same state. Therefore, one can imagine an equivalence relation on address pairs in which two pairs are considered equivalent if they differ in only finitely many places; an infinite supertile boundary as a whole corresponds to an equivalence class of this relation.

In particular, suppose we restrict our attention once again to the useful class of *eventually periodic* addresses.

As mentioned in section 5.1, if an individual tile address is described as an initial segment and a repeating segment, then its containing infinite supertile is defined by the repeating segment alone. Pairs of infinite supertiles bordering on each other are defined by a cyclic path within the winnowed DFA. By searching for those cycles in increasing order of length, it is possible to automate the process of enumerating the infinite supertile boundaries in the eventually-periodic class. An analysis similar to this is begun for the Spectre tiling in [Pao]; this DFA technique permits it to be automated for any tiling.

### 6.3.1 Finding out why a substitution system was ambiguous

If the substitution system was originally ambiguous, and Algorithm 9 was used to turn it into an unambiguous one admitting a transducer, then a different analysis of this kind can be used to find addresses in the unrefined system which correspond to more than one address in the refined one – in other words, to find the particular hard-to-distinguish tilings which *gave rise* to the ambiguity in the substitution system.

Some of this information can be extracted from an attempt to determinise a transducer for the original (coarse) tiling. If the section 4.3.1 technique is used to detect that determinisation has failed, then a by-product is the ability to identify a particular input to the transducer with two possible outputs, via the cycle found in the graph  $G$  and a path to that cycle from the start state. However, this only describes *one* ambiguous input – whichever was the first one to be detected during the failed transducer construction. The following technique will find them all systematically.

To do this, we first make a DFA which matches the ‘diagonal’ subset  $\mathcal{D} \subset \mathcal{T} \times \mathcal{T}$  of pairs of tile addresses in the refined system: the language of strings made by zipping the *same* tile address with itself. This is matched by a DFA isomorphic to the one for  $\mathcal{T}$  itself, consisting of a START state, and a state for each  $(\textit{layer}, \textit{tile type})$  pair, with transitions derived from the substitution system in an obvious manner. We aim to find a pair of distinct tile addresses  $A, A'$  accepted by this DFA which have the same image under the ‘forgetful’ map  $\phi$  which discards tile subtypes to recover the corresponding address in the original unrefined system.

If  $A, A'$  have the same subtype for their  $n$ th-order supertiles, for some  $n$ , then they must exactly match in all lower-order tile subtypes as well, because the subtype of any tile together with a subtype index uniquely determines the type of the next lower-order tile, and so on inductively. So if  $A \neq A'$ , then there must be some  $k \geq 0$  such that the two addresses exactly match in the first  $k$  symbols, and thereafter, have *no* symbol in common.

Now consider what happens if we zip together the addresses  $A, A'$  into a combined string containing ordered pairs of a symbol from each address, and use that as input to the product DFA  $\mathcal{D} \times \mathcal{D}$ . While processing the initial  $k$  symbols, the product DFA will remain in a ‘diagonal’ state, i.e. one of the form  $(s, s)$ . After that, every transition will be on a pair of symbols which match in their coarse tile type, and subtype index, but *never* match in their tile subtype from refinement.

We can construct a subset of  $\mathcal{D} \times \mathcal{D}$  matching all such strings by starting from every diagonal state and using only transitions on symbols of the form  $((t), (t'))$  or  $((\overset{i}{\leftarrow} t), (\overset{i}{\leftarrow} t'))$  for tiles  $t, t'$  which are distinct refinements of the same coarse tile type. Any infinite path in this subset DFA corresponds to the tail of some pair of ambiguous tile addresses, and a full ambiguous tile address can be constructed by prefixing to it any path from the DFA start state to the diagonal state it began from.

## 7 Results

In this section we shall present some results of applying these algorithms to well-known tilings. Full-page figures at the end of the article give the complete details of each substitution system suitable for input to these algorithms: the edge types and edge deflation rules are shown (constituting the ‘geometric source code’ described in section 2.7), and each deflation diagram is shown in full, with both sides of each edge labelled with an appropriate  $\mathbf{E}_{u,v}$  or  $\mathbf{I}_{i,j}$  symbol, so that the full combinatorial adjacency maps can be read off these diagrams, or cross-checked against them if regenerating them from the geometry.

Where a refinement of the system is needed to make it unambiguous, that refinement is also shown in a figure. The refinement diagrams do not need to repeat the detailed adjacency maps from their source tiling, since those are unchanged; they only need to show how many subtypes of each original tile type exist, and which subtypes appear in each deflation.

### 7.1 Penrose P2 and P3 tilings

The Penrose P2 tiling of kites and darts, and the P3 tiling of thin and thick rhombs, can each be generated by either a substitution system of Robinson triangles, or one made from the whole tiles. Both systems have strengths. The Robinson-triangle systems are geometrically simple in that each tile’s deflation occupies the

same region of the plane as the original tile (if scaled appropriately), and preserve all the symmetry in the original tilings. On the other hand, the whole-tile system is naturally more practical if your aim is to generate actual Penrose tilings for display, since it does not require a post-processing step of recombining the two triangular halves of each tile.

(As a practical matter, this recombination could be done by a separate software layer consuming the output of a transducer, but another approach would be to augment the substitution system with a one-off base layer whose parent is the main layer of Robinson triangles, deflating one half of each tile into the tile itself and the other half into an outline doubling back on itself and enclosing no area.)

All four of these substitution systems –  $\{ \text{P2 and P3} \} \times \{ \text{triangles, whole tiles} \}$  – are unambiguous. Algorithm 6 successfully constructs a deterministic transducer for each one.

Figures 20, 21 and 22 show the P2 triangle system in full; figures 26, 27 and 28 show the P2 whole-tile system; figures 23, 24 and 25 show the P3 triangle system; figures 29, 30 and 31 show the P3 whole-tile system.

## 7.2 Ammann-Beenker tiling

The Ammann-Beenker tiling is usually described as a two-tile system, consisting of a square and a rhombus. However, the rhombus comes in two mirror-image forms (although these are indistinguishable if you do not show the vertex markings that force the tiling to be aperiodic). For the purposes of these algorithms, mirror-image tiles must be counted as different.

When choosing a substitution system for the Ammann-Beenker tiling, one also has a similar choice to the Penrose tilings: either bisect the square tile into a pair of right triangles so that each tile deflates to a patch of subtiles occupying the same area of the plane, or leave the square whole and instead complicate the shapes of the deflation maps.

As mentioned in section 4.3.2, the Ammann-Beenker tiling is ambiguous, because when eight rhombus tiles appear around a single vertex, they can only do so in one way, which requires a particular arrangement of the two mirror-image forms (see Figure 14). This is equally true of either substitution system. Moreover, both systems require two passes of Algorithm 9 to refine them from the original three- or four-tile system into one that admits a deterministic transducer.

The unambiguous refinements of both systems involve eight variants of the rhombus (four of each of the two mirror-images). When the square is left whole, there are eight variants of that too; when it is bisected, each half-square splits into *five* variants, which can combine in a subset of the possible combinations.

Figures 32, 33 and 34 show the Ammann-Beenker substitution system involving two rhombus tiles and the two triangular halves of the square, and Figure 35 shows its unambiguous refinement. Figures 36, 37 and 38 show the system with a whole square, and Figure 39 shows the unambiguous refinement of that system.

## 7.3 Spectre tiling

[SMKGS24b] presents two substitution systems for the Spectre tiling. One, shown in figure 2.1 of the paper, is a minimalist system containing two tile types: a single Spectre, and the ‘Mystic’ double tile consisting of two Spectres at  $30^\circ$  to each other. The other, spread across figures 4.2, 5.1, and 5.3, involves nine hexagonal metatiles and eight different types of edge, with one set of deflation rules turning hexagons into more hexagons, and a second set turning them into Spectre tiles.

Both of these systems can be represented in the combinatorial form required as input to these algorithms. The 9-hexagon system is essentially in that form already, but the simpler Spectre/Mystic system is more difficult to represent, because the paper does not state how the edges of a single Spectre or Mystic correspond to the edges of the patch of tiles deflated from each one. However, such an edge mapping does exist; information equivalent to it is available in various sources such as [Che], and the author is indebted to Pieter Mostert in particular for discussions involving the related ‘comet-rhomb tiling’ from which it can be derived.

To specify the edge mapping for the Spectre/Mystic system, we first classify the edges into two distinct types, and assign a direction to each one. The edge types correspond to the direction of the edge in the plane: edges whose direction is a multiple of  $60^\circ$  have one type, and those at an odd multiple of  $30^\circ$  the other type. Directions are assigned in alternation around the 14 edges of the tile (counting the long edge as two collinear edges, as usual).

This assignment of edge types separates the previously identical Spectre tiles into two distinct types, again depending on their orientation mod  $60^\circ$ , with most Spectres being of one type, and a small number being the ‘skew’ Spectres with all the edge types swapped. Each skew Spectre is then fused with one of its neighbours to make the Mystic double-tile. Figure 40 shows the resulting two tile types, with their edge markings and directions.

With the edges distinguished in this way, it is now possible to write down a pair of deflation rules that turn each edge consistently into a pattern of other edges. Figure 42 shows these deflation rules.

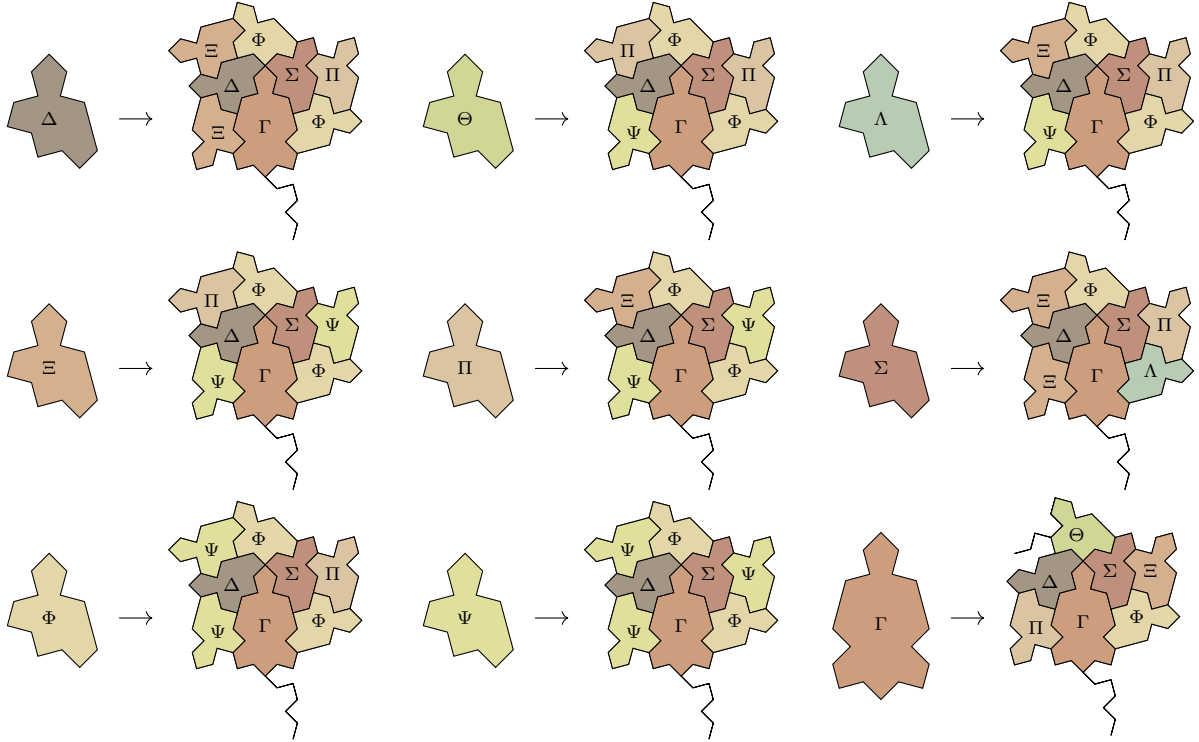


Figure 17: The 9-tile refinement of the Spectre/Mystic substitution system

If the Spectre and Mystic outlines are deflated by applying those rules, each one generates an output region which can be tiled with a number of Spectres, including one skew one forming half of a Mystic. However, since the Spectre deflation reflects the plane, these two regions must either be tiled with reflected Spectres, or be reflected themselves before tiling with Spectres in the original handedness. (We have chosen the latter approach in our diagrams.)

The deflated outline also includes some zero-thickness spurs. In both outlines a long spur of six edges protrudes outwards from the patch outline, and then retraces its steps to its starting point. The Mystic deflation also includes two further spurs, one intruding *inward* into the region and crossing over interior edges of its tiling with Spectres, and one running back and forth along part of the outline.

Figures 41 and 43 show the deflation diagrams for the two tiles in full<sup>10</sup>. The difficult spurs in the Mystic deflation are shown detached from the main tiling, with an indication of where they should properly start from.

The algorithms in this article take all of this complication in their stride. The adjacency maps for the two deflations describe the complicated spurs in the same way as described in section 2.3, mapping some  $\mathbf{E}_{u,v}$  to each other, and whenever two pairs of edges coincide, making an arbitrary choice about which one to map to which<sup>11</sup>.

The alternative 9-hexagon system is not shown in full here, partly because [SMKGS24b] gives all the details required, and also because it is redundant, for the following reason.

The 9-hexagon system is unambiguous. If it is transcribed into a combinatorial description in the style of this article, with a ‘Spectres’ layer and a ‘hexagonal metatiles’ layer and two sets of deflation rules, then that description admits a deterministic transducer.

On the other hand, the Spectre/Mystic system is ambiguous: it does not admit a deterministic transducer. However, one pass of Algorithm 9 refines it into an unambiguous system consisting of nine tile types: eight different variants of the single Spectre tile, and still only one Mystic.

The unambiguous system generated by Algorithm 9 *exactly* corresponds to the 9-hexagon system: each of its 9 tile types corresponds to one of the hexagons, and every deflation diagram in the refined system matches the corresponding diagram in Figure 5.1 of [SMKGS24b], *except* that the metatile shapes are Spectres and

<sup>10</sup>As a practical matter, when generating a Spectre tiling from this system, one could add a base layer to the substitution system which separates the Mystic tile into its two Spectres. This is a simple transformation, and left to the reader.

<sup>11</sup>The adjacency map in Figure 43 shows a particular choice of which edges to map to which, but this is not critical to the algorithm. For example, the diagram shows the mappings  $\mathbf{E}_{15,-4} \leftrightarrow \mathbf{E}_{12,-2}$  and  $\mathbf{I}_{2,9} \leftrightarrow \mathbf{I}_{3,4}$  on a pair of edges which coincide if the separate spur is replaced at its proper starting point (shown by a red diamond). The alternative choice  $\mathbf{E}_{15,-4} \leftrightarrow \mathbf{I}_{3,4}$  and  $\mathbf{I}_{2,9} \leftrightarrow \mathbf{E}_{12,-2}$ , mapping the top side of each of those edges to the bottom side of the *other* one, would work equally well and make no difference to the success of the algorithms.

Mystics instead of hexagons. Figure 17 shows these deflation diagrams in full, with the same tile names (and colours) as [SMKGS24b] uses for the corresponding hexagons.

Moreover, a deterministic transducer constructed from the 9-hexagon system is *equivalent* to one constructed from the refined Spectre/Mystic system shown here. Having labelled the tile types compatibly, tile addresses in the two systems look essentially the same (up to differences of detail such as whether the lowest-order Spectre is labelled directly with one of the nine types, or whether it is deflated from a lowest-order hexagon with the same type), and the two transducers agree on the neighbour address for any input tile. This occurs because *after* the transducer is built, there are no remaining references to the edges of any supertile, so the fact that the supertiles are hexagonal in one system and Spectre-shaped in the other is no longer visible.

So applying the refinement algorithm to the Spectre tiling has not generated a new and interesting substitution system. Instead, it has re-derived one of the systems in the paper from the other one (with the small difference of more complicated tile shapes but fewer edge types). However, even without any new discoveries, the fact that the two analyses agree is a useful check that the algorithms presented here are behaving as expected.

Also, it is useful to have re-derived the 9-tile system as a refinement of the Spectre/Mystic system, because we now have an explicit mapping between the two systems. Therefore it becomes possible to apply the procedure from Section 6.3.1 to find out details of *why* the Spectre/Mystic system did not already admit a deterministic transducer: what infinite-order supertile(s) have multiple representations?

Running that algorithm reports that there is just *one* ambiguous infinite supertile, with three distinct addresses in the refined system which all look the same in the unrefined Spectre/Mystic system. In the unrefined system, the ‘simplest’ address of a tile in the ambiguous supertile is a Spectre tile which is subtile 7 of a larger Spectre (in the arbitrary indexing of subtiles used in Figure 41), which is subtile 7 of its still larger parent, and so on for ever:

$$\text{spectre} \xleftarrow{7} \text{spectre} \xleftarrow{7} \text{spectre} \xleftarrow{7} \text{spectre} \xleftarrow{7} \dots$$

In the refined system, this address separates into three. One of them has the same tile type  $\Psi$  at every level, so that it is invariant under deflation. The other two alternate between the  $\Xi$  and  $\Pi$  tile types, so that each one deflates to the other:

$$\begin{aligned} \Psi &\xleftarrow{7} \Psi \xleftarrow{7} \Psi \xleftarrow{7} \Psi \xleftarrow{7} \dots \\ \Xi &\xleftarrow{7} \Pi \xleftarrow{7} \Xi \xleftarrow{7} \Pi \xleftarrow{7} \dots \\ \Pi &\xleftarrow{7} \Xi \xleftarrow{7} \Pi \xleftarrow{7} \Xi \xleftarrow{7} \dots \end{aligned}$$

In fact, the two infinite supertiles with  $\Pi, \Xi$  tiles are neighbours. Specifically, a transducer constructed from this substitution system reports that each of the following two edge addresses maps to the other one:

$$\begin{aligned} (\Xi, 0) &\xleftarrow{7} \Pi \xleftarrow{7} \Xi \xleftarrow{7} \Pi \xleftarrow{7} \dots \\ (\Pi, 9) &\xleftarrow{7} \Xi \xleftarrow{7} \Pi \xleftarrow{7} \Xi \xleftarrow{7} \dots \end{aligned}$$

So these two supertiles occur in the same Spectre tiling of the plane, side by side. This is interesting because it means that some rigid motion of the plane – in fact, a  $\frac{1}{6}$  rotation – maps one of these identical supertiles to the other, and therefore, leaves an infinite region of the plane invariant. Under the same rotation, what happens to the rest of the plane?

A plausible answer would be that the whole plane is symmetric under that rotation. There are Spectre tilings with a rotational symmetry. However, there are none with *6-way* rotational symmetry, only 2-way and 3-way. The answer in this case is more interesting: the Spectre tiling containing these two infinite supertiles is singular in the same sense as the Penrose infinite cartwheel pattern, in that *almost* all of the plane is invariant under that  $60^\circ$  rotation, with only a small number of narrow paths of tiles varying. Figure 44 shows the central section of this singular tiling (which can be found by other methods too).

The third version of the same infinite supertile, involving a  $\Psi$  tile at every level, occurs in a separate but extremely similar Spectre tiling. It also has  $60^\circ$  near-symmetry, but moreover, if the two tilings are overlaid so that the  $\Psi$  supertile corresponds to one of the  $\Pi, \Xi$  supertiles, then they match each other almost completely, with only one of the asymmetric paths varying between the two tilings. (Which path varies depends on which of  $\Pi, \Xi$  and  $\Xi, \Pi$  you overlaid the  $\Psi$  supertile on.)

## 7.4 Hat tiling

[SMKGS24a] presents two substitution systems for the hat tiling. One, shown in figure 2.11 of the paper, is a minimalist system very similar to the Spectre/Mystic system, consisting of two tiles, of which one is a single hat, and the other is a fusion of a reflected hat with one of its neighbours, in exactly the same way that the Mystic is a fusion of the rare skew Spectre with a normally oriented neighbour. These deflate to patches of hats

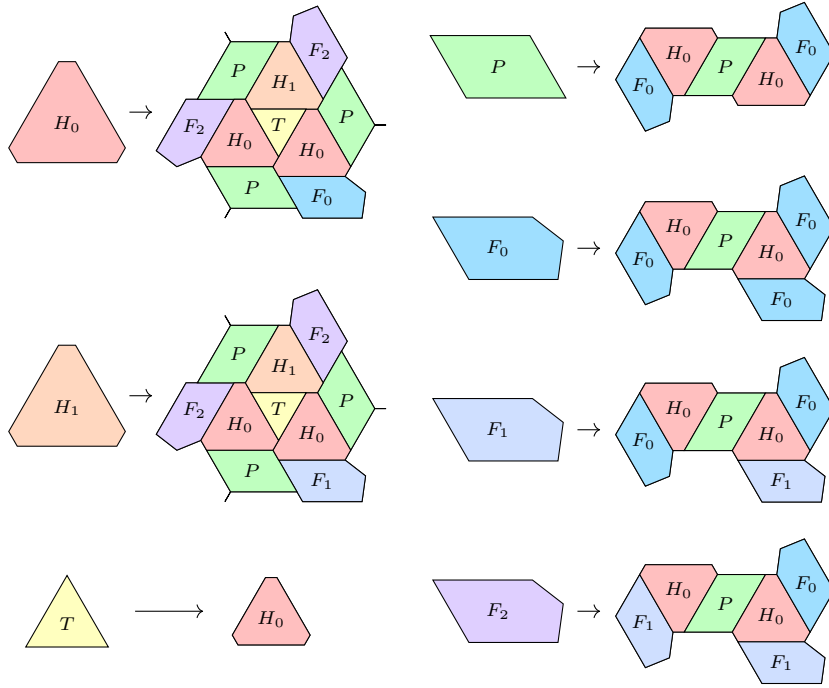


Figure 18: The *HHTPFFF* substitution system

labelled  $H_8$  and  $H_7$  respectively. The other system consists of four metatiles  $H, T, P, F$  in simple polygonal shapes, with one deflation rule to turn them into more metatiles, and another to turn them into hats (shown in figures 2.8 and 4.1 of the paper respectively).

As with the Spectre/Mystic system, in order to handle either of these hat substitution systems using the techniques in this paper, we first need to know exactly how the edges match up between each tile type and its deflation.

The rules for the  $\{H_7, H_8\}$  system are very similar to those for the Spectre/Mystic system: as in that system, we classify the edges into two types based on orientation<sup>12</sup>, and assign directions in alternation around the tile. Figure 45 shows the two tiles marked in this fashion, and Figure 47 shows the deflation rules for the two edge types.

Transforming each edge of the two tile types via these rules expands each one into a patch which can be tiled by one double-hat fusion and either 6 or 7 ordinary hats. Figures 46 and 48 show the results of this process<sup>13</sup>.

The *HTPF* system is presented in two forms. In one form, the deflation diagrams of the metatiles overlap; in the other, selected metatiles are removed from each deflation diagram so that each tile has a unique supertile. For these algorithms, only the non-overlapping form is suitable.

Edge annotations for the non-overlapping *HTPF* system are derived in [BGS25] (figures 4 and 5), and reproduced here in Figure 50 (showing the edges subdivided as mentioned in section 2.4, with edge types and directions), and Figures 51 and 52 showing the rules for transforming each edge type into a sequence of sub-edges during deflation of metatiles to other metatiles or hats respectively. The resulting adjacency maps are shown in Figures 53 and 54.

*Both* of these substitution systems are ambiguous. In each case, refinement via Algorithm 9 resolves the ambiguity by creating a system with more tile types.

The unambiguous version of *HTPF* is a substitution system one might call *HHTPFFF*: it consists of two variants of the original  $H$  tile, three variants of  $F$ , and just one variant of each of  $T$  and  $P$ . These are shown in Figure 18.

The unambiguous version of the  $\{H_7, H_8\}$  system derived by the same procedure involves seven variants of the single hat tile, and still just one variant of the double-hat. These are shown in Figure 19.

As in the previous section, we can apply the algorithm in section 6.3.1 to each of these refined systems, to discover the reason why each system was originally ambiguous.

<sup>12</sup>In the hat tiling, this classification of edge types also matches the difference in length: the hat tiling inherits from its underlying kite tiling the property that an edge of length 1 and one of length  $\sqrt{3}$  always differ in orientation by an odd multiple of  $30^\circ$ .

<sup>13</sup>As with the Spectre system, one might wish to add a base layer to this system separating the double-hat tile back into its two individual hats. Another useful optional base layer, in this or the *HTPF* system, is one that divides each hat into the eight kites of the underlying kite tiling, which allows the output of these algorithms to be handled in a discrete manner as subsets of the kites in that grid.

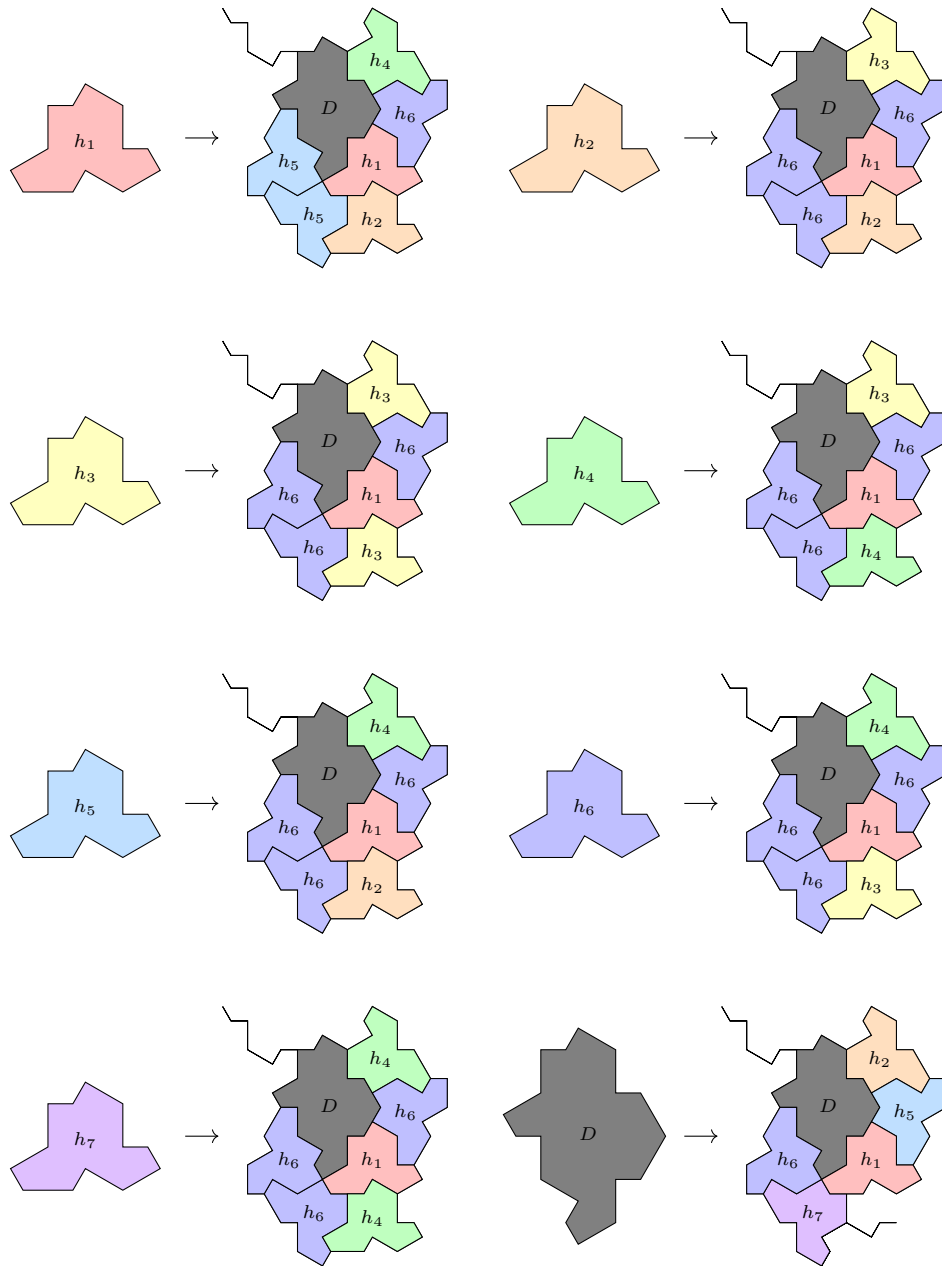


Figure 19: The 8-tile refinement of the  $H_7/H_8$  system for hats

For the 8-tile refinement of the  $\{H_7, H_8\}$  system, the answer is extremely similar to the answer for the Spectre/Mystic system, described in the previous section. Again, there is just one infinite supertile in the unrefined system which has three distinct representations in the refined system. Moreover, again, two of those are neighbours within the same tiling of the plane, rotated  $60^\circ$  relative to each other – and, also just like the Spectre case, that tiling has 6-way rotational near-symmetry. The third identical infinite supertile occurs in a distinct tiling of the plane, but a very similar one.

The unrefined address of a tile in this infinite supertile consists of a hat which is subtile number 6 of a larger hat, which is subtile 6 in turn of the next larger hat, and so on for ever:

$$\text{hat} \stackrel{6}{\leftarrow} \text{hat} \stackrel{6}{\leftarrow} \text{hat} \stackrel{6}{\leftarrow} \text{hat} \stackrel{6}{\leftarrow} \dots$$

In the refined system, the three corresponding addresses each have the same type of hat at every layer (unlike the Spectre case, where two of the addresses alternated tile types):

$$\begin{aligned} h_2 &\stackrel{6}{\leftarrow} h_2 \stackrel{6}{\leftarrow} h_2 \stackrel{6}{\leftarrow} h_2 \stackrel{6}{\leftarrow} \dots \\ h_3 &\stackrel{6}{\leftarrow} h_3 \stackrel{6}{\leftarrow} h_3 \stackrel{6}{\leftarrow} h_3 \stackrel{6}{\leftarrow} \dots \\ h_4 &\stackrel{6}{\leftarrow} h_4 \stackrel{6}{\leftarrow} h_4 \stackrel{6}{\leftarrow} h_4 \stackrel{6}{\leftarrow} \dots \end{aligned}$$

The two of these supertiles that appear together in the same tiling are the ones with  $h_2$  and  $h_4$  tile types. The tiling itself is shown in Figure 49. Like the singular Spectre tiling, the asymmetric paths come in two forms; unlike the Spectre tiling, one of those forms is a straight line rather than a wiggly path. (If the hats are instead drawn as turtles, the straight lines are aligned naturally to the underlying kite tiling.)

The third copy of this infinite supertile, involving the  $h_3$  address, is part of a second 6-way singular hat tiling. If the two tilings are overlaid so that the  $h_3$  supertile corresponds to the  $h_4$  supertile, then the two tilings differ only in a single straight line of hats; if instead the two tilings are overlaid so that the  $h_3$  supertile corresponds to  $h_2$ , then they instead differ in a wiggly path. [Soc23] exhibits these two tilings and their two minimal differing paths.

Applying the section 6.3.1 algorithm to the *HHTPFFF* substitution system instead of the 8-tile refinement of  $\{H_7, H_8\}$  reveals no new interesting cases. In this system, there is again a single infinite supertile with multiple representations, which in the unrefined *HTPF* system has an address consisting entirely of  $F$  metatiles, with each one being subtile number 5 of its supertile (in the numbering of Figure 53):

$$\text{hat} \stackrel{0}{\leftarrow} F \stackrel{5}{\leftarrow} F \stackrel{5}{\leftarrow} F \stackrel{5}{\leftarrow} F \stackrel{5}{\leftarrow} F \stackrel{5}{\leftarrow} \dots$$

This infinite supertile has just two possible representations in the refined *HHTPFFF* system, because both  $F_0$  and  $F_1$  can appear as subtile 5 of some version of  $F$ , but  $F_2$  cannot. For each of  $F_0$  and  $F_1$ , subtile 5 is the same type as itself, so the two possible addresses are

$$\begin{aligned} \text{hat} &\stackrel{0}{\leftarrow} F_0 \stackrel{5}{\leftarrow} F_0 \stackrel{5}{\leftarrow} F_0 \stackrel{5}{\leftarrow} F_0 \stackrel{5}{\leftarrow} \dots \\ \text{hat} &\stackrel{0}{\leftarrow} F_1 \stackrel{5}{\leftarrow} F_1 \stackrel{5}{\leftarrow} F_1 \stackrel{5}{\leftarrow} F_1 \stackrel{5}{\leftarrow} \dots \end{aligned}$$

These correspond exactly to the  $h_3$  and  $h_2$  supertiles from the other substitution system. The  $h_4$  variant of that supertile does not appear separately in this system.

## 8 Future possibilities

One useful operation not implemented by this suite of algorithms is the ability to translate the same tiling from one substitution system to another, by creating a transducer that would consume an address in the first system and emit an address in the second.

Such a transducer would not necessarily be able to keep the invariant seen in the transducers here, of emitting exactly one output symbol per input symbol, because not all substitution systems for the same tiling deflate by the same factor. For example, there is a ‘half-deflation’ system for the P2 and P3 Penrose tilings [de 81a] which deflates each one to the other, such that two deflations return to the same tiling you started with, having performed what would normally be a full deflation. [mat] also presents systems for the hat tiling which take two deflations to repeat the effect of a single deflation in the  $\{H_7, H_8\}$  or *HTPF* systems (although in this case the intermediate tiling is still a hat tiling).

If an algorithm of this form were possible, then it might also be possible to use it to match a substitution system against *itself*, to determine if there exist any pairs of distinct addresses which give rise to an identical tiling of the plane. For example, the system in [mat] has such pairs, because in some cases, half-inflating

a perfectly symmetric instance of the hat tiling leads to a ‘singular’ (nearly symmetric) instance, and so the tile addresses in the symmetric tiling must break its symmetry in order to specify which way round the not-quite-symmetric singular deflation will be.

## 9 Implementation

An implementation of the algorithms in this article, written in Rust, is in the `crates.io` package repository under the name `substitution-tiling-transducers`.

## 10 Acknowledgments

I am grateful to Robin Houston, Craig Kaplan, Pieter Mostert and mathBlock for useful discussions and encouragement.

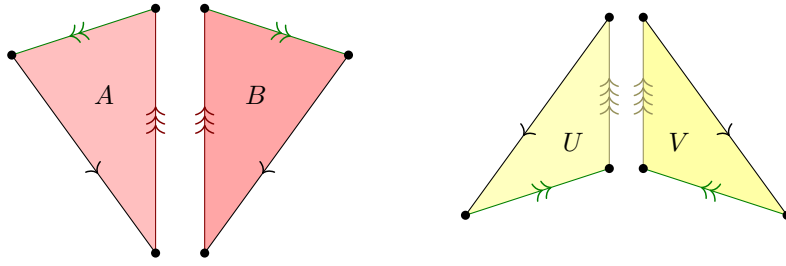


Figure 20: Diagrams of the P2 Robinson-triangle tiles, with labelled edges

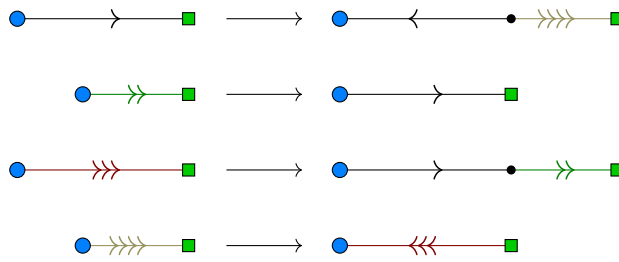


Figure 21: Edge deflation rules for P2 Robinson triangles

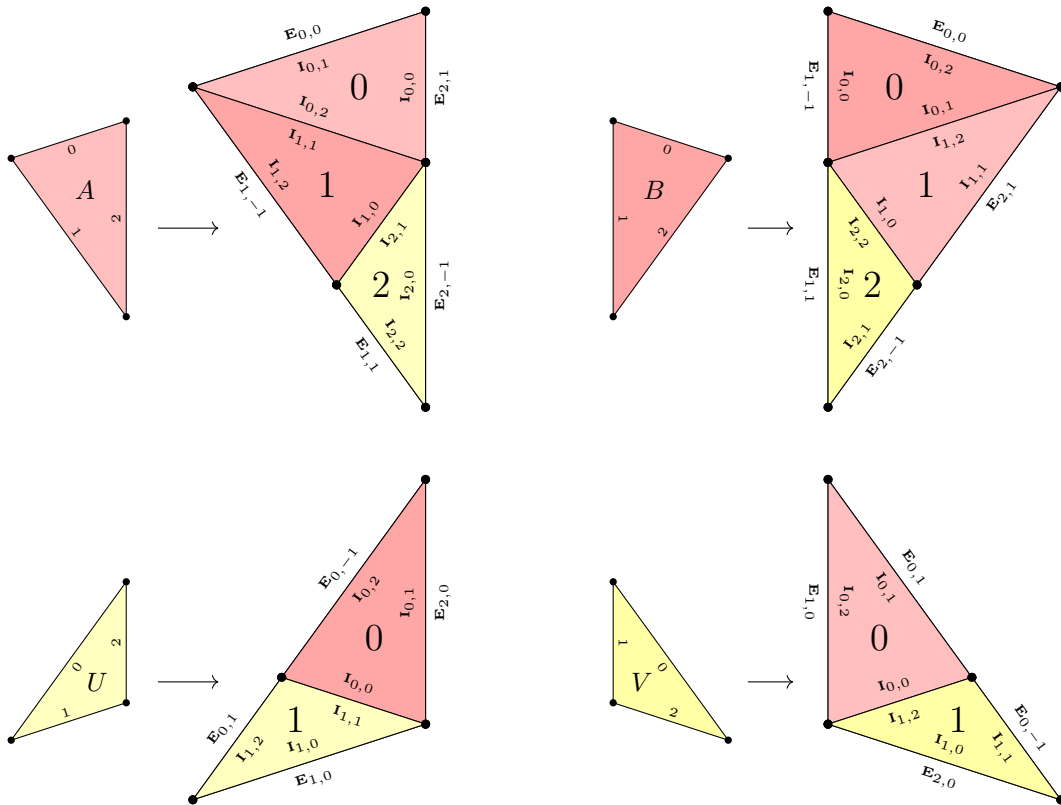


Figure 22: Adjacency maps for P2 Robinson triangles

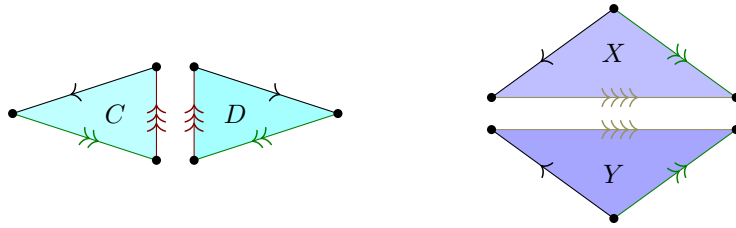


Figure 23: Diagrams of the P3 Robinson-triangle tiles, with labelled edges

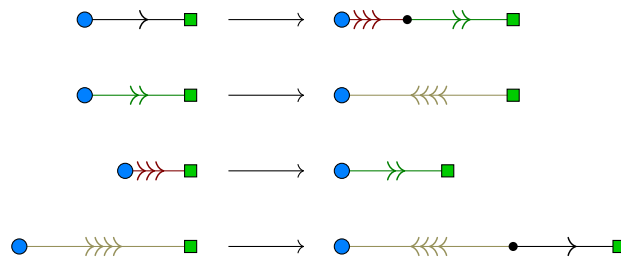


Figure 24: Edge deflation rules for P3 Robinson triangles

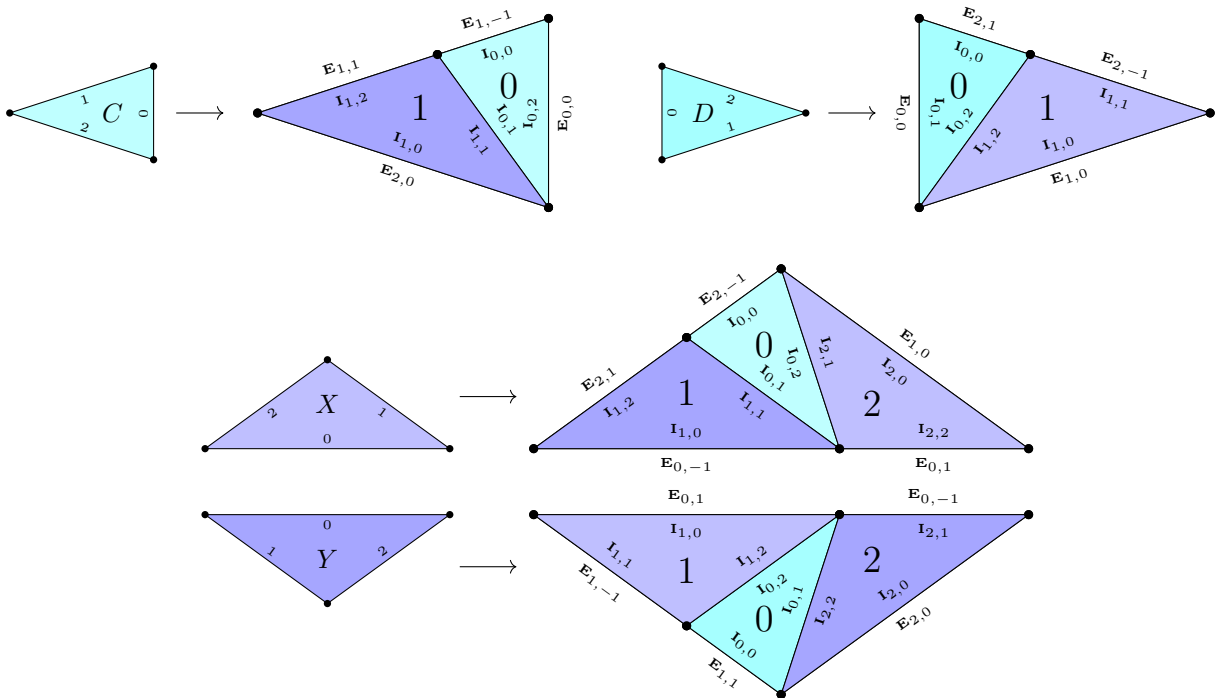


Figure 25: Adjacency maps for P3 Robinson triangles

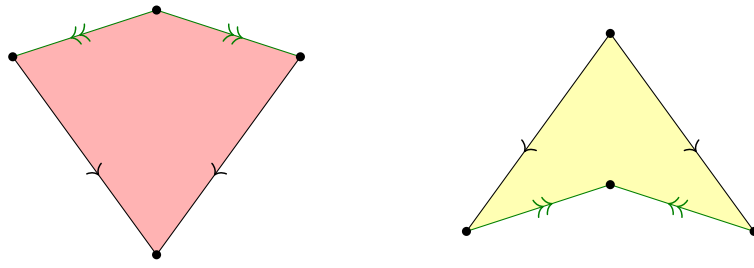


Figure 26: Diagrams of the P2 whole tiles, with labelled edges

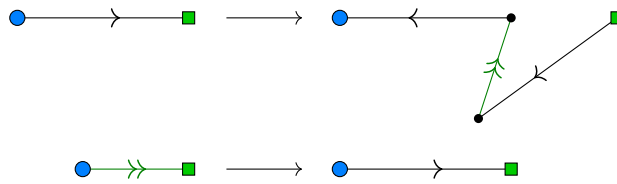


Figure 27: Edge deflation rules for P2 whole tiles

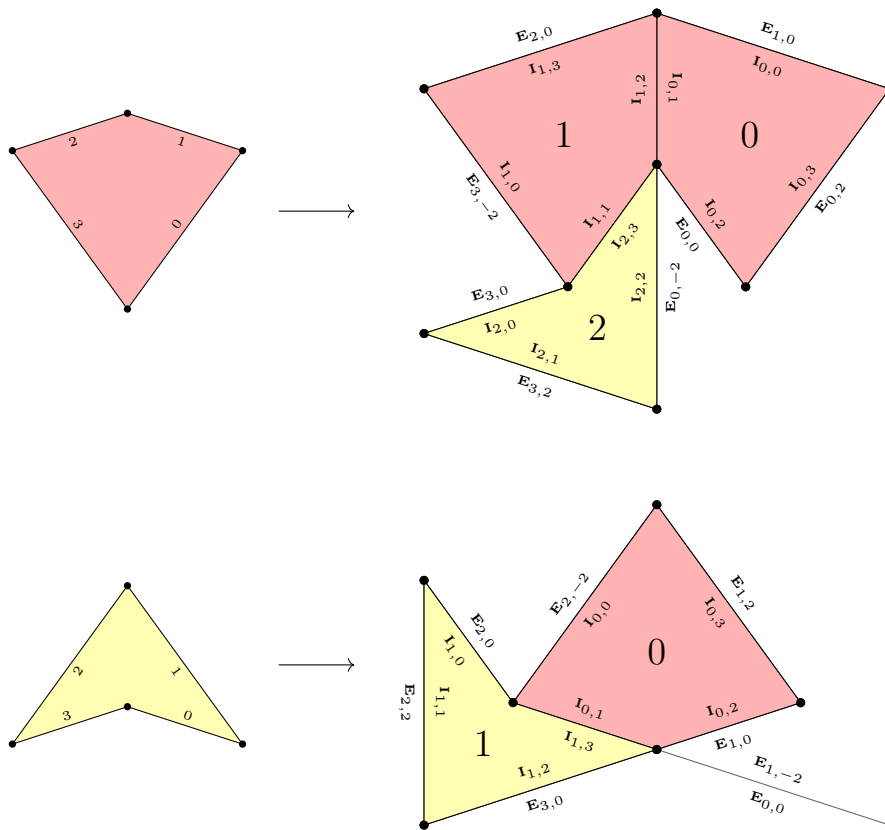


Figure 28: Adjacency maps for P2 whole tiles

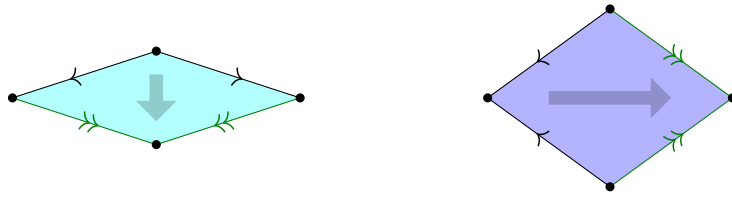


Figure 29: Diagrams of the P3 whole tiles, with labelled edges

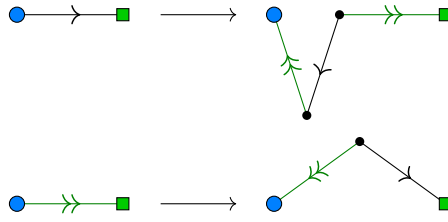


Figure 30: Edge deflation rules for P3 whole tiles

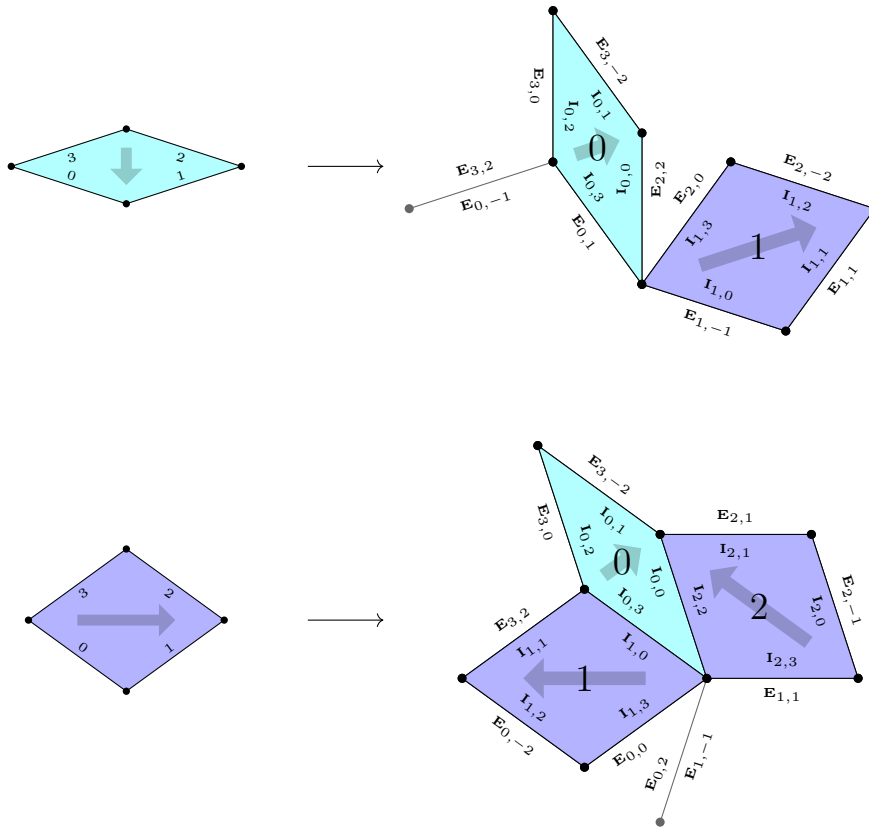


Figure 31: Adjacency maps for P3 whole tiles

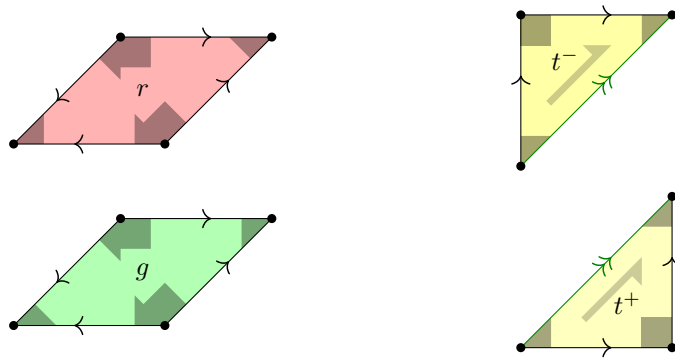


Figure 32: Diagrams of the Ammann-Beenker tiles (with the square bisected), with labelled edges

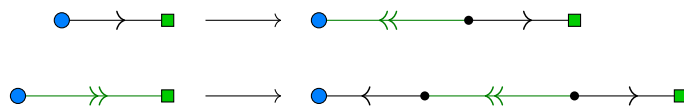


Figure 33: Edge deflation rules for the Ammann-Beenker tiling

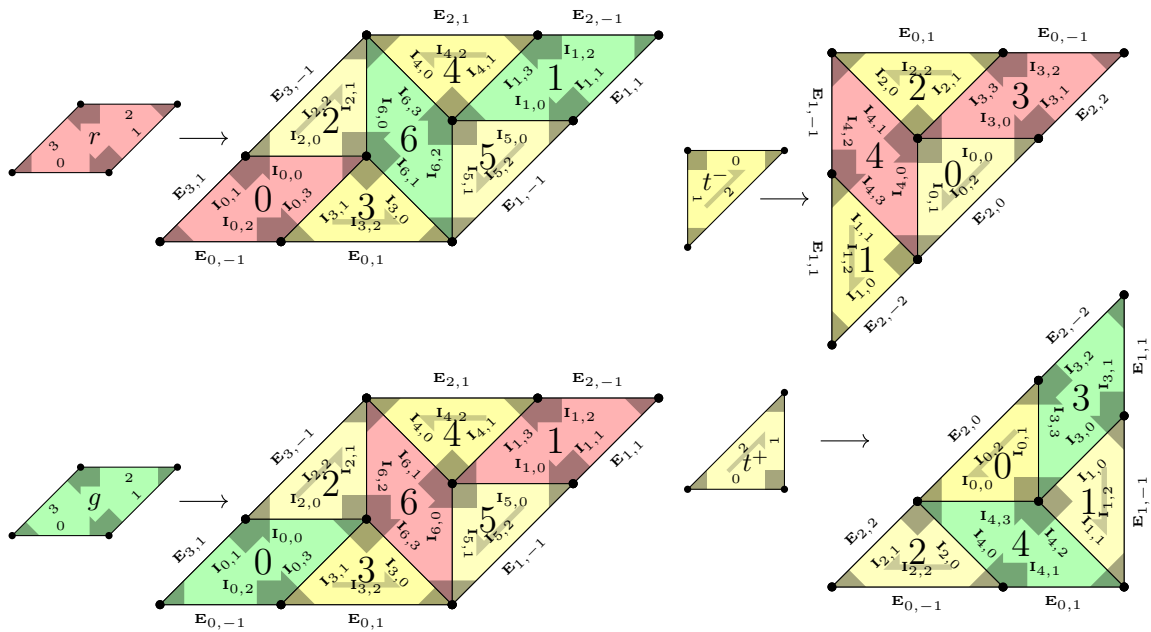


Figure 34: Adjacency maps for the Ammann-Beenker tiling

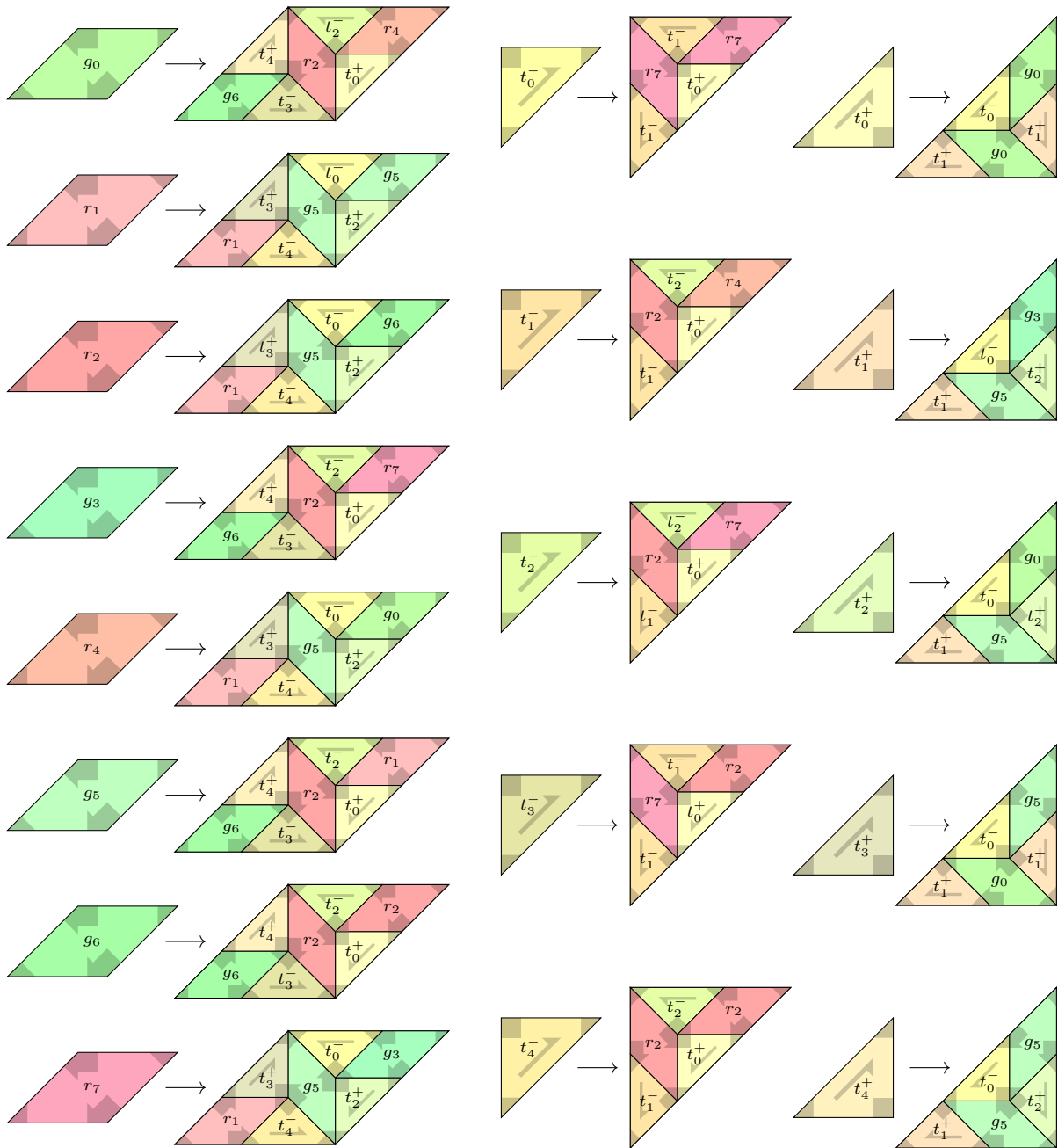


Figure 35: Unambiguous refinement of the Ammann-Beenker system, with the square bisected

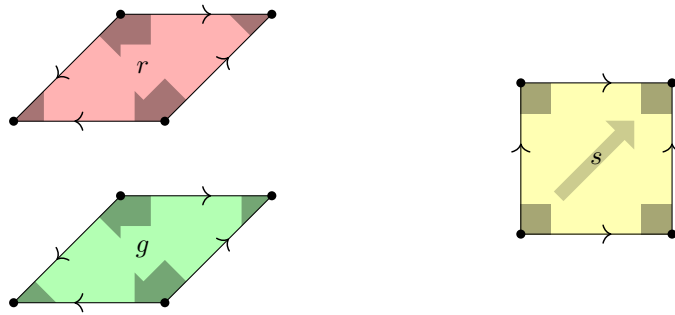


Figure 36: Diagrams of the Ammann-Beenker tiles with the square whole, with labelled edges

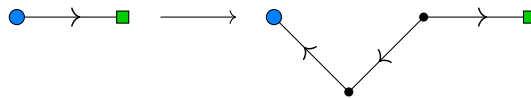


Figure 37: The single edge deflation rule for the Ammann-Beenker tiling with the square whole

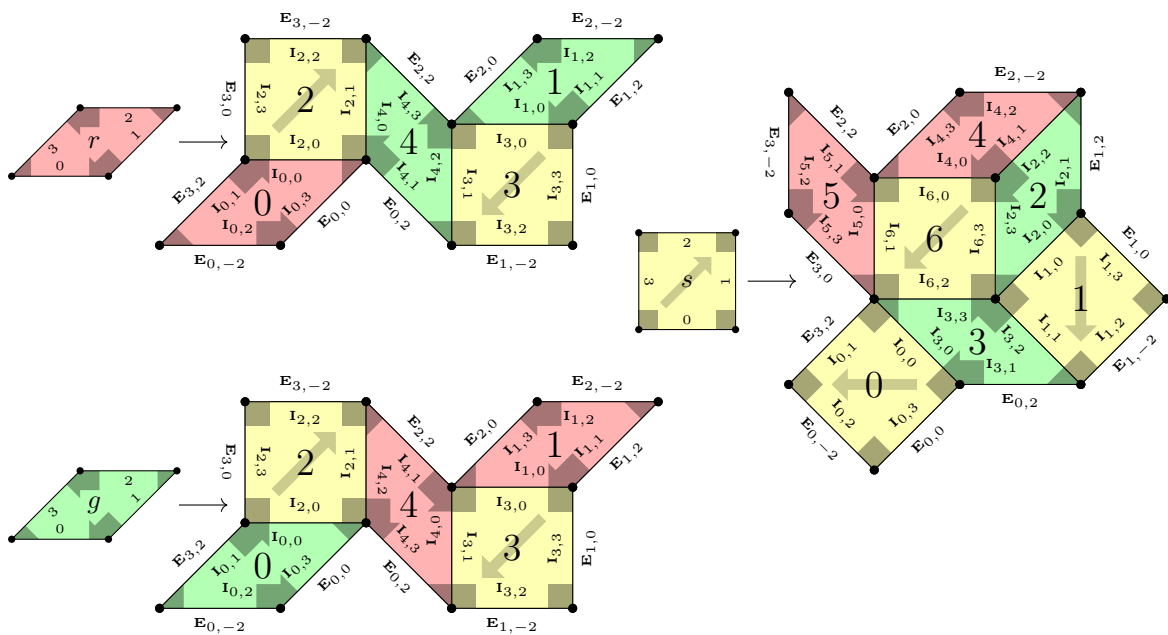


Figure 38: Adjacency maps for the Ammann-Beenker tiling, with the square whole

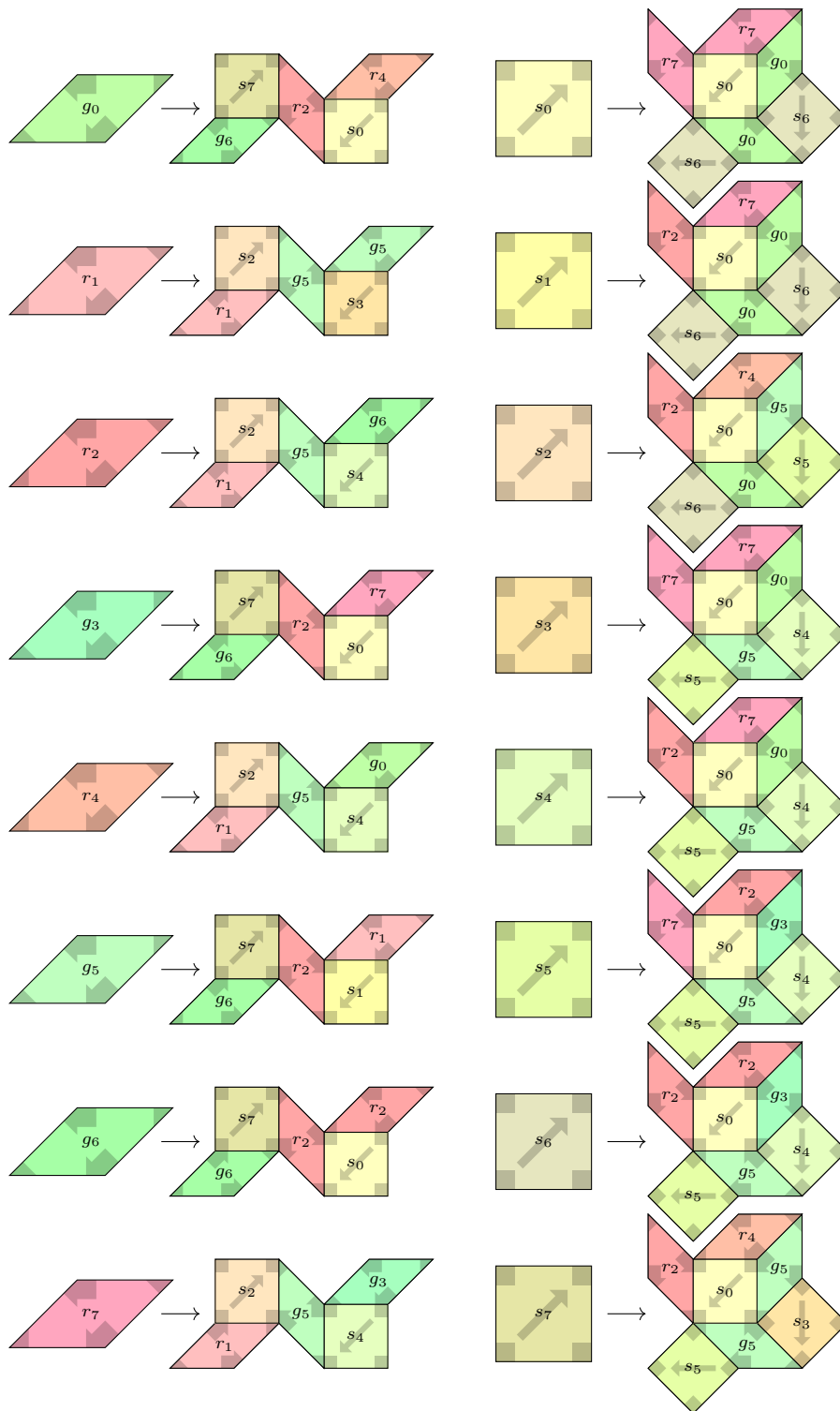


Figure 39: Unambiguous refinement of the Ammann-Beenker system, with the square whole

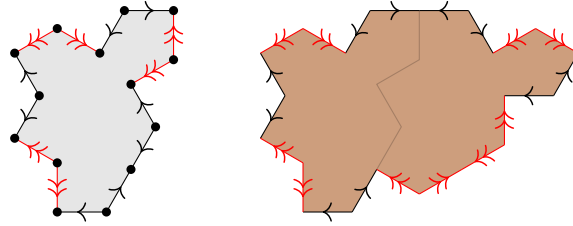


Figure 40: Tile diagrams for the Spectre/Mystic system, with labelled edges

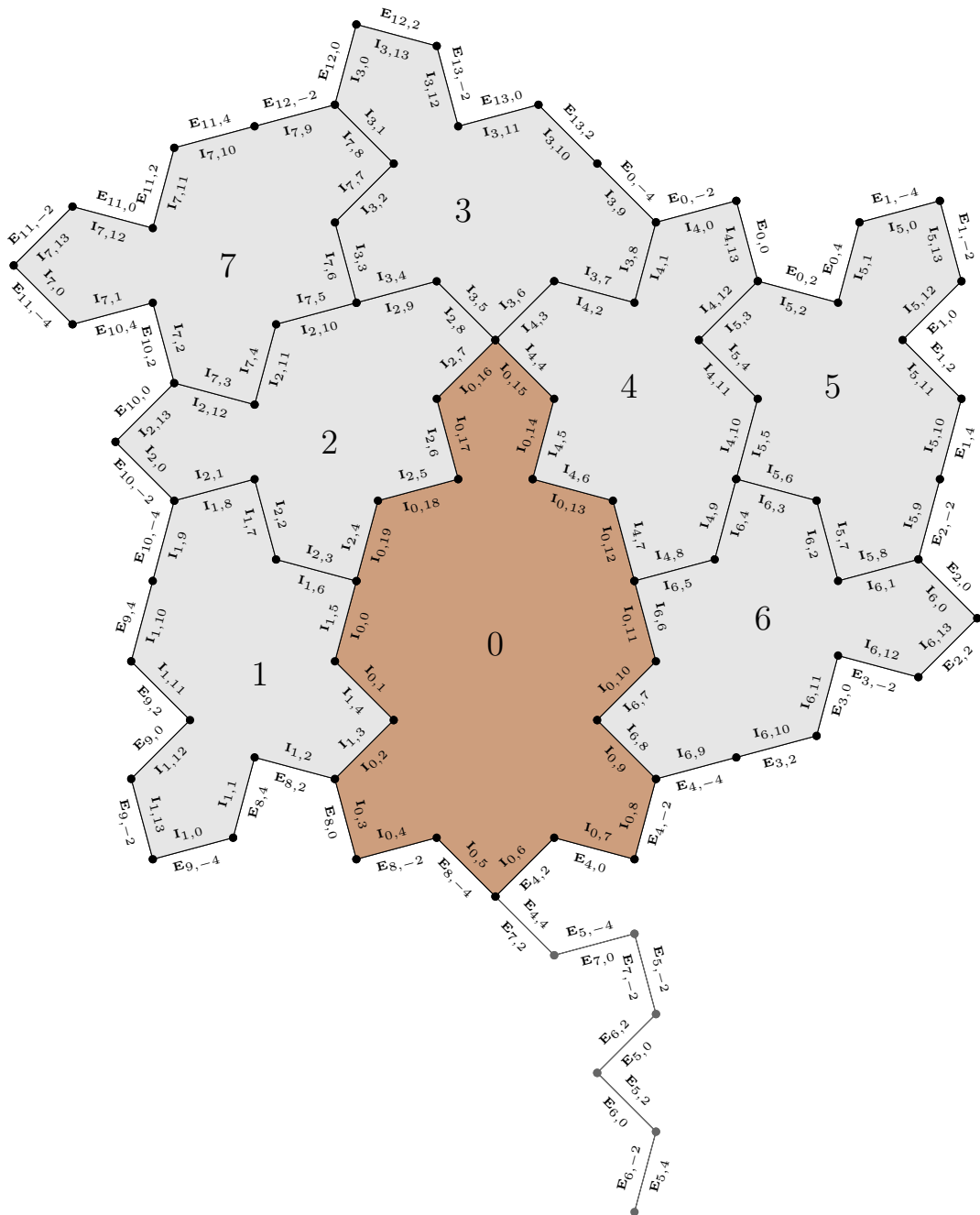


Figure 41: Adjacency map for deflating a Spectre to a patch of Spectres

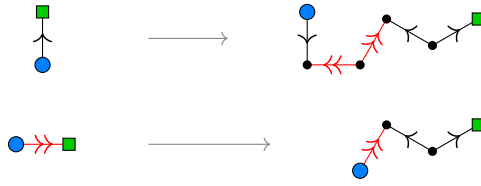


Figure 42: Edge deflation rules for the Spectre/Mystic substitution system

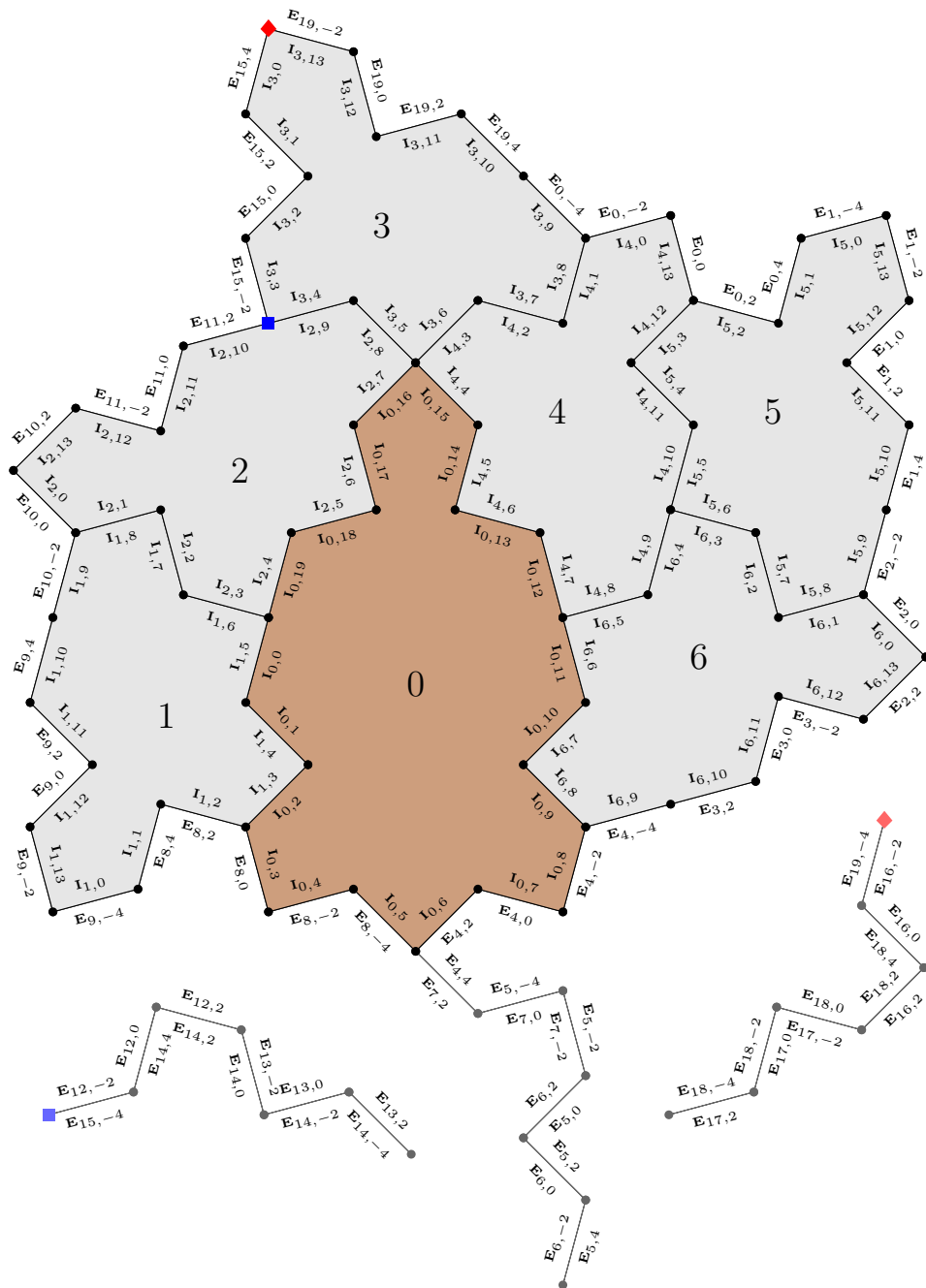


Figure 43: Adjacency map for deflating a Mystic to a patch of Spectres (two spurs are shown displaced from their true locations to avoid overlapping text)

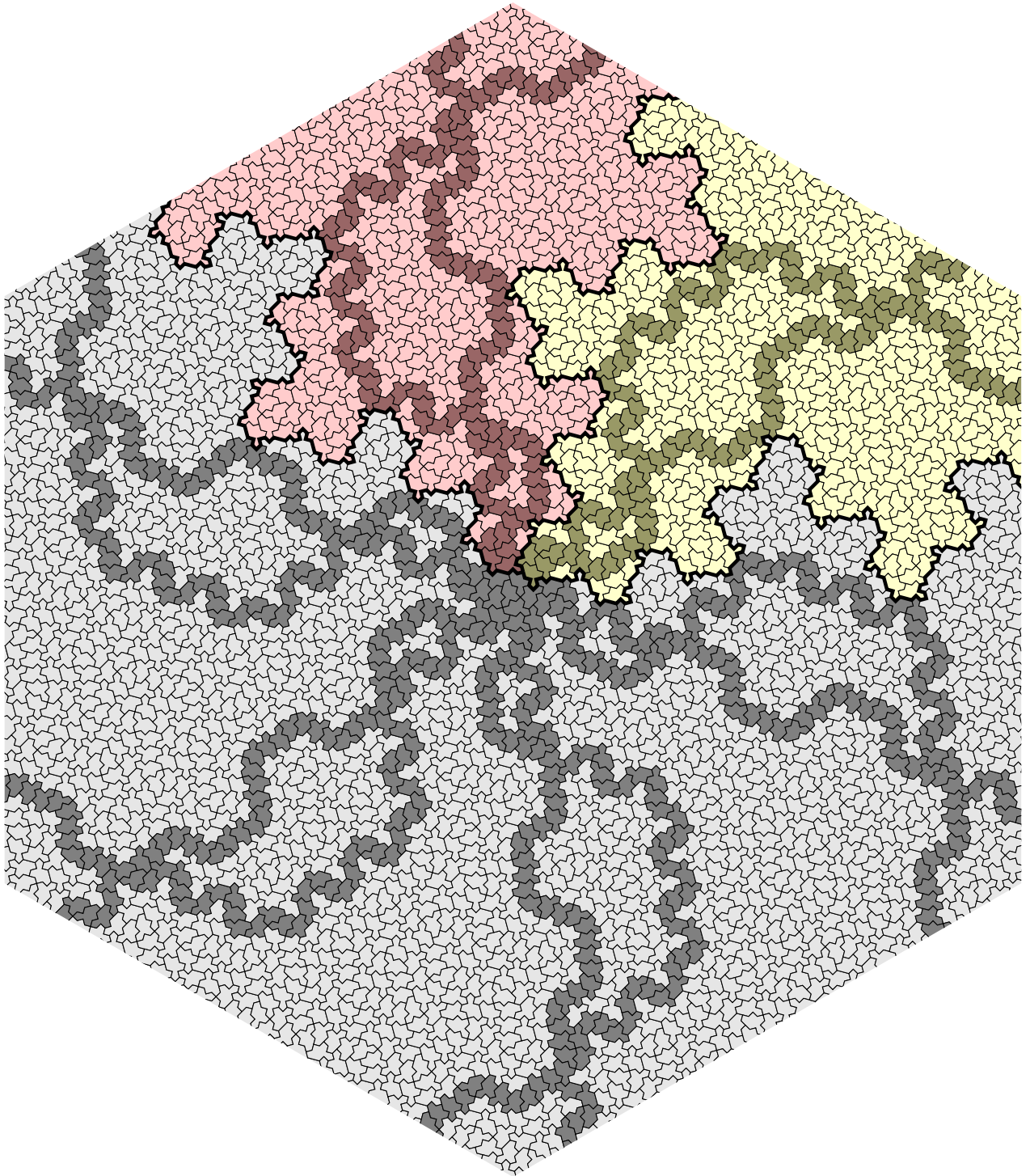


Figure 44: The singular Spectre tiling containing two congruent infinite supertiles  $(\Pi, \Xi)$  and  $(\Xi, \Pi)$  (red and yellow, top). The light tiles are invariant under any rotation by a multiple of  $60^\circ$ .

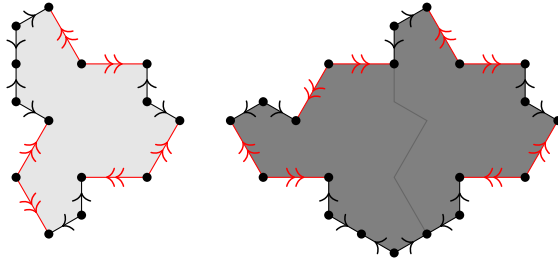


Figure 45: Marked hat tiles in the  $\{H_7, H_8\}$  substitution system

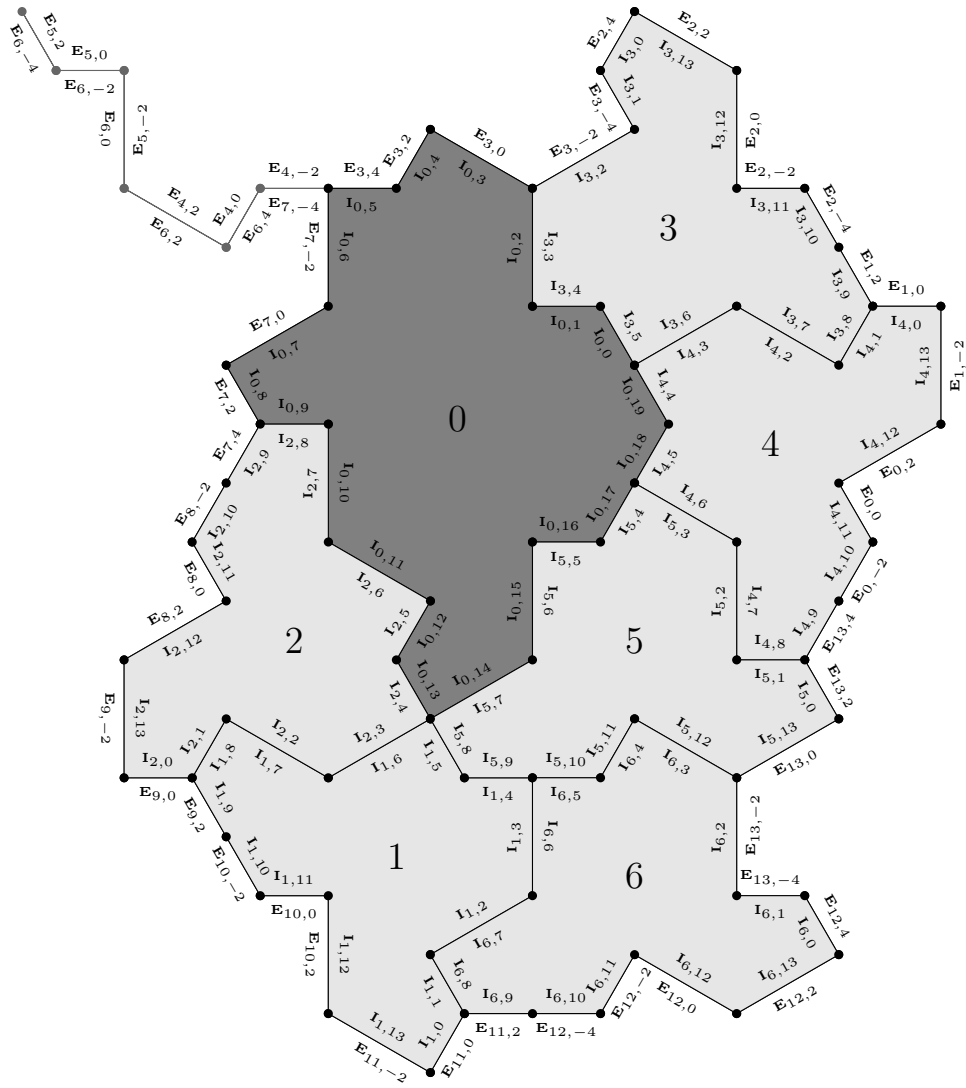


Figure 46: Adjacency map for deflating a single hat to an  $H_8$  patch

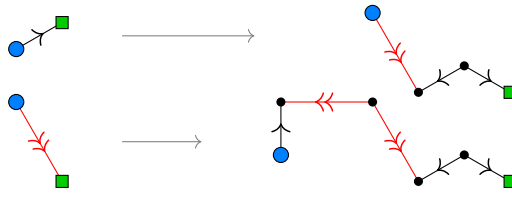


Figure 47: Edge deflation rules for the  $\{H_7, H_8\}$  substitution system

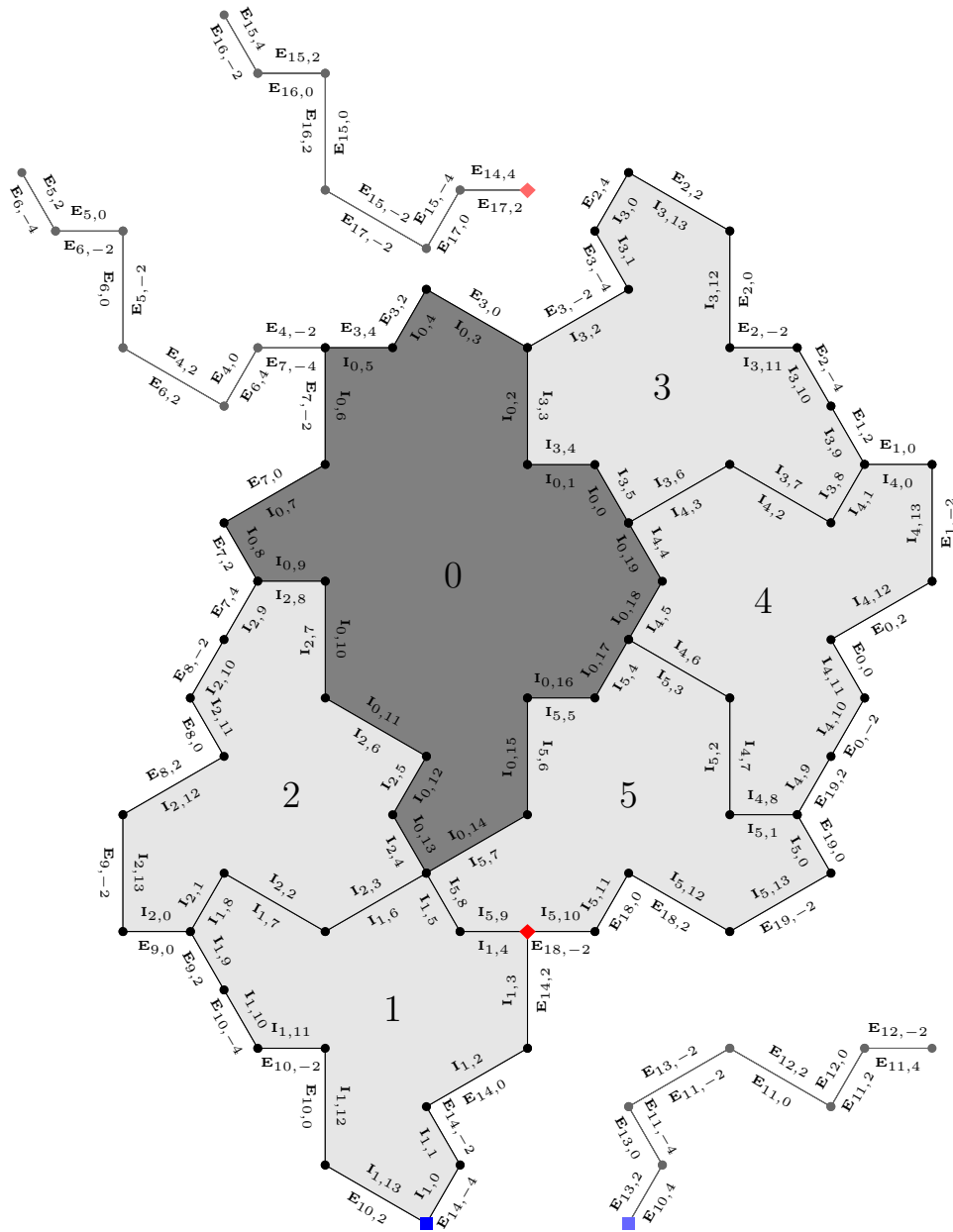


Figure 48: Adjacency map for deflating a double hat to an  $H_7$  patch (two spurs are shown displaced from their true locations to avoid overlapping text)

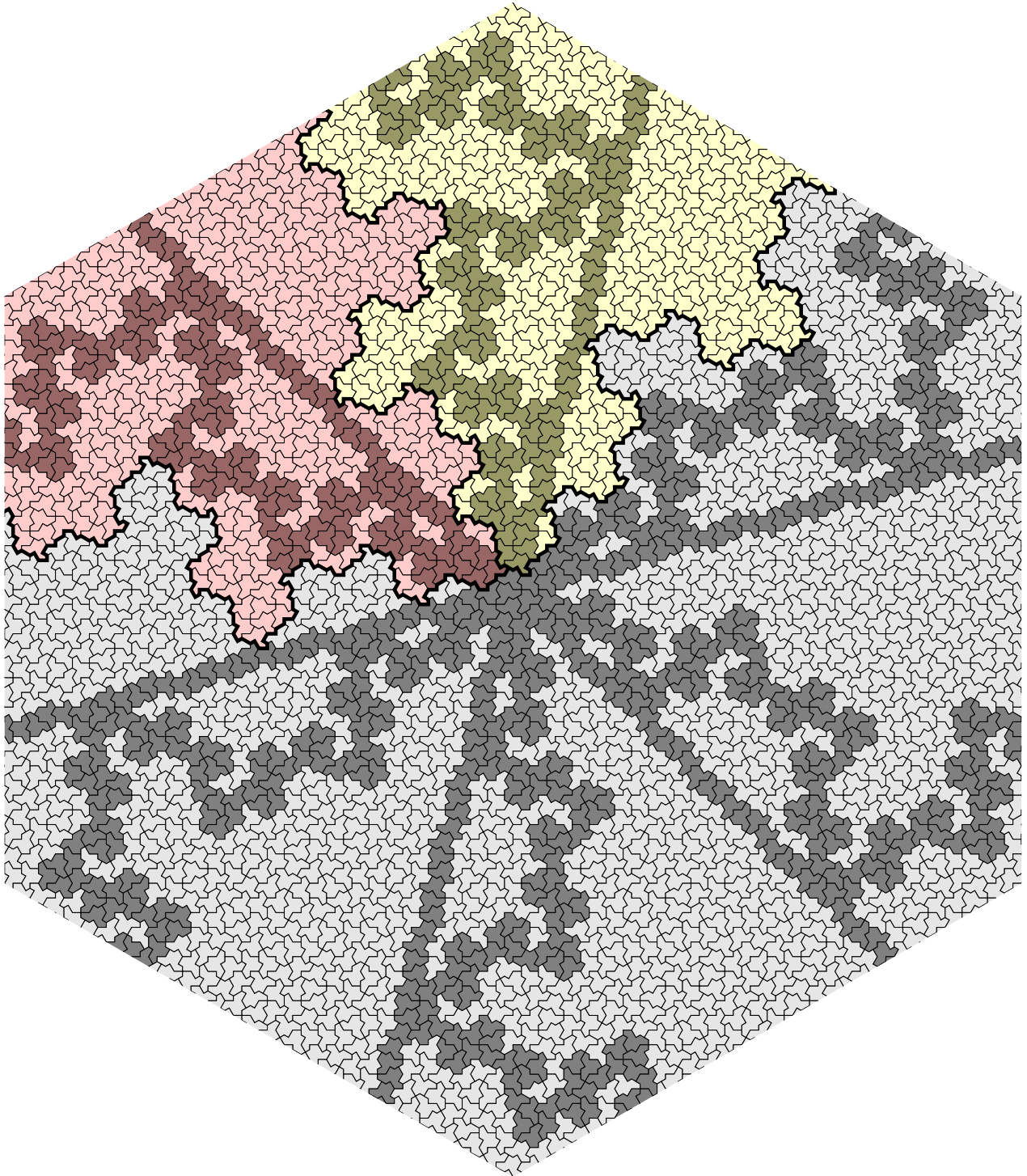


Figure 49: The singular Hat tiling containing two congruent infinite supertiles ( $h_2$ ) and ( $h_4$ ) (red and yellow, top). The light tiles are invariant under any rotation by a multiple of  $60^\circ$ .

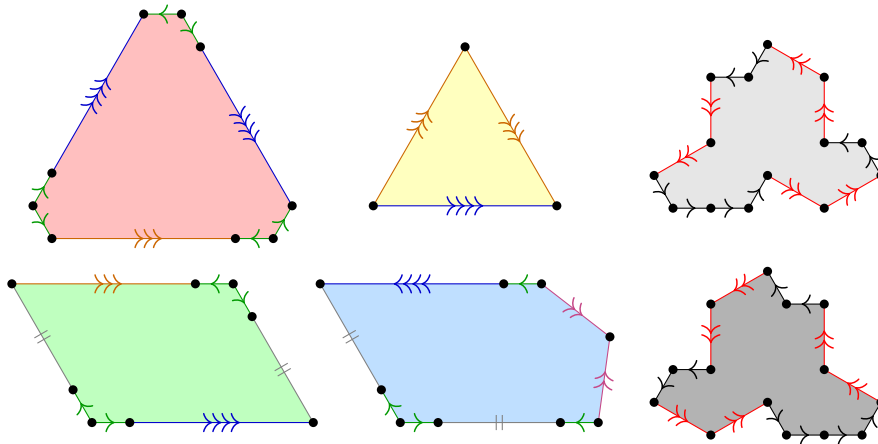


Figure 50: Diagrams of the *HTPF* metatiles and the hat, with labelled edges

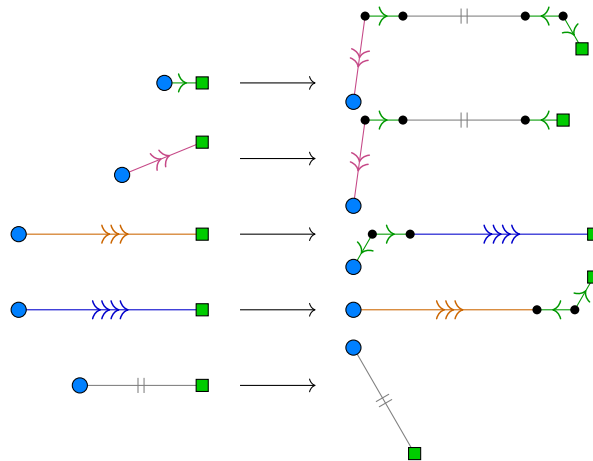


Figure 51: Edge deflation rules for *HTPF* metatiles to other metatiles

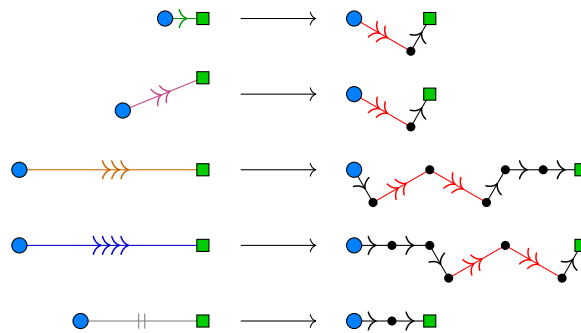


Figure 52: Edge deflation rules for *HTPF* metatiles to hats

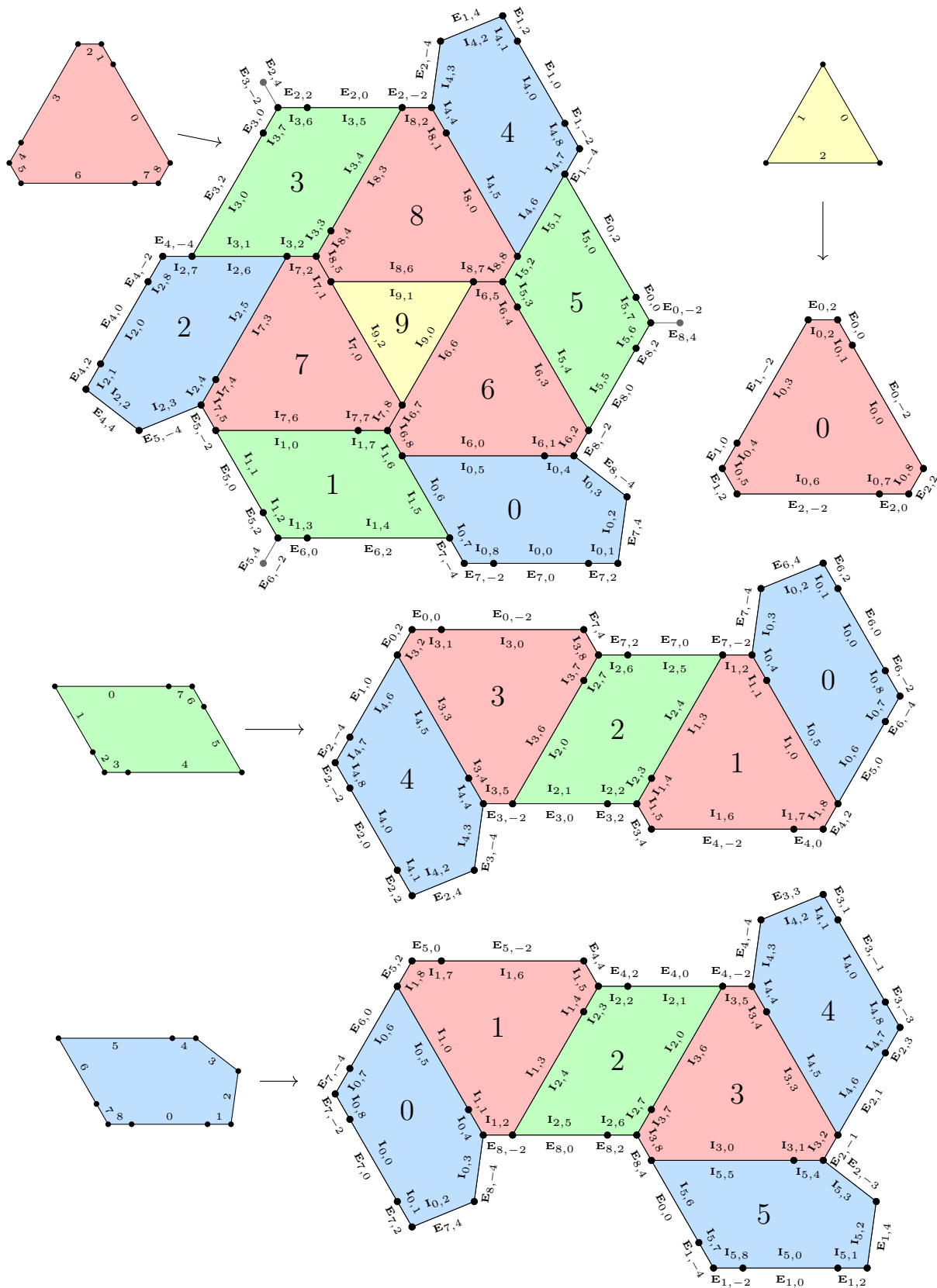


Figure 53: Adjacency maps for deflating *HTPF* metatiles to more metatiles

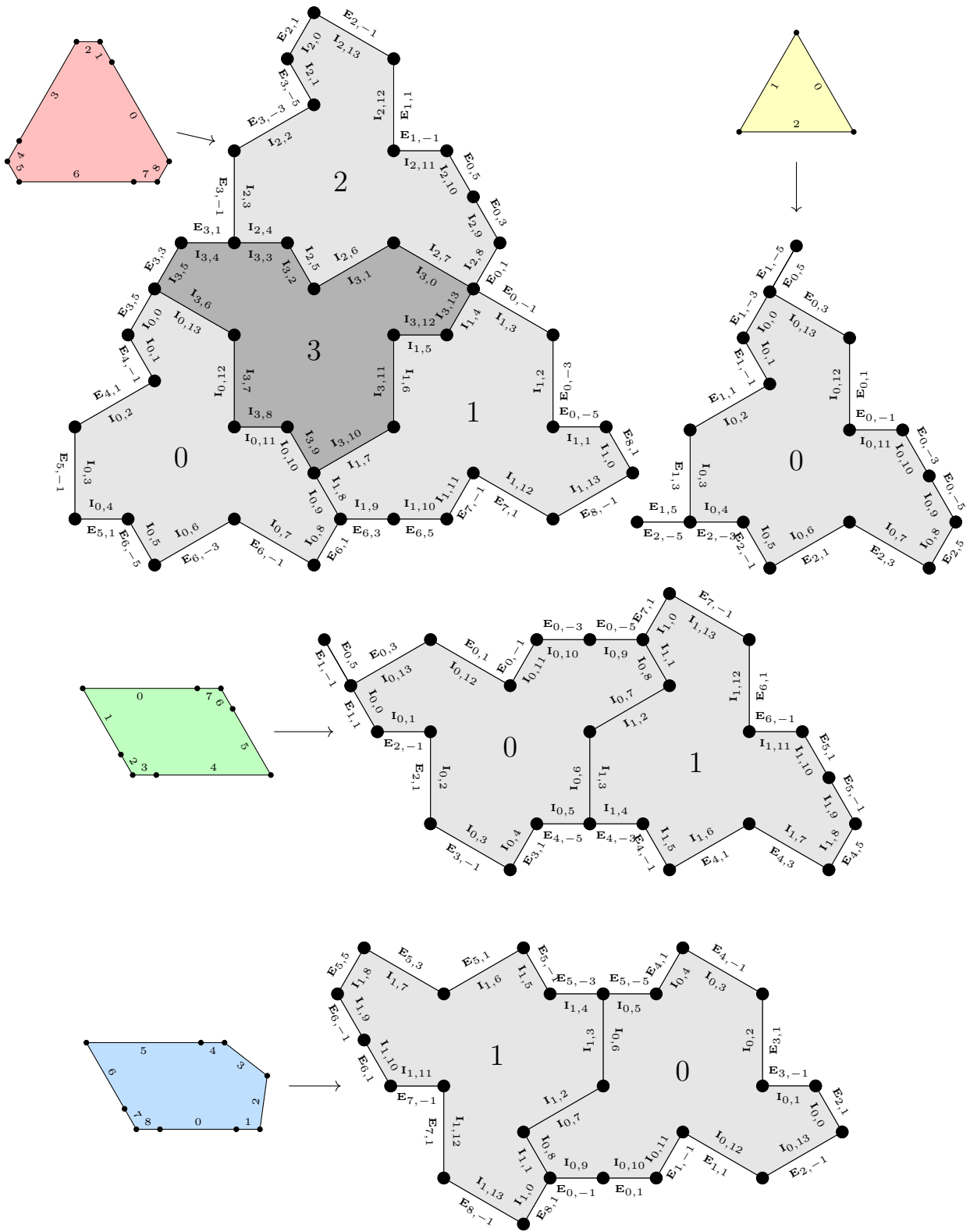


Figure 54: Adjacency maps for deflating *HTPF* metatiles to hats

## References

- [Ang82] Dana Angluin. Inference of reversible languages. *J. ACM*, 29(3):741–765, July 1982. doi:10.1145/322326.322334.
- [BGS25] Michael Baake, Franz Gähler, and Lorenzo Sadun. Dynamics and topology of the hat family of tilings. *Israel Journal of Mathematics*, June 2025. URL: <https://dx.doi.org/10.1007/s11856-025-2780-8>, arXiv:2305.05639, doi:10.1007/s11856-025-2780-8.
- [Che] 4d lift of the tilings by the Smith et al. aperiodic monotile. <https://www.math.univ-toulouse.fr/~cheritat/2023-monotile/4D-lift/>. Accessed: 2025-09-12.
- [de 81a] N.G. de Bruijn. Algebraic theory of Penrose’s non-periodic tilings of the plane. i. *Indagationes Mathematicae (Proceedings)*, 84(1):39–52, 1981. URL: <https://www.sciencedirect.com/science/article/pii/1385725881900160>, doi:10.1016/1385-7258(81)90016-0.
- [de 81b] N.G. de Bruijn. Algebraic theory of Penrose’s non-periodic tilings of the plane. ii. *Indagationes Mathematicae (Proceedings)*, 84(1):53–66, 1981. URL: <https://www.sciencedirect.com/science/article/pii/1385725881900172>, doi:10.1016/1385-7258(81)90017-2.
- [GS86] Branko Grünbaum and G C Shephard. *Tilings and patterns*. W. H. Freeman & Co., USA, 1986.
- [GS99] Chaim Goodman-Strauss. Aperiodic hierarchical tilings. In J. F. Sadoc and N. Rivier, editors, *Foams and Emulsions*, pages 481–496. Springer Netherlands, Dordrecht, 1999. doi:10.1007/978-94-015-9157-7\_28.
- [mat] Turtle Tiles Footnote 1: Altered metatiles and half-inflations. <https://mathblock8128.wordpress.com/2025/07/13/turtle-tiles-footnote-1-altered-metatiles-and-half-inflations/>. Accessed: 2025-11-16.
- [Pao] Maurizio Paolini. Spectre tilings with given Conway signatures. [https://dmf.unicatt.it/paolini/einstein/spectre\\_tilings\\_by\\_sig.html](https://dmf.unicatt.it/paolini/einstein/spectre_tilings_by_sig.html). Accessed: 2025-09-12.
- [Pen79] R. Penrose. Pentaplexity: A class of non-periodic tilings of the plane. *The Mathematical Intelligencer*, 2(1):32–37, Mar 1979. doi:10.1007/BF03024384.
- [Rob75] Comments on the Penrose tiles. Mimeographed notes, preprint of the University of California Berkeley, 1975.
- [SMKGS24a] David Smith, Joseph Samuel Myers, Craig S. Kaplan, and Chaim Goodman-Strauss. An aperiodic monotile. *Combinatorial Theory*, 4(1), July 2024. URL: <https://dx.doi.org/10.5070/C64163843>, arXiv:2303.10798, doi:10.5070/c64163843.
- [SMKGS24b] David Smith, Joseph Samuel Myers, Craig S. Kaplan, and Chaim Goodman-Strauss. A chiral aperiodic monotile. *Combinatorial Theory*, 4(2), September 2024. URL: <https://dx.doi.org/10.5070/C64264241>, arXiv:2305.17743, doi:10.5070/c64264241.
- [Soc23] Joshua E. S. Socolar. Quasicrystalline structure of the hat monotile tilings. *Physical Review B*, 108(22), December 2023. URL: <https://dx.doi.org/10.1103/PhysRevB.108.224109>, arXiv:2305.01174, doi:10.1103/physrevb.108.224109.